A pilot study to characterize racing wheelchair propulsion biomechanics in virtual reality and the real-world for a 1500-meter indoor track

by

Sydney Maria Turai Hampshire

A thesis submitted in partial fulfillment of the requirements for the degree of

Master of Science

in

Rehabilitation Science

Faculty of Rehabilitation Medicine
University of Alberta

Abstract

Many of the 65 million wheelchair users in the world rely on their upper extremity to propel themselves in a manual wheelchair. Unfortunately, the human shoulder is not designed for the imbalanced and extreme forces required to propel a manual wheelchair in our built environments. Upper extremity pain and pathologies associated with manual wheelchair propulsion arise quickly after confinement to a manual wheelchair. Understanding propulsion styles and remedial training of manual wheelchair users is vital, something that may be done effectively in a virtual reality simulation.

The purpose of this pilot study was to develop a research protocol, identify issues with the virtual reality simulation, and examine dynamics measurements taken in the real-world and compare them to dynamics measurements taken in virtual reality. The long-term goal of this research is to optimize a wheelchair track athlete's performance and enable them to propel themselves with a more efficient propulsion technique that also minimizes their risk of injury. Doing so should assist all manual wheelchair users by creating balance in the muscles of the upper extremities and reduce what are currently inevitable injuries.

This was a confirmatory research, longitudinal study. It explored the hypotheses that there was no difference between in dynamics measures and reported perceived experience in the real-world and in a virtual world.

Ten healthy and physically active non-disabled individuals were observed as they propelled a racing wheelchair for 1500-meters around a track in the real-world and a representation of the track in a virtual environment. Participants were 20 – 24 years old. The virtual world incorporated an instrumented wheelchair ergometer capable of simulating the inertia of the participants and wheelchair. Dynamic (ergometer and wearable

dynamic device) and qualitative data on perceived presence and exertion as well as upper extremity pain in the virtual environment (questionnaires) were gathered. Participants propelled at their own set pace in both environments and were not full-time manual wheelchair users.

Steady state cadence, acceleration, steady state and ramp up phase power, ramp up phase force, and the time interval were not different between the two test environments, implying that overall power and the rolling resistance were also not different. Whole test cadence, ramp up and average velocity, distance traveled, time taken to complete the test, ramp up energy, and ramp up push number were all different between the two test environments. Presence and immersion in VR can still be improved, supported by a relatively low average reported presence. Visually induced motion sickness was not experienced by study participants. Shoulder pain in daily living was reported as zeroes or "not performed" and did not differ between the two test environments. The shoulder and overall test areas had different levels of reported exertion between the two test environments. The 1500-meters time point was the most similar test time point between the two test environments. No significant differences between the RW pretest and post-test shoulder pain, but there were significant differences between the VR pretest and post-test shoulder pain.

The study failed to reject the null hypothesis that there was no significant differences between the dynamics measurements and perceived experiences of the study participants in the two environments. This was likely due to a high variance in the mechanical parameters of the virtual simulation. Participants reported a moderate visual representation of the real-world in the virtual world, no motion sickness, a relatively low

level of exertion, and no shoulder pain. However, the virtual world did not fully represent the real-world in a physical way. The dynamics settings of the wheelchair ergometer need to be further adjusted, specifically the inertia weight settings.

This pilot study shows significant differences in dynamic and self-reported measures between the two environments. Improvements to the design of the virtual reality system were identified and procedures for collecting training session data and calibrating the ergometer system were developed.

Preface

This thesis is an original work by Sydney Maria Turai Hampshire. The research project, of which this thesis is a part, received research ethics approval from the University of Alberta Research Ethics Board, Project Name “Wheelchair athlete training using immersive virtual reality ergometer”, Pro00075648, 1/4/2018.

The materials presented in this work are original research conducted in Rehabilitation Robotics Lab, University of Alberta, led by Dr. Martin Ferguson-Pell. The systems developed for this thesis were designed and developed by Sydney Maria Turai Hampshire with the help of Dr. Martin Ferguson-Pell and Mr. John Christy Johnson. The new sensors used in the study; the track compensator indicator device and desktop dial, were designed by Sydney Maria Turai Hampshire with the assistance of Dr. Martin Ferguson-Pell. The data collection and analysis in chapter 3 and 4 are my original work. I was responsible for the data collection and analysis as well as the thesis composition. Mr. John Christy Johnson assisted with the data collection. Dr. Judy Chepeha was my co-supervisor author and was involved with concept formation and thesis composition.

This thesis is an original work by Sydney Maria Turai Hampshire. No part of this thesis has been previously published.

Dedication

This thesis is dedicated to my parents.

It's no *Sand County Almanac*,

but it should do.

– Syd.

Acknowledgements

I would like to acknowledge the hard work of a handful of individuals, without which this project could not have occurred. For it is true when they say that we walk in the footsteps of those who have gone before. Without them to break way, to cut the trail, we could not go that little bit further into the unknown, and, in the pursuit of knowledge, that is what we all strive to do. We all do our part to chisel away at the façade, to bring the obscure to daylight.

First, to Dr. Zohreh Salimi, I give my immense thanks. From the very first time I met her up until this day she has been a steadfast support and resource of knowledge. Her innovative work with the Rehabilitation Robotics Laboratory's wheelchair ergometer is the foundation for this, all of our current, and all future work.

Mr. Kenton Hamaluik and Ms. Lucie Eliasova I thank for their work on the virtual reality immersion system in the Rehabilitation Robotics Laboratory. Hamaluik's dedication to developing a robust simulation is tangible still in today's *ConsoleErgometer* code and LabVIEW software. Eliasova's attention to detail and willingness to get engrossed in the project is what has led to such a fantastic visual simulation of the real-world Universiade Pavilion indoor track.

I would also like to extend my thanks to Mr. John Christy Johnson for his commitment to and aid in every test session. There could not have been a more loyal comrade with a stronger sense of duty to the team.

To all of the individuals who volunteered for this study, I thank you immensely. Not only did all of you selflessly partake in the study, you were all also incredibly enthusiastic to take part. Every one of you were dedicated to the task at hand and took great steps to try to understand the experience of manual wheelchair users.

Additionally, I would like to thank the Para Athletics team at the Steadward Centre for Physical and Personal Achievement in Edmonton for their support. Specifically, I would like to thank Maegan Ciesielski, the head coach, for her assistance and for letting our team borrow their large red racing wheelchair for use in this study.

Dr. Judy Chepeha I thank for her extensive guidance characterizing and understanding upper extremity pathology and function. Any individual who works to understand human biomechanics for rehabilitative purposes should have guidance from a mentor like Dr. Chepeha. It is critical that we understand not only the mechanism behind the movement but also the functional goal associated with that movement, for this is what is associated with the person.

Lastly, to Dr. Martin Ferguson-Pell, the architect of this endeavor, I acknowledge his hand in everything. Without Dr. Ferguson-Pell, this work could never have been realized. In many ways, the student is only as good as their teacher since, in the beginning, much depends on the teacher's ability to instruct such that, in the future, the student has the tools necessary to problem solve on their own. I met Dr. Ferguson-Pell in 2015 and it would not suffice to say that he has been steadfastly supportive and rigorous the entire time. Never one to let me accept "good enough" or allow me to believe I had reached the end of my ability to learn. He urged me to acquire new knowledge and skills for this research project and push the boundaries of my understanding. Always there to both answer a research question and hear a theory, he enables high quality research in the area of manual wheelchair propulsion.

Table of Contents

List of Tables

List of Figures

List of Abbreviations

ARC	Arching
C	Central
DLOP	Double Looping Over Propulsion
ECHA	Edmonton Clinic Health Academy
ER	Experienced Realism
G	General
GI	Gastrointestinal
ICF	International Classification of Functioning
INV	INVolvement
IPQ	Igroup Presence Questionnaire
IV	Independent Variable
MSAQ	Motion Sickness Assessment Questionnaire
MWUs	Manual Wheelchair Users
P	Peripheral
PSL	Paint Stick Length
RPE	Rating of Perceived Exertion
RR	Rolling Resistance
RRL	Rehabilitation Robotics Laboratory
RU	Ramp Up
RW	Real-World
S	Sopite-Related
SS	Steady State
SC	Semi-circular
sEMG	Surface Electromyography
SLOP	Single Looping Over Propulsion
SP	Spatial Presence
T	Total
VAS	Visual Analog Scale
VIMS	Visually Induced Motion Sickness
VR	Virtual Reality
WUSPI	Wheelchair User's Shoulder Pain Index

1. Introduction

1.1 Background

Globally, an estimated 65 million people require daily use of a wheelchair (WHO, 2010). Many will be required to or chose to use a manual wheelchair and rely on their upper extremity strength to get around in their day-to-day life. Many manual wheelchair users (MWUs) have one of the following conditions which requires that they use a manual wheelchair: spinal cord injury, lower-limb amputation, a stroke, multiple sclerosis, rheumatoid arthritis, spinal bifida, poliomyelitis, hip fracture, and/or chronic pain (Finley & Rodgers, 2004; Engel et al., 2009).

The human shoulder is not suited to the repetitive and strenuous forces required to propel a manual wheelchair, thus upper extremity pain and pathology often arise after confinement to a wheelchair (Kentar et al., 2018). Manual wheelchair propulsion is an inefficient means of locomotion, with a gross mechanical efficiency that rarely exceeds 10% (van der Woude et al., 1988a; van der Woude et al., 1988b). It is also associated with musculoskeletal stress and upper extremity injuries, the likelihood of which increases with increased years of manual wheelchair propulsion (Gellman et al., 1988; Cooper et al., 1998; Curtis et al., 1999a; Finley & Rodgers, 2004; van der Woude et al., 2001). In a study of 451 individuals with paraplegia, upper extremity pain was reported by about 81% of the study's participants (Kentar et al., 2018).

The long-term goal of the Rehabilitation Robotics Laboratory's (RRL) research into manual wheelchair propulsion is to allow a MWU to propel their wheelchair in a simulated environment as they normally would in the real-world (RW). In doing so, wheelchair propulsion can be studied in a controlled environment to allow objective conclusions to be drawn and minimize upper extremity problems in MWUs.

1.2 Statement of Purpose

This study examined racing wheelchair propulsion through biomechanical monitoring of a 1500-meter race using an immersive virtual reality (VR) ergometer system, developed in the RRL at the University of Alberta (Salimi & Ferguson-Pell, 2013; Salimi, 2017). This research is thought to be best conducted in the VR environment, as technology and measurements can be combined to sequence the athlete's push style without affecting the

inertial characteristics of propulsion, as long as the virtual environment can be designed to be an accurate simulation of the RW racetrack. It is critical that measurements be combined when studying wheelchair propulsion so that a more complete examination of different propulsion techniques can be conducted (van der Woude et al., 2001). Dynamics, joint angle, and muscle recruitment must be studied together to characterize different propulsion styles, and this can most easily be done in VR where data gathering systems do not impede a participant's ability to propel their wheelchair as they normally would. Once VR can confidently be used to conduct performance testing, these different measurements can be explored.

This study's purpose was to examine wheelchair racing dynamics measurements taken in the RW and compare them to measurements taken in VR to confirm that the VR environment adequately represents the RW environment. By creating an accurate racing wheelchair simulator, the RRL introduces the means to optimize the performance of elite wheelchair track athletes and to provide a controlled training environment. Doing so may lead to the creation of accessible exercise guidelines and propulsion style recommendations. Long-term, this should assist all MWUs and help reduce what are currently inevitable overuse injuries associated with wheelchair propulsion.

1.3 Relevance of Research

In the past, many have studied the biomechanical and physiological mechanisms behind wheelchair propulsion to understand and help reduce the likelihood of upper extremity pathology (Rodgers et al., 2000, Mercer et al., 2006, Qi et al., 2015). However, there exists a knowledge void such that dynamics, joint angle, and muscle recruitment are not studied together and this knowledge is not readily translated into exercise guidelines for MWUs, which could reduce pain and pathology in MWUs (Curtis et al., 1995a; Curtis et al., 1995b; Kobayashi et al., 2017; Martin Ginis et al., 2018). Such studies might be undertaken in a virtual environment where the participant is stationery; consequently, motion capture and surface electromyography (sEMG) might be used. It is known that the propulsion technique employed by MWUs affects the recruitment of muscle groups during manual wheelchair propulsion (Qi et al., 2014). Studies using sEMG in VR may be able to shed light on which muscles are recruited during wheelchair racing propulsion and comment on how this differs in an

individual with spinal cord injury. Additionally, studying normal and abnormal propulsion styles in wheelchair athletes at the whole-body level could inform new exercise guidelines for MWUs. This may improve rehabilitation and prevent shoulder pathology by either recommending proper propulsion techniques or urging MWUs to not use certain harmful propulsion techniques. Thus, the question remains, how effectively does a simulated environment replicate RW conditions for research and training purposes?

We cannot completely generalize our future findings with wheelchair racing athletes to everyday MWUs. There are some different mechanics at play in the propulsion style employed by the racing athlete and the fact that that racing athletes lean forward to lessen the effects of drag substantiates this. Thus, it is less likely that results from studies with wheelchair racing athletes will lead to recommendations on proper propulsion techniques in everyday MWUs. Instead, it is more likely that it will lead to recommendations to not use certain harmful propulsion techniques. This information will improve rehabilitation by reducing imbalance in the muscles of the upper extremity. It aligns well with the definition of rehabilitation being to allow individuals to return to return to their home, live independently, and participate in society (WHO, 2011). Individuals do not lose their desire to partake in sport and recreation after experiencing a permanent or semi-permanent disability. Parasports allow individuals to remain active after injury & retain social benefits of competitive sport. Doing so optimizes patient outcomes in the community (AHS Strategy, 2016). A large part of accomplishing this goal is developing customized propulsion techniques for MWUs to reduce what are currently inevitable injuries in the upper extremities.

Beyond using the VR ergometer system to comment on manual wheelchair propulsion and shoulder biomechanics, there exists the possibility of using VR to train wheelchair athletes. Globally, there is mounting interest in health and wellness by all citizens to improve their quality and quantity of life through better nutrition, exercise, and recreation. MWUs also partake in this movement, in part through wheelchair sports. Wheelchair racing athletes are at an even greater risk of developing overuse injuries in their upper extremities, if they do not propel safely, due to the extreme forces they employ and intense speeds they travel at (30 km/hour or greater) (Heyward, 2017). Interestingly, Finley & Rodgers (2004) found no difference in the incidence of shoulder pain, past or present, between athletes and non-athletes who were MWUs. This begs the question, “If proper techniques are employed, as racing

wheelchair athletes do at high speeds, can increased shoulder injury be minimized in manual wheelchair propulsion?"

While completing this study, I also met with a former wheelchair racing athlete to discuss wheelchair racing and steering. She told me that there was much she needed to learn when she began wheelchair racing but that not a lot of information was available to athletes online (Sierra Roth, Personal communication, May 16, 2020). Additionally, this athlete, Sierra, had a direct channel of communication with the Team Canada Paralympic coach for track racing but still decided to withdraw from the sport of wheelchair racing in favor of joining rowing. Sierra commented that wheelchair racing on a track is very difficult because it requires the racer to set their steering mechanism, their track compensator, every time they race and when they change lanes. The track compensator steering mechanism is very sensitive and can even affect the steering dependent on the flooring material installed on the indoor racing track. Finally, Sierra commented that wheelchair racing took a lot of effort from her shoulders as she has a higher level of spinal cord injury. Often steering would require her to use her shoulders to advance one wheel more than the other in a wheelie so she could turn. A wheelie can be performed in one of two ways: due to a great enough torque being applied to the rear wheels by an athlete's hands or by an athlete shifting their weight to left or right relative to the wheelchair. Individuals with lower levels of spinal cord injury or more core innervation are more able to shift in their seats to steer instead of overexerting using their shoulders. These individuals can use their body weight to move the front wheel left or right when they wheelie to steer. Currently, a huge gap exists between the elite wheelchair racing group racing for Team Canada and the amateur-level athlete in Edmonton. There are very few wheelchair racing programs with the tools necessary to train wheelchair racing athletes in Canada. Additionally, the common difficulty with steering the racing wheelchair using the track compensator seems to not be addressed by any athlete or research groups. Addressing wheelchair steering is novel and can be done in a VR simulation.

Once a VR environment can be built to represent the RW, future studies with VR ergometers may address how training and performance can be optimized for maximum performance potential. van der Woude et al. (2006) noted the critical role that wheelchair sports, and the subsequent technological research conducted because of sports, play in enhancing the lives of everyday MWUs. As such, this study intends to determine if a VR

simulator can provide a representative training environment for wheelchair track athletes and inform our understanding of push styles in everyday MWUs. The purpose of such research would be to enable manual wheelchair athletes to meet their goals while minimizing the risk of injuries associated with these goals. Learning what is the most efficient propulsion style for function and protection of the shoulder in wheelchair athletes will inform our understanding of propulsion efficiency in everyday MWUs.

2. Review of Relevant Literature

In this section, current information relevant to the study is presented. This includes pathology associated with the various styles of wheelchair propulsion, the types of immersive simulations that could be used to study wheelchair propulsion, and two methods of replicating over-ground wheelchair propulsion. Additionally, two systems for measuring RW dynamics factors are introduced.

2.1 Manual Wheelchair Propulsion

Shoulder pain affects a MWU's ability to go about their day and reach their functional goals. Since this study is focused on wheelchair-racing, it is worth noting that a study by Derman et al. (2016) found that overall Paralympic athletes have a higher injury incidence than Olympic athletes and that injuries in Paralympic sport are more likely to occur in the shoulder joint.

The daily median activity for MWUs, as reported by Sonenblum et al. (2012), was 1.6 km over 54 minutes broken up into 90 bouts of mobility, or instances of movement. On a typical day, their study's participants completed about ten bouts of movement per hour that they were seated in their wheelchairs. The median bout of movement lasted 21 seconds and had the participant travel 8.6 meters at 0.43 m/s. 85% of bouts of movement recorded by Sonenblum et al. (2012) were less than 1 min and consisted of the individual moving less than 30 meters. However, the day-to-day variability was considerable in all variables studied, with occupancy time varying the least. These average daily movements tend to put MWUs below national health guidelines for weekly activity. Additionally, because our built environments are not designed for manual wheelchair propulsion, MWUs experience novel stressors, like frequently raising their arms above shoulder height at home and work (Reid et al., 2003; Troy et al., 1997). Thus, the functional activities that MWUs complete daily increase their likelihood of shoulder pain. Contention exists between staying active while in a manual wheelchair and reducing one's risk of injury (National Institute of Health, n.d.).

Increased shoulder pain in MWUs has been shown to contribute to more sedentary lifestyles yet exercise guidelines to help prevent shoulder injury in MWUs are scarce, furthering the progression of shoulder pathology (Executive Committee for the International

SCI Data Sets Committees et al., 2006; Martin Ginis et al., 2018). Guidelines that do exist tend to be clinical and not readily accessible to MWUs, such as *Clinical Practice Guideline for Health-Care Professionals* written by the Consortium for Spinal Cord Medicine (2005). Additionally, MWUs often report pain in more than one area, such as various combinations of shoulder, wrist, and elbow pain (Kentar et al., 2018), which may increase a MWU's level of disability. However, an increase in shoulder strength does not necessarily lead to a more optimal push strategy and less pain; increasing muscle mass alone does not better equip an individual in a manual wheelchair for wheelchair propulsion (Ambrosio et al., 2005). Specificity in strength training and teaching proper propulsion techniques are more critical to maximize the effectiveness of the task. Additionally, overuse injuries are believed to be related to the cadence of the MWU and incorrect propulsion style (Consortium for Spinal Cord Medicine, 2005). Therefore, proper propulsion techniques must be used by MWUs and researched by the scientific community. These techniques should reduce the likelihood of injury by creating muscle balance in the upper extremities.

A MWU's propulsion stroke has been classically divided into two phases: a shorter push phase and a longer recovery phase (Allen et al., 2008). The push phase is the phase where the MWU applies force to the wheelchair to propel, while the recovery phase is the phase where the MWU repositions their arm back to the start of the push cycle for the next push phase. The push phase begins with the shoulder abducted, extended, and internally rotated. As the MWU continues through the push, the shoulder flexes more in the horizontal and sagittal planes. It is generally agreed that the greatest overall movement of the shoulder joint occurs in the directions of flexion and abduction. Although there is disagreement in the maximum and minimum ranges of movement in each

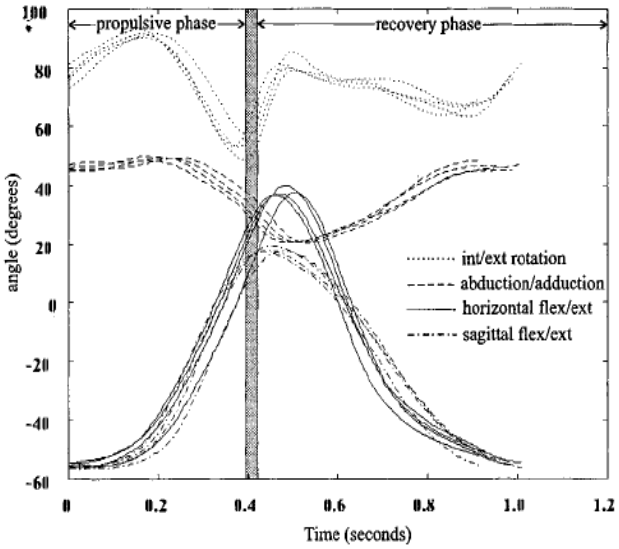

Figure 1. Shoulder range of motion throughout four consecutive wheelchair propulsion strokes for a single individual. The transition from propulsive phase to the recovery phase is marked by the grey bar. (Boninger et al., 1998).

plane. Figure 1 illustrates the range of motion at the shoulder with a typical wheelchair propulsion stroke.

This study focused on the push phase of manual wheelchair propulsion, as this is the period where forces are the most substantial. The components of the push phase were characterized using dynamic measurements. Dynamic measurements are force, distance, time, acceleration, and velocity, and will be explained later. The velocity, cadence (pushes/minute), and push length are all interrelated and characterize the push (Cooper et al., 2010). The muscles involved in the push phase are the anterior deltoid, sternal pectoralis major, supraspinatus, infraspinatus, serratus anterior, and long head of biceps brachii (Mulroy et al., 1996). The recovery phase muscles include the medial and posterior deltoids, subscapularis, supraspinatus, and middle trapezius (Mulroy et al., 1996). Research to date indicates that the rotator cuff is the most at risk of overuse injuries via repetitive strains during manual wheelchair propulsion (Mulroy et al., 1996, Veeger et al., 2002). A rotator cuff tear is injury to one or more of the tendons or muscles of the rotator cuff: the supraspinatus, infraspinatus, teres minor, and subscapularis (University of Sheffield Learning Media Unit, 2005). Imbalance in the shoulder muscles occurs when some muscles are strengthened or overused and others are weakened or underused, which can lead to shoulder complaints. The rotator cuff is at risk of developing imbalance-linked pathologies as a result of push phase propulsion because some of the rotator cuff muscles are activated and strengthened during the push phase while others are not used in the push phase and may weaken over time. This imbalance can create long-term health complications which can be further exacerbated by the fact that MWUs often experience poorer health outcomes as compared to the general population (Krahn et al., 2015; Stillman et al., 2017).

There are four common everyday propulsion styles employed by MWUs: semi-circular (SC), single looping over propulsion (SLOP), double looping over propulsion (DLOP), and arcing (ARC) (Figure 2) (Shimada et al., 1998; Boninger et al., 2002; Herrera et al., 2018). SC is characterized by the hands falling below the hand rim during the recovery phase. It is usually preferred for long distances as it is smoother, generally more efficient, and reduces shoulder strain. SLOP is characterized by the hands rising above the hand rim during the recovery phase. Boninger et al. (2002) found SLOP to be the most common propulsion style in their study at 45%, followed by DLOP at 25%. DLOP is characterized by the hands rising above the hand

rim, crossing over it, and dropping under the hand rim during the recovery phase. Boninger et al. (2002) also found that SC and DLOP had the lowest cadence, both were significantly lower than SLOP ($p<0.5$ for all comparisons) patterns and ARC ($p<0.01$ for all comparisons). ARC occurs when the hand follows an arc along the push rim during the recovery phase. It is often used when going up inclines, as it can lead to a faster cadence and more control in the push.

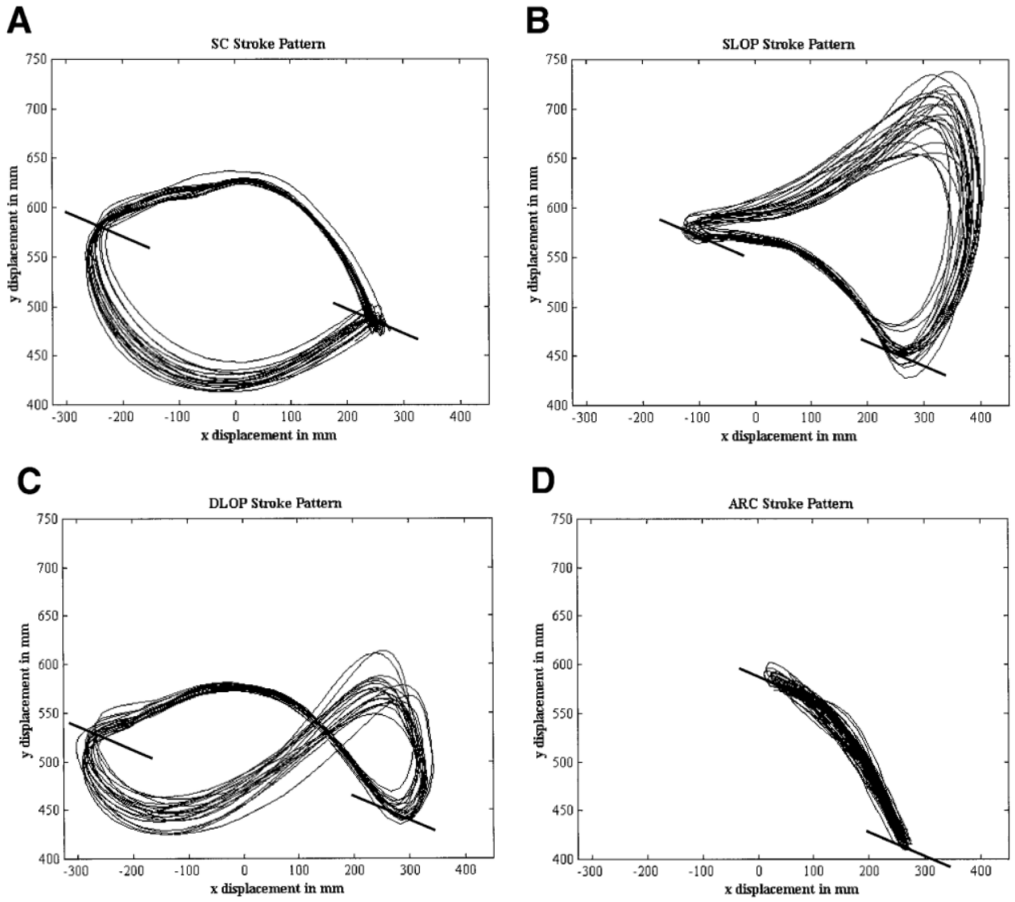

Figure 2. Four propulsion styles: A) SC, B) SLOP, C) DLOP, and D) ARC. The dark bars to the right of each pattern represent the beginning of the propulsive stroke, while the dark bars to the left represent the end of the propulsive stroke and the beginning of the recovery phase. (Boninger et al., 2002).

Wheelchair racing athletes tend to be taught to use the para-backhand propulsion (PBH) technique (Morse et al., 1994). In this style, the fingertips contact the hand rim with a bit of support by the thumb. In everyday wheelchair propulsion, more of the center of the fingers and thumb contact the rim. To accommodate this, wheelchair racing athletes must wear gloves, which are specialized for increased adhesion and protection. The PBH style has five phases: the catch, drive, release, lift-and-stretch, and acceleration phases. First, the racer grabs the top of the hand rim with the thumb in a "hitchhiker's pose" while also flexing their wrist

to the thumb side in radial deviation (Figure 3A). Contact in the catch phase begins between 1:00 and 1:30, as on a clock face (Figure 3B). In the drive phase, the last joint on the thumb squeezes against the hand rim while the base of the thumb holds close to the tip of the index finger to disperse the force. The hand travels around the hand rim and the contact point changes to the base of the thumb and index-/middle-finger cuticles at 5:00 to 7:00 (Figure 3B). In the release phase, the thumbs move in front and around the hand rims, the hands are flexed to the pinkie-finger side of the wrist (ulna deviation) (Figure 3C). The elbows are forcefully lifted up and behind (shoulder extension) (Figure 3D). With the shoulders extended, a stretch in the chest and anterior shoulder muscles is created and the acceleration phase begins (Figure 3 E). In this stroke, the arms gain speed to enhance the force of the catch and drive phases. Figure 3F shows the whole push cycle from the catch phase to the acceleration phase.

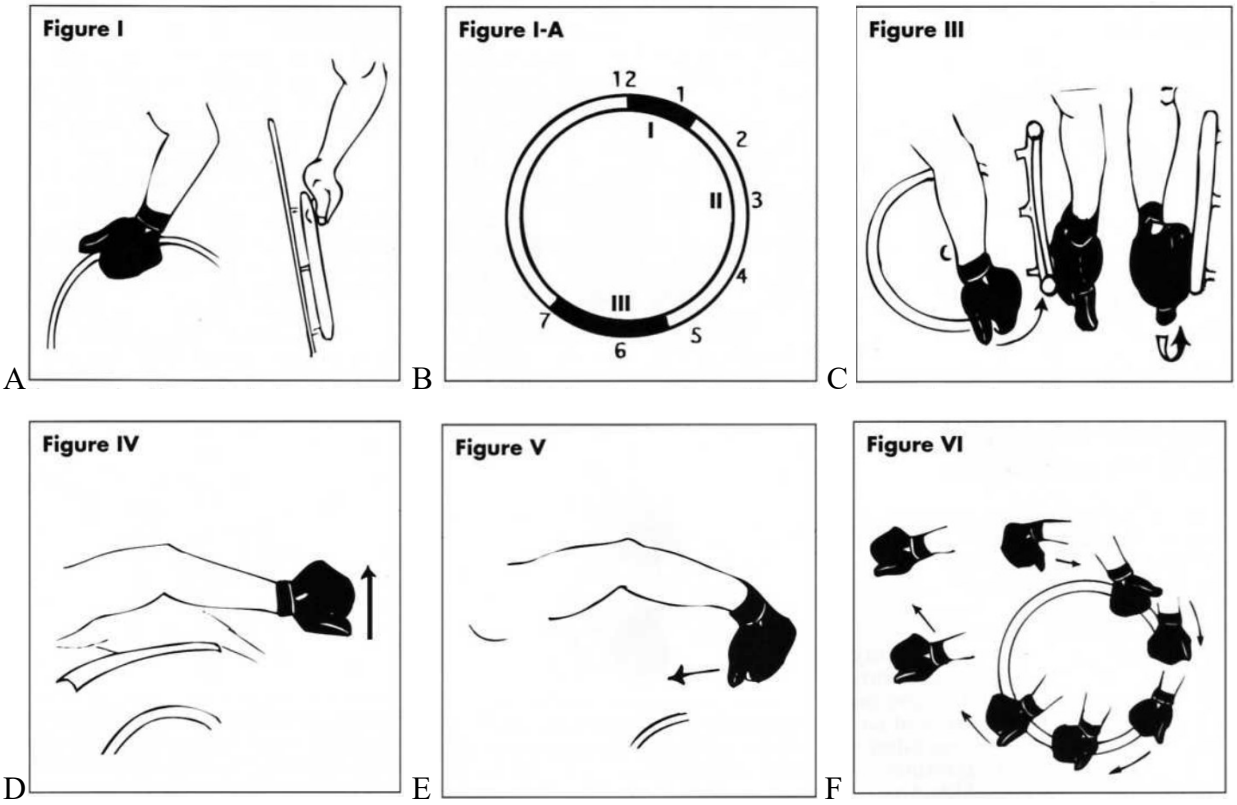

Figure 3. Outline of the para-backhand propulsion technique. The catch (A), drive (B), release (C), lift-and-stretch (D), and acceleration (E) phases (Morse et al., 1994).

Wheelchair propulsion beyond dynamics and propulsion style has not been extensively explored, largely because of environmental limitations. For example, a motion capture space to study manual wheelchair propulsion would have to be much longer than is typically built in order to accommodate a moving wheelchair. Even then, it will most likely only be long enough

to measure one or two propulsion strokes. A stationary wheelchair ergometer placed inside an immersive VR environment could solve this problem by allowing researchers to use more monitoring technology unobtrusively on a stationary participant. Research with full-time racing MWUs is rarely done in VR and is thus innovative. The opportunity for added technology will allow for future exploration of novel measures, like joint angle and muscle sequencing, in addition to traditional biomechanical measures, like force and distance (van der Helm & Veeger, 1996). First though, an accurate representation of the RW must be created in VR.

2.2 Racing Wheelchairs

Figure 4. A four-wheeled racing wheelchair.

Prior to the 1990s, racing wheelchairs had four wheels (Figure 4), which offered more stability to the chair and was safer than the modern three-wheeled wheelchair (Figure 5) (Viger, 1988). Presently, three wheeled chairs are the standard track racing wheelchair as they allow for faster speeds around corners, quicker acceleration, better drafting, and are lighter (Viger, 1988).

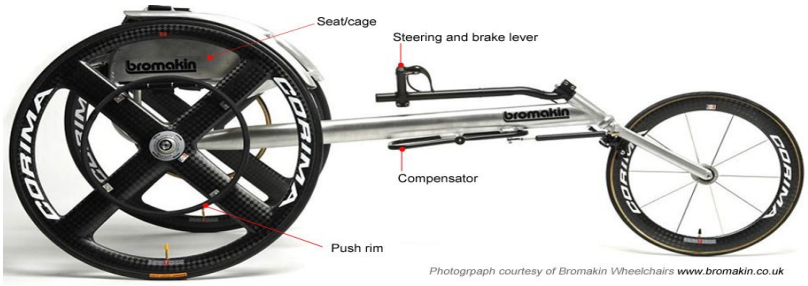

Figure 5. A typical modern-day racing wheelchair for track events complete with track compensator.

When steering their wheelchair, a wheelchair racer has only two options: a standard manual steering mechanism or a pre-set and automatic device called a track compensator. While a manual steering mechanism was used historically in four-wheeled racing wheelchairs, and still is used today during some road races, a more automated mechanism is needed to be competitive in modern sprint races. A track compensator (Figure 6) allows a racer to turn their wheelchair at a pre-set angle without needing to push differentially on their hand rims. The

track compensator typically uses two setting dials that allow the athlete to adjust the angle of travel depending on the track's geometry and the athlete's lane assignment.

Figure 6. A typical modern-day racing wheelchair for track events complete with track compensator.

The track compensator is a cylindrical rod attached to a square or oval track control device (Figure 7). The track control device is set at two specific angles: one to travel in a straight line and one to travel at an angle around the corners of the racetrack. This is needed because wheelchair track racers do not steer their wheelchair by differentially pushing, as civilian MWUs do. When a wheelchair athlete enters a corner and continues around the bend, they are still pushing straight. Instead of steering their wheelchair manually, a wheelchair racer will hit the control device from the left side of the chair to move it to the right. In doing so, they move the front wheel to the pre-assigned angle of the track. When they exit the curve, the racer will hit the control device from the right to push it back into a line of straight travel.

Figure 7. Close up of the track compensator mechanism (HowIRoll. . . [accessed 2019]).

The track compensator is adjusted using two "stops" on the track control device (Figure 8). These stops are dials which turn in or out to set the angle of the turn, the left stop, and to set the straight path of travel, the right stop. In this way, the racer will turn the left dial out to make the curve more aggressive. A racer will almost never change the right position of the right stop; however, the racer will change the position of the left stop with every race dependent on the lane they are assigned. The racer sets the angle to the inside, or left, line of their assigned lane. When completing this study, I met with a current wheelchair triathlon athlete and learnt that most track racing wheelchairs use the same steering design (Erin Jackson, Personal communication, February 7, 2019).

Figure 8. Full view of a racing wheelchair's steering mechanism.

2.3 Immersive Simulations for Manual Wheelchair Propulsion

Wheelchair propulsion studies conducted in the RW are the most realistic and have the greatest context validity; however, current RW testing for wheelchair athletes has significant draw backs. Equipment used for evaluation on an indoor track in the RW can slow down a wheelchair athlete or alter their propulsion form. In a treadmill environment, racers lose the ability to self-select their speed and the ability to use visual cues to gauge performance intensity. Stephens and Engsberg (2010) studied manual wheelchair propulsion in the RW and on a treadmill and found that the differences were significant between the two test environments for both the left and right wheels. In another study, Koontz et al. (2012) compared wheelchair propulsion on a level tile surface to wheelchair propulsion on a dynamometer at a self-selected speed. They found that push length, cadence, and total force were similar between the two environments; however, they could not replicate the rolling resistance (RR) of the tile surface on the dynamometer. Additionally, the researchers did not include the effects of the subject's inertial mass during the simulation and there was no visual feedback during the dynamometer propulsion. Inertia is the quality of matter which resists change in motion; it resists acceleration. Both studies did not include a means to simulate inertia, which greatly decreases how realistic the simulation was.

This study overcame many of these issues by using the RRL's immersive VR ergometer system. The system combines features of an ergometer and dynamometer with a 3D visual experience. Without the EON ICube Mobile VR semi-immersive system, participants lose periphery vision immersion, which decreases validity and presence in VR (Salimi, 2017).

For an effective simulated wheelchair propulsion experience conducted in a controlled lab environment, visual feedback is needed to increase presence, engage the participant, and allow the participant to respond to the simulated environment. This is done because, when simulating over-ground propulsion, it is necessary for participants to be able to complete tasks that are as close as possible to RW conditions (Cooper et al., 2010; Richter et al., 2011; Vanlandewijck et al., 2001; Koontz et al., 2012). Visual feedback could be provided through non-immersive systems, semi-immersive systems, or fully immersive head-mounted display systems. In the past, non-immersive systems have been used to study wheelchair propulsion

and have relied heavily on measurements like propulsion speed (Gooset-Tolfrey et al., 2010), muscle activity (Qi et al., 2012), applied force, cadence, and distance traveled (Cooper et al., 2010; Rice et al., 2010; Richter et al., 2011) as their outcome variables because they often do not use much more than a high-resolution computer monitor for visual feedback. Conversely, a fully immersive head-mounted display systems usually mean that the participants lose periphery vision immersion, have increased motion sickness, and experience decreased presence (Salimi, 2017). Semi-immersive systems might allow the participant to fully engage with their environment and feel the VR environment as the RW. This is because semi-immersive systems blend the two systems mentioned above.

To create an accurate replication of RW wheelchair propulsion on a wheelchair ergometer in VR, it has been proposed that there are at least seven biomechanical factors that need to be similar between the two environments (Salimi et al., 2018; de Klerk et al., 2020). These factors are:

- Velocity,
- Acceleration,
- Applied Force,
- Resistive Force,
- Energy Consumption,
- Inertial Effects, and
- Trunk Swing.

These factors were examined in this study for consistency between the VR environment and RW. There was also the question of how realistic the VR environment was in terms of its visual and tactile feedback. This aspect was addressed by studying the participant's perceived presence, exertion, and shoulder pain level via questionnaires. Presence in VR is the sense of being immersed in the virtual environment and experiencing it as real. Level of exertion is an individual's experienced degree of physical and mental effort when completing a task.

Results from this study helped to create an immersive VR ergometer system that can replicate RW track performances. They also provide a proof of concept for a tool to be used for more effective physiological evaluation of wheelchair athletes. Moreover, in the future, this system could provide a safe and controllable environment for wheelchair athlete training. This innovative work in VR may shed light on the contributing biomechanical causes of shoulder pathology in MWUs and has the potential to expand our understanding of wheelchair push styles. Multiple variables can be controlled in the VR simulated environment, making it

an ideal place for research in this field. If reality can be adequately simulated in this study, a brand-new realm of research can be explored.

2.4 Wheelchair Ergometer and Dynamometer

An ergometer can measure speed, work, and power during wheelchair propulsion (Wu, 2012). A dynamometer is a device that can measure torque, or rotational force, and speed of rotation through sensors installed on the axles of the roller (DiGiocine et al., 2001; Sauret et al., 2011). Both can measure quantities of interest in manual wheelchair propulsion and be used to control the RR of the system with the correct attachments. RR is the force that resists an object's motion when it rolls on a surface. Controlling RR is critical because as the RR increases the effort to propel increases, which can decrease immersion in VR and the realness of the simulated wheelchair propulsion. Both ergometers and dynamometers perform similar functions with the main takeaway being that ergometers primarily measure work and dynamometers primarily measure force. A dyne is a derived unit of force specified in the centimeter–gram–second system of units. It is 1 gcm/s^2 whereas a newton is 1 kgm/s^2. An erg is the amount of work done by a force of one dyne exerted for a distance of one centimeter ($g \cdot cm^2/s^2$). When using these systems, participants can push at their own set speed and change propulsion metrics quickly as desired or in response to the simulated propulsion task. Both ergometers and dynamometers consist of a pair of parallel steel rollers (Figure 9).

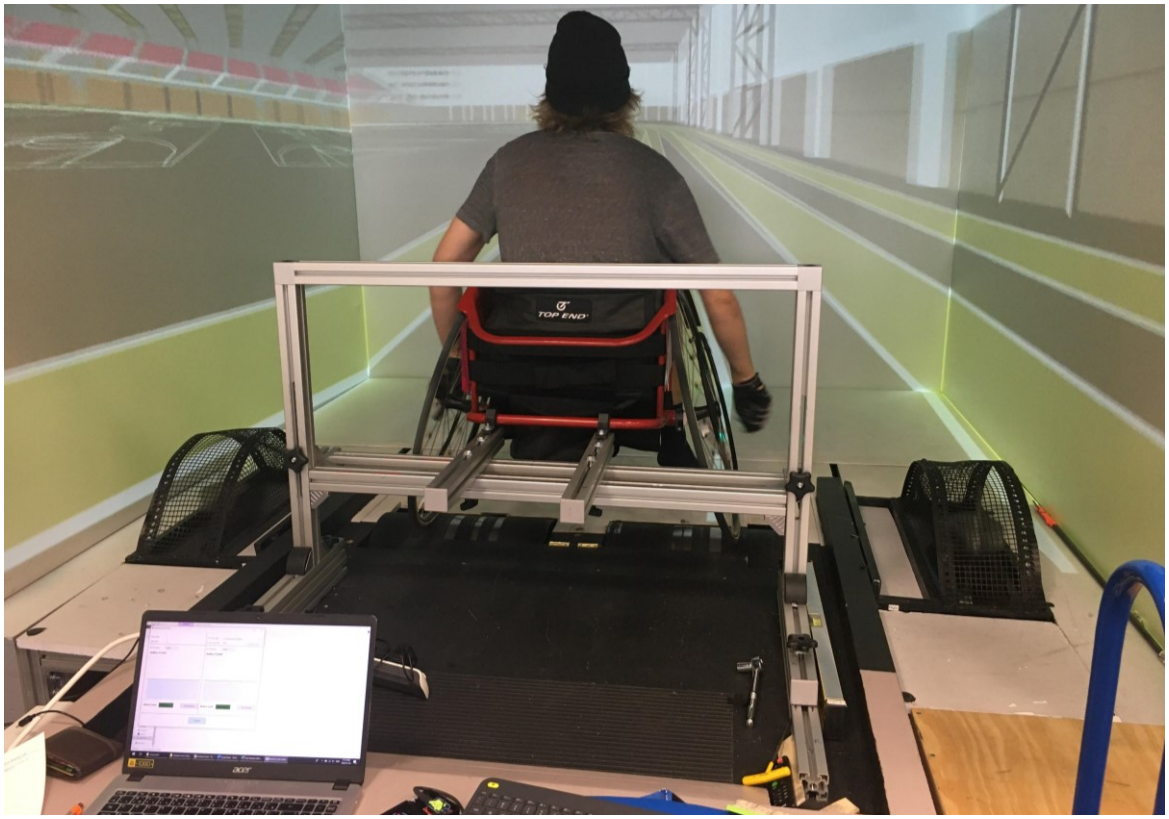

Figure 9. The Rehabilitation Robotics Laboratory's wheelchair ergometer, wheelchair bracing system, and EON ICube virtual reality system (Salimi & Ferguson-Pell, 2013). This photo also shows the ergometer being used in one of this study's test sessions. The computer with Redliner is running in the lower left corner of the frame

The wheelchair ergometer system used in this study replicated that used in studies on wheelchair biomechanics at the University of Pittsburgh and University College London (UK) (Shimada et Al., 1995; Hills, 2011). One of the benefits of this is that the inertia and resistance are easily determined (DiGiovine et al., 2001). Thus, the results of our studies can be compared to other institution's results. The ergometer system in the RRL (University of Alberta, Edmonton, AB, Canada) has been in operation since 2012 (Qi et al., 2014; Salimi & Ferguson-Pell., 2012) and has been previously validated for dynamics measurements using video analysis by Naicker, G in 2017.

2.5 Real-World Dynamics Measurement Devices

Naicker (2017) validated Redliner using the SMART^{wheel} (Cowan et al., 2008) and the RRL's wheelchair ergometer (Salimi, 2017). Redliner is a lightweight non-contacting battery-powered activity monitor that can be attached to the spokes of a manual wheelchairs user's wheels (Salimi & Ferguson-Pell, 2012). The device has two accelerometers, one near the axle of the wheel and the other near the hand rim, which continuously collect the angular acceleration of the wheels (Figure 10). A microcontroller onboard collects and records the data from both accelerometers continuously and records a timestamp for each reading. The data is saved to a microSD card as a CSV file and analyzed as outlined in Section 4.1.2.

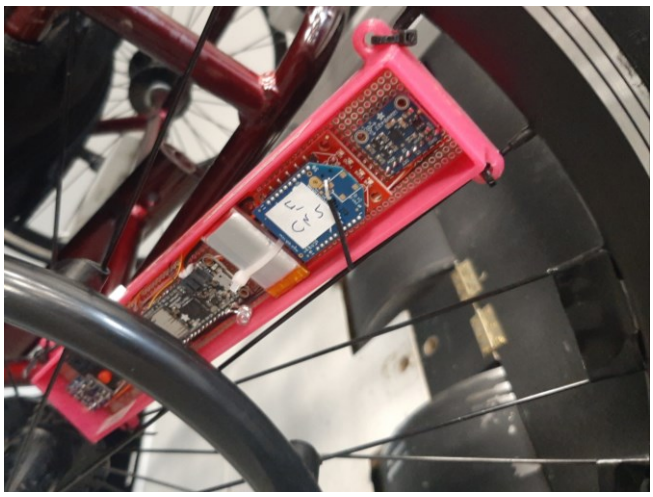

Figure 10. A picture of Redliner mounted on the wheel of a manual wheelchair. The accelerometers are shown at either end and the black microcontroller sits in the middle of the device next to the battery.

The SMART^{wheel} (Cowan et al., 2008) is a measurement device that attaches to most manual wheelchairs and communicates with a computer via Wi-Fi to collect and display propulsion information. The SMART^{wheel} measures three-dimensional forces (tangential, radial, and axial) and moments (N) applied to the push rim. It is a clinical and research tool that allows users to gather push force (N), stroke frequency (Hz), stroke length (m), distance traveled (m), and wheelchair velocity (m/s). The SMART^{wheel} is an entire new wheel that replaces the existing wheel on a manual wheelchair (Figure 11). It uses three strain gauges to collect the deflection of the push rim during propulsion and then uses those deflection values to calculate the force imparted to the push rim. Within the main body of the SMART^{wheel} are various accelerometers that track the kinematic movement of the wheel.

Figure 11. A photo of the SMART^{wheel} designed by Cowan et al. (2008) mounted on the RRL's Quickie four-wheeled manual wheelchair.

3. Study Design

This study was a confirmatory research, longitudinal study with a mixture of paired measurements and descriptive questionnaire data. Randomizing the test environment for the first test session was considered. However, no learning effect should exist as the study demographic did not know how to propel a racing wheelchair. Additionally, to comment on how realistically the VR environment represented the RW, the participants needed to complete the RW trial prior to the VR trial. Thus, the participants were not randomly assigned to their first test environment.

3.1 Participant Recruitment

Recruitment for the study was based on who was available and willing to be a part of the study. The wheelchair racing community in Alberta is very small, with only about 5 – 10 amateur-level racers present in the Edmonton area. Given the fact that all of these individuals may not be willing or able to partake in the study, a cohort of individuals who are not full-time manual wheelchair users was recruited for this pilot study.

3.1.1 Inclusion Criteria

Only healthy and physically active non-disabled individuals were selected, with the knowledge that experience-related differences exist in over-ground manual wheelchair propulsion (Symonds et al., 2016). Participants were allowed to partake if they were 18 – 50 years old. Participants actually recruited for the study were 20 – 24 years old. The study recruitment was a convenience sample by word of mouth.

3.1.2 Exclusion Criteria

For their safety, the following excluded a potential participant:

- history of abuse of alcohol and/or controlled substances,
- uncontrolled exercise-induced asthma,
- heart condition or high blood pressure,
- chest pain at rest or during physical activity,
- obesity (BMI > 30),
- musculoskeletal injury or pain in the upper extremities,
- a bone or joint problem that could be made worse by intense physical activity,
- severe motion sickness,

- vestibular condition,
- concussion, and/or
- visual impairment.

3.2 Sample Size

A comparison of means was used to calculate sample size: $\frac{(u + v)^2.(\sigma_1^2 + \sigma_0^2)}{(\mu_1 - \mu_0)^2}$

Figure 12 shows the results of the power analysis using data from the literature. It suggested that the sample size be 10 subjects for heart rate measurements and 15 subjects for sEMG measurements. A power analysis of the pilot study data showed that an average of 15 participants would be needed to compare the two test environments for dynamic measures while 26 would be needed for metabolic measures in future studies.

Heart Rate: **= 9.7 subjects**
% VO_{2peak}: **= 55.1 subjects**
sEMG: **= 14.6 subjects**

Pilot Study:
Dynamic Measures: **= 14.5 subjects**
Metabolic Measures: **= 26.0 subjects**

Figure 12. Power analysis results. See Appendix A for calculations.

Given the Central Limit Theorem and assumptions of normality, a sample size of 20 is typically suggested in research studies. Using this rule of thumb and the above power analysis while also understanding that metabolic data will not be used in this study, a sample size of **15 subjects** was proposed before the study started.

3.3 Predicted Variables to Be Studied

The independent variable (IV) in this study was the test environment, RW or VR environment. The predicted variables that could be studied from Redliner and the wheelchair ergometer were ratio and were cadence (pushes/min), power (W/s), energy (J), applied and resistive force (N), velocity (m/s), acceleration (m/s^2), distance (m), and time (s). The aggregated score from each questionnaire becomes the dependent variable for each paired t-test or paired samples test.

The next sentences are about the remaining seven biomechanical factors that need to be similar between the two environments, as reported by Salimi et al. (2018). Rotational inertial effects were considered to be minimal in this mostly straight-line propulsion experiment. Straight-line inertia was compensated for in this study using an inertial weight compensator device attached to the ergometer rollers (Figure 13). Due to time constraints, trunk swing and energy consumption could not be measured between the two environments. However, for racing wheelchair users the technique of propulsion involves much less trunk swing than traditional wheelchair propulsion as the participants lean forward throughout the propulsion cycle. In the future, trunk movement can be assessed using an inertial measurement unit, in the RW, and motion capture technology, in both environments, as done by Salimi and Ferguson-Pell (2013). This will also demonstrate the feasibility of using motion capture in VR. Additionally, energy consumption between the two environments could be compared using the mechanical work done: $Energy\ Consumption = Force\ (N)\ \times distance\ (m)$.

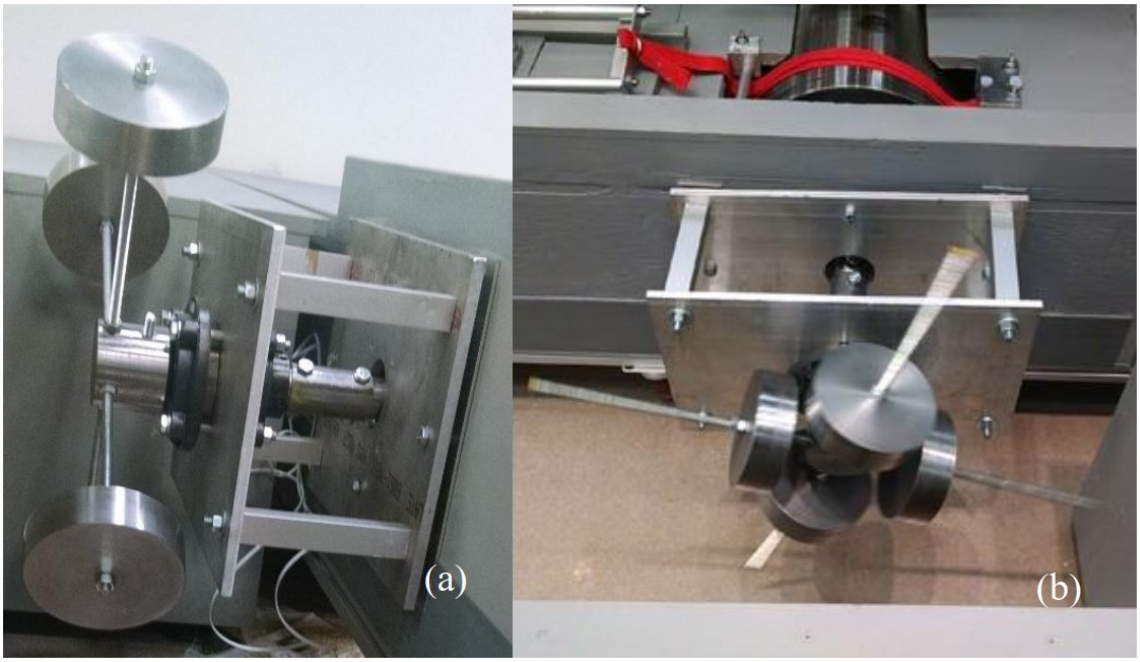

Figure 13. The inertia system developed for straight line propulsion showing the inertia system adjusted to two different weight settings (18.8cm [a] and 3.0cm [b]).

3.4 Ethics

Ethics approval was received in January of 2018 for this study. It included updates to study forms and the possibility of using motion capture and the inertial measurement unit (Appendix B). It added that participants would undergo fitness and performance testing, which might have caused minor physical stress, fatigue, musculoskeletal related injuries. The potential risk to the participant was no greater than what would be experienced by an individual while undertaking regular exercise, due to the planned acclimating session. The participant might have developed blisters if they pushed too intensely, but gloves were provided to minimize this risk. If at any point the participant exhibited discomfort, they were asked if they wished to continue. If they did not want to proceed, the facilitator immediately ceased testing. If appropriate, a facilitator would check their blood pressure and heart rate to ensure they were within safe parameters. If a participant would have been injured, they would have been accompanied to the appropriate health services for evaluation and treatment.

Participants all gave prior consent to be a part of the study and their names were never associated with their data. After measurements were recorded, data was downloaded onto an RRL computer and assigned a random number. Only the anonymized number was used to identify the individual from that point forward. Names and personal information are stored separately from the data. Study information will be kept for five years on a secure computer or in a locked cabinet in the RRL and then destroyed.

3.5 Hypotheses

The overall goal of this research study was to characterize push style dynamics during racing wheelchair propulsion. The following primary hypotheses was tested:

Ho 1: There is no observable difference in the dynamics mechanics experienced when a participant propels their racing wheelchair in virtual reality and the real-world.

The primary hypotheses were tested in two environments as part of a continued effort to validate the VR environment. Therefore, measures of presence in VR, as well as perceived exertion and shoulder pain, were tested. The following secondary hypotheses were tested

Ho 2: There is no observable difference in the participant's perceived experience when a participant propels their racing wheelchair in virtual reality and the real-world.

Ho 2.1: Using an established methodology, no difference is detected in perceived presence while completing an exercise test in the two environments.

Ho 2.2: Using an established methodology, no difference is detected in perceived exertion while completing an exercise test in the two environments.

Ho 2.3: Using an established methodology, no difference is detected in perceived shoulder pain while completing an exercise test in the two environments.

4. Materials & Methods

This chapter outlines the tools of measurement used in the study, study experimental procedure, calibration of the various study measurement tools, considerations for wheelchair propulsion in racing wheelchairs in VR, and initial method used to calibrate the ergometer rollers when they were coupled for racing wheelchair propulsion.

4.1 Explanation of Measurement Tools

In this study, a wheelchair ergometer, RW dynamics measurement device, VR immersion system, and five questionnaires were used to assess dynamic measures and perceived experience between the two test environments.

4.1.1 RRL Wheelchair Ergometer

The wheelchair ergometer used in this study is comprised of two rollers, which have inertial characteristics matched to those encountered when propelling a wheelchair in the RW. Two magnetic brakes are available to adjust the RR of the ergometer in real-time and also to simulate the resistance associated with rotational inertia. For a participant to turn the ergometer, the wheel furthest from the center of rotation is rotated at a greater speed than the opposing wheel, causing the chair to travel in an arc. In a RW situation, the participant would feel a slight resistance to rotation due to the forces required to accelerate their mass about the center of rotation. This resistance can be equated to the rotational moment of inertia of the combined mass of the wheelchair and participant. Applying a variable torque to the shaft of each roller provides mechanical feedback to the participant equal to the rotational resistance, simulating that of the RW. The wheelchair brace system ensures that the wheelchair is safely secured during testing and in an accurate location on the rollers throughout the test. These systems have been inspected by the University of Alberta Hospital Clinical Engineers and meet electrical safety requirements.

It is helpful going forward to have a good understanding of the interaction of systems and data routing used for the VR immersion system and wheelchair ergometer system. Figure 14 outlines the pathway of data processing beginning with the rollers inside the VR immersion system, the EON ICube, and their corresponding encoder, to the Teensy and MFP-c5 computer

on the desktop, onto the *ConsoleErgometerRacing* program on the MFP-c5 computer, and ending with either LabVIEW and the magnetic braking system or the two EON-hosting servers. The program on the Teensy counts the number of times the encoders each rotate and then sends this data to the *ConsoleErgometerRacing* program (Figure 13). If the linear velocity is to be modified, it is modified in the *ConsoleErgometerRacing* program in Microsoft Visual Studio. The custom LabVIEW program records the ergometer velocity, acceleration, and time in a CSV file and displays this data graphically to the system technician in real-time (Figure 13). The magnetic brakes identified in Figure 13 were not found to be necessary for this study, as explained later. The track compensator indicator device and the remote dial will be explained in Section 4.4 to outline how they affect the EON ICube projection and roller velocity through the *ConsoleErgometerRacing* program.

The custom LabVIEW program built by Dr. Zohreh Salimi and Mr. Matthew McKenzie previously (Figure 15) was modified to accommodate the National Instruments BNC-2100 and USB-6212 devices. These two devices allow a voltage to be applied to the rollers to brake them magnetically. The National Instruments BNC-2110 and USB-6212 wire directly into the computer instead of communicating over an Ethernet connection. As a result, the communication rate between the rollers and the computer, or time interval, is a consistent 0.02 sec. While adding the two devices, it became necessary to initiate two analog out channels in the second frame structure for use in the For Loop as this is the protocol for wiring in LabVIEW with the BNC-2110. These two analog out channels are used to apply the variable voltage to the two rollers separately. Once this was completed, two more variables were added to the Ergometer.vi (Figure 16, red circle) so that the Dial Value and Track Compensator Value could be written to the CSV file as well (Figure 17). These variables are used later in the thesis to examine steering accuracy in the VR environment. While completing this work, it was discovered that velocity was being written to the spreadsheet in m/s and not in rad/s, as was stated in the excel sheet, and this mistake was corrected.

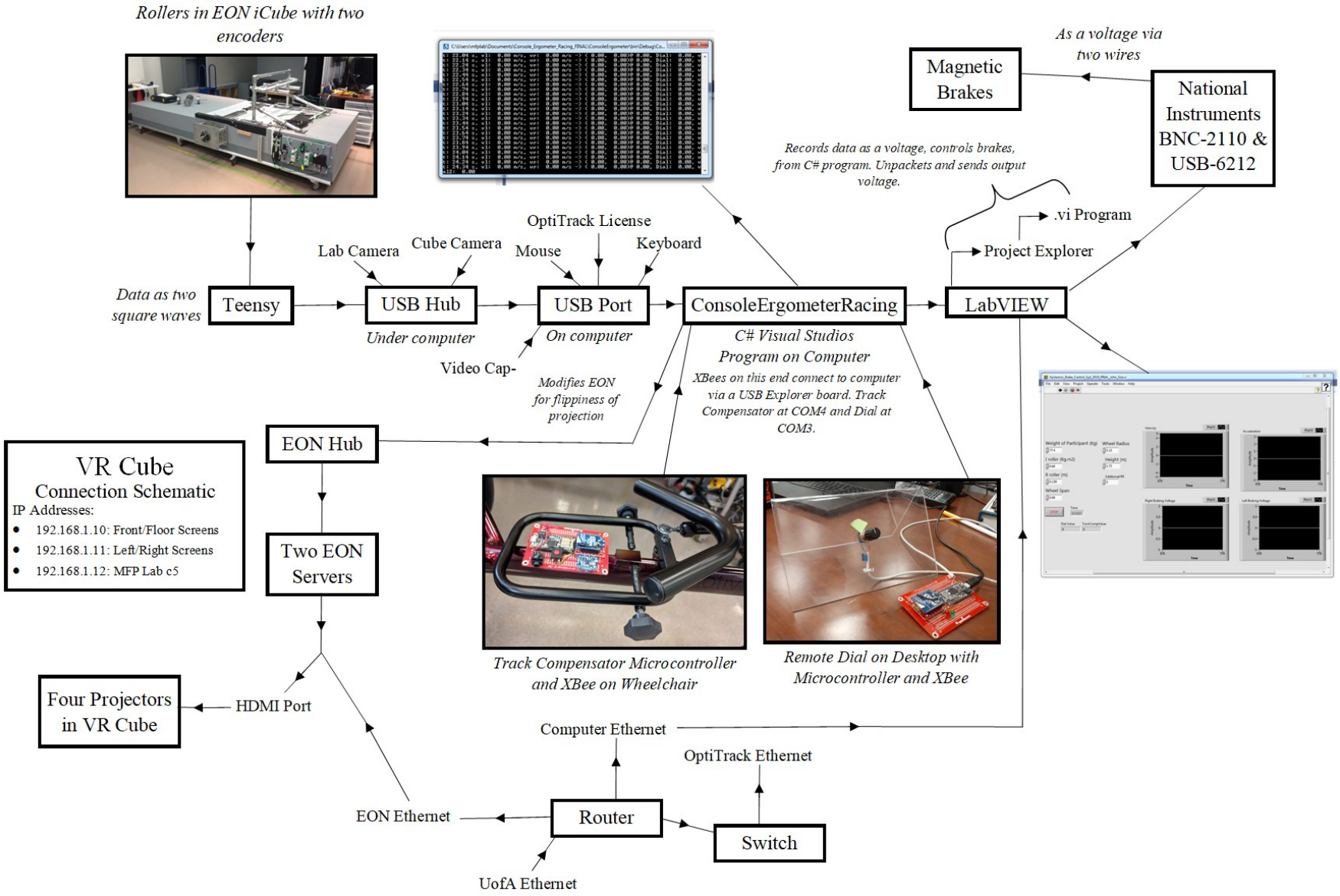

Figure 14. Schematic of current wheelchair ergometer and EON ICube set up. The IP addresses for each of the Ethernet connections are also displayed. Also shows the operating custom LabVIEW program (top black box) and custom *ConsoleErgometerRacing* program (right grey dialogue box) during a test session.

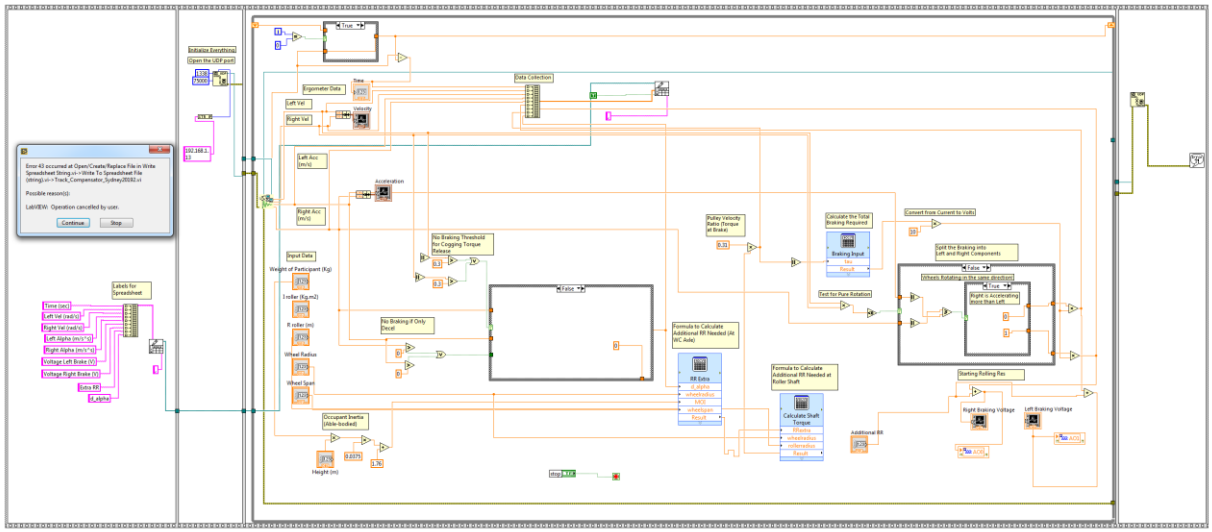

Figure 15. Original LabVIEW program which stopped working when we switched to the National Instruments BNC-2110 and USB-621 modules.

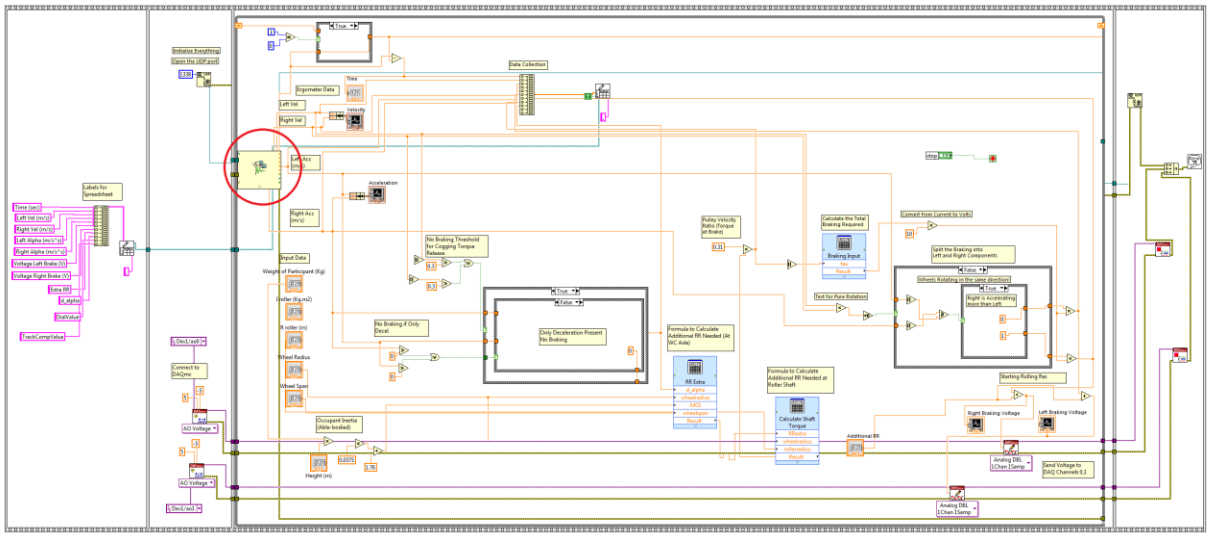

Figure 16. Updated LabVIEW program to include the separate analog out channels.

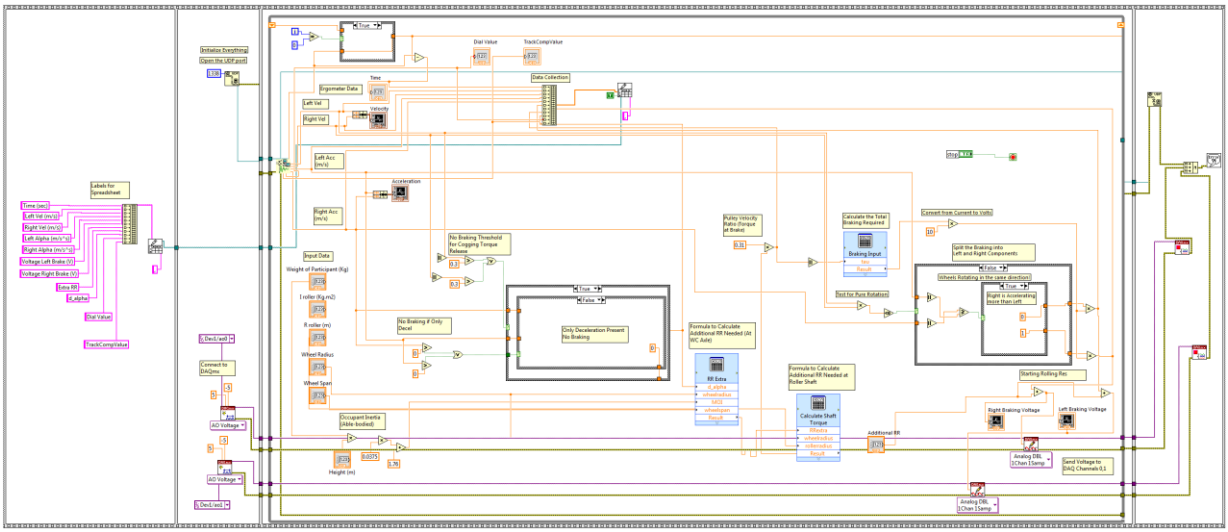

Figure 17. The current LabVIEW wiring structure.

The LabVIEW program converts the Teensy signal from the two encoders that interface with the two rollers into linear velocity (m/s) and acceleration (m/s^2). It also records the elapsed time (s) and can apply an output voltage to the magnetic brakes to slow them or replicate the RR of a different environment. Time and current velocity are direct outputs from the ergometer. The velocity can be averaged throughout the test to get average velocity in a session, as long as the technician ensures the participant does not stop and trims the start/end times. Using the wheelchair ergometer data, the distance traveled is gathered by integrating the velocity and summing it throughout the session (Figure 18).

$$Distance\ Traveled\ in\ the\ First\ Row\ of\ Movement\ (m) = \left[\ v_{current} \times \left(t_f - t_{f-1}\right)\right]$$
$$= 0.001 m/s \times (3.94s - 3.92s) = 2 \times\ 10^{-6} m$$
$$Total\ Distance\ Tracveled\ (m) = \sum_{t_1}^{t_n} \int\ v_{current} dt$$

*Summed across each row throughout the entire test.

Figure 18. Calculating the total distance traveled from the ergometer velocity data.

4.1.2 Redliner Device

Average and peak velocity (m/s) and acceleration (m/s^2), as well as distance traveled (m), were collected using Redliner (University of Alberta, Edmonton, Canada). Using angular acceleration gathered by Redliner, linear velocity and acceleration of the wheelchair, and thus the participant, as well as distance traveled can be calculated. The distance is calculated by integrating velocity while the acceleration is calculated by differentiating velocity. All data gathered using Redliner is time stamped so that it can be synchronized with the other measures. Redliner is more likely to accumulate sensor error than the wheelchair ergometer because of this integration and differentiation.

The angular velocity, or omega, (rad/s) was calculated for this study as in Figure 19. The change in the X accelerometer was found by subtracting the top accelerometer X value from the bottom accelerometer X value for each moment in time for each Redliner. Change in X was divided by the distance between the two sensors and square rooted to get omega. Omega was smoothed using a second-order Butterworth low pass filter cut off at 1Hz. Omega smoothed was multiplied by 0.33 meters, the radius of the racing wheelchair, to get the linear

velocity (m/s) at any moment. This was completed with a custom MATLAB program (Appendix C).

$$\Delta X\ Accelerometer = abs(Top\ X - Bot\ X)$$

$$Omega\ (rad/s) = \sqrt{\frac{\Delta X}{sensor\ distance}}$$

*Sensor distance was 0.184 m for each Redliner.

$$Linear\ Velocity\ (m/s) = OmegaSmooth\ \times Wheel\ Radius$$

* use a 2nd order Butterworth low pass filter cut off 1Hz to create *OmegaSmooth*

Figure 19. Calculations used to find the linear velocity of the wheelchair using Redliner.

Redliner data can also be used to calculate distance traveled by integrating the linear velocity and acceleration by differentiating the smooth velocity trace outlined in Figure 19. These calculations are outlined in Figure 20.

$$Distance = abs(Linear\ Velocity \times dt) = abs(Linear\ Velocity\ \times Time\ Interval)$$

$$Alpha\ (rad/s^2) = \frac{OmegaSmooth\ (rad/s)_n - OmegaSmooth\ (rad/s)_{n-1}}{Time\ Interval\ (s)}$$

$$Linear\ Acceleration\ (m/s^2) = AlphaSmooth\ \times wheelchair\ Radius\ (m)$$

* use a 2nd order Butterworth low pass filter cut off 1Hz to create *AlphaSmooth*

Figure 20. Calculations to compute distance traveled and linear acceleration using Redliner accelerometer data.

4.1.3 EON ICube

This study used the EON ICube Mobile VR immersion system to simulate the RW environment in the RRL. The EON ICube projects a VR environment onto four screens, one on the floor and three surrounding the participant (Figure 9). In this system, the participant can see their body and wheelchair, which should increase their sense of presence. This system provides a visual representation akin to the RW conditions. The VR simulations are run on the two servers next to the MFP-c5 computer (Figure 14). The servers are used to open the EON Viewer program in order to project the Universiade Pavilion simulation onto the four projection screens.

The *ConsoleErgometerRacing* program can modify the linear velocity received from LabVIEW and is responsible for sending this velocity data to the two EON servers. The RW

speed of the two moving rollers leads to changes in the EON ICube visual simulation according to how fast the rollers are moving and in what ratio to each other. If the speed is larger, the simulation moves faster and further. If the ratio between the two rollers is the same, the individual will travel straight. If one roller moves more quickly than the other, the simulation will turn away from the faster moving roller.

4.1.4 Perceived Presence - Questionnaires [IPQ/MSAQ]

Perceived presence in VR is vital for the accurate simulation of the RW. It must be continually improved and validated if it is to be used to assist those with mobility challenges. Data gathered from the Igroup Presence Questionnaire (IPQ) and Motion Sickness Assessment Questionnaire (MSAQ) was used to evaluate presence. Improving the VR immersion system through quantitative and qualitative feedback on perceived presence should lead to more conclusive experimental results.

An IPQ was one of the metrics used to test the sense of presence in VR (Schubert & Regenbrecht, 2002) (Appendix D). The IPQ is made up of 4 subcategories asked in 14 questions: INVolvement (INV), Experienced Realism (ER), Spatial Presence (SP), and General (G). In addition to the original 14 questions, three more questions were added to the IPQ to specifically ask the participants their views on the similarities and differences between the RW and VR environment. The IPQ was collected after the VR test session.

A MSAQ was also used and it measured Visually Induced Motion Sickness (VIMS), as performed previously in the RRL (Appendix E; Salimi, 2017; Gianaros et al., 2001). VIMS is a nauseating experience that can throw off the VR users' sense of presence and adversely affect how they perform in VR. VIMS may come on rapidly during a VR session and persist for hours or even days after the VR experience, which may have negative consequences when the user returns to normal activities. The MSAQ consists of 16 questions in 4 subcategories (5 scores): Total (T), Gastrointestinal (GI), Central (C), Peripheral (P), and Sopite-Related (S). As per previous work, the MSAQ scale was changed to a scale of 0 to 9 instead of 1 to 9 to create a maximum score of 100 for the test. Training sessions were thought to be critical during the study in order to reduce VIMS. Salimi (2017) found that four acclimatization sessions reduced T, GI, and C VIMS significantly in maneuverability tasks. The MSAQ was asked after each test session in each test environment.

4.1.5 Perceived Exertion - Borg's Rating of Perceived Exertion

Borg's Rating of Perceived Exertion (RPE) is widely used in sports physiology to monitor performance and technique (Borg, 1998). The Borg Scale used in this study is included in Appendix F.

RPE provided quantitative insight into the participant's view on their propulsion and the validity of the VR environment. Any failures in the functionality of the system, such as improper RR, may be realized through a participant's RPE. Reliable training on how to report RPE was critical during the study but it may also impact the participant in their day-to-day life. Perhaps future studies may look at training a MWU to gauge an event that might stress their shoulders using RPE.

Perceived exertion was measured using the 15-point Borg RPE Scale. Even though RPE is a subjective measure, it can provide an interesting look into perceived heart, respiration, breathing, and sweating rates as well as muscle fatigue (Qi et al., 2015). RPE was taken at 750-meters, 1500-meters, and 5-minutes post-test. Participants were asked to score their perceived exertion on the 6-20 scale for their Shoulders, Center, and Overall. Central RPE refers more to cardiovascular effort, while overall RPE couples shoulder muscle fatigue and cardiovascular fatigue.

4.1.6 Perceived Shoulder Pain - Wheelchair User's Shoulder Pain Index [WUSPI] & Visual Analog Scale [VAS] for Pain

The Wheelchair User's Shoulder Pain Index (WUSPI) (Curtis et al., 1995a) is a questionnaire that was designed to measure shoulder pain in MWUs (Appendix G). The RRL has used this index many times before and it was also used in the pilot study for this study. The 15-item functional index assesses shoulder pain in the functional activities of MWUs. It has excellent test-retest reliability and internal consistency (Curtis et al., 1995b). The WUSPI was used to understand shoulder pain in the daily activities of the participants. It was collected after each test sessions in each test environment.

A Visual Analog Scale (VAS) measured change in pain before and after the test session and was also compared between the two environments (Appendix H). The VAS consists of a

straight line with endpoints for the extreme limits such as ‘no pain at all’ and ‘pain as bad as it could be’ (Haefeli & Elfering, 2006). The participant marked along the line their current pain level between the two end points. This data was collected pretest and post-test in both test environments.

4.2 Experimental Protocol

Each participant underwent two trials, one test on the Butterdome/Universiade Pavilion indoor track at the University of Alberta (RW test) and one test in the RRL on the wheelchair ergometer (VR test). The participant’s performance was measured with a wheelchair ergometer, in the VR environment, and a wheelchair-attachable activity monitor, in both environments. The wheelchair ergometer allows the self-regulation of exercise intensity and continuous measurement of acceleration, velocity, and distance traveled. The wheelchair ergometer was set up inside the EON ICube Mobile VR immersion system in the RRL within the Edmonton Clinic Health Academy (ECHA). Each participant propelled their wheelchair at a self-selected speed for 1500 meters. They were not taught a specific propulsion style to use throughout the race but employed whichever style was most comfortable for them. This push style was not recorded but participants were monitored throughout the test to ensure they were propelling safely. The participants completed at least one practice lap in each environment, were taught to wheelie in the RW environment, and rested for 5 minutes after the practice lap before starting each test.

Before starting the exercise tests, participants received an orientation on how to report and answer questions relating to their RPE, IPQ, MSAQ, and WUSPI. During the 1500-meter race, three recordings of RPE were taken, once at 750 meters, once at 1500 meters, and once 5 minutes post-test. At each interval, participants were asked to score their RPE for their shoulders specifically, center specifically, and overall RPE. IPQ, WUSPI, and MSAQ were collected at the end of each test only, with IPQ only being collected after the VR test session. VAS was collected before and after each test.

4.2.1 Real World: Butterdome/Universiade Pavilion and Lab (~1 hour)

The participant was taken to the RRL, gave informed consent to be a part of the study, and introduced to the VR environment. They were instructed to move in VR to acclimatize to the environment for one lap or approximately 5 minutes. They were then taken to the Butterdome/Universiade Pavilion and asked to complete a 1500-meter race, about six laps, on the running track in lane 5. The participant was given time to practice pushing the wheelchair around the track before the test session. Their wheelchair had Redliner on it and they propelled at their own set pace. They filled out a RPE questionnaire during testing, a WUSPI and MSAQ questionnaires after the testing, and a VAS questionnaire before and after testing.

4.2.2 Virtual Reality: Rehab Robotics Lab (~1 hour)

After the RW test session, the participant was brought back to the RRL to complete the VR test session. The time between the RW test and the VR test was anywhere from 30 to 50 minutes. However, four participants came back a different day to do their VR test due to technical failures with the VR system which prevented the participants from completing both sessions in the same day. The four participants who came back a different day came back anywhere from 2 – 7 days later. The VR test was conducted exactly like the RW test but was instead done in VR in the RRL. All the equipment used in the RW was used in VR. The individual filled out a RPE during testing, a IPQ, WUSPI, and MSAQ, after testing, and VAS before and after testing.

4.2.3 Statistical Analysis

IBM Statistical Package for the Social Sciences version 25 (SPSS, Chicago, IL, USA) was used to examine the data from this study. The quantification of the observed differences between the two test environments used parametric and nonparametric statistics as the data required. Since there is no literature on standard deviation in VR, it was assumed that the standard deviations in the two environments are the same.

The primary means of comparing the two test environments was a paired t-test. Vanlandewijck et al. (2001) suggest that each individual be their own control as it reduces error due to between-subjects variation. Before the paired t-tests were completed on any variable, SPSS boxplots were used to check for significant outliers visually and the Shapiro-Wilk test of normality was used to check for significant differences. If these conditions were

met, a paired t-test was done. If outliers were present in the dataset and the Shapiro-Wilk test of normality was significant, a paired-samples sign test was done instead as the distribution of differences between paired observations was not symmetrical. The questionnaires in this study all provide data that is meaningful when the scores are aggregated for each statistical test.

4.3 Calibration

Before the experiment outlined above was completed, a calibration of the wheelchair ergometer was done to ensure the distance traveled, velocity, movement in the 3D simulation, and RR were correct.

4.3.1 Roller Correction Factor

The velocity of the rollers, as reported by LabVIEW, was examined experimentally to determine if it was correct. The manual racing wheelchair was videotaped while being propelled by a lab member on the rollers while also collecting the data coming out of the rollers via LabVIEW. The rollers were timed for how long it took to complete ten roller rotations on the video once the rollers reached a constant speed. This equated to 10 meters of distance traveled by the wheelchair as the circumference of the roller is ~1 meter. This distance of 10 meters was then divided from the ergometer distance.

This revealed that LabVIEW and the video recording were not presenting the rollers moving at the same speed as the ergometer distance traveled was 15.8 meters instead of 10 meters. Thus, there was a problem to fix and it was the result of an incorrect correction factor being applied to the roller's linear velocity in the *ConsoleErgometerRacing* program. It was decided that it would be better to experimentally determine a new correction factor while using a powered wheelchair instead of a manual wheelchair. This way the speed of the rollers would be constant, which would allow simple calculations to find velocity and distance traveled over time in order to calculate the new correction factors. The non-constant speed of the manual racing wheelchair meant that velocity over time was not constant and couldn't be directly translated into distance traveled.

With the powered wheelchair, the constant speed meant that ten rotations of the roller by the powered wheelchair was ~10 meters of travel, as the circumference of the rollers is ~ 1 meter. The calculations for finding the first two new correction factors are shown in Figure 21.

The initial correction factor present in the original *ConsoleErgometer* program, which the *ConsoleErgometerRacing* program was built off of, was 0.195 m/rev and resulted in 15.8 meters of travel instead of 10 meters of travel. Once a new correction factor was found for a trial, this new corrector factor was inputted into the *ConsoleErgometerRacing* program and a new test was done with ten more rotations of the rollers. Five testing sessions were completed and the results from all tests are shown in Appendix I. After five test sessions, the correction factors in Table 1 were gathered. These factors ensure that propelling on the rollers with them uncoupled did result in equal distances traveled by both rollers and straight-line propulsion in the VR environment.

$$Offset\ Ratio = \frac{Ergometer\ Distance\ (m)}{Video\ Distance\ (m)} = \frac{15.8\ m}{10\ m} = 1.58$$

$$First\ Correction = \frac{Inital\ Correction\ (\frac{m}{rev})}{Offset\ Ratio} = \frac{0.195\ (\frac{m}{rev})}{1.58} = 0.1234\ (\frac{m}{rev})$$

$$Trial\ Two\ Left\ Offset = \frac{Ergometer\ Distance\ (m)}{Video\ Distance\ (m)} = \frac{12.13689\ m}{10\ m} = 1.213689$$

$$Second\ Left\ Correction = \frac{First\ Correction\ (\frac{m}{rev})}{Trial\ Two\ Left\ Offset} = \frac{0.1234(\frac{m}{rev})}{1.213689} = 0.1017(\frac{m}{rev})$$

$$Trial\ Two\ Right\ Offset = \frac{Ergometer\ Distance\ (m)}{Video\ Distance\ (m)} = \frac{12.40143\ m}{10\ m} = 1.240143$$

$$Second\ Right\ Correction = \frac{First\ Correction\ (\frac{m}{rev})}{Trial\ Two\ Left\ Offset} = \frac{1.234(\frac{m}{rev})}{1.240143} = 0.0995(\frac{m}{rev})$$

Figure 21. First two calculations of the new correction factor. Each wheel of the wheelchair had its own correction factor as the left roller was found to usually take longer to slow down.

Table 1. The new experimentally determined correction factors for the *ConsoleErgometer Racing* program.

Left Correction Factor (m/rev)	Right Correction Factor (m/rev)
0.0948424803	0.0939070754

As explained later in this section, the racing wheelchair required that the rollers be coupled together and move in sync. After the above experiment, the rollers were coupled, but sometimes the correction factors would no longer keep the wheelchair moving straight in the simulated environment. It was suspected that this occurred if the encoders were jostled or if the wheelchair was held on top of the rollers in a slightly different position. Once the

wheelchair was checked to ensure that it was in the correct position, the Right Correction Factor could be adjusted. It was found to be faster to experimentally determine the correct value to set the correction factor by varying the Right Correction Factor. An individual was asked to push the wheelchair down the first straight away and try to reach the first curve, about 60 meters away, before they started to veer. If they veered to the right, the right correction factor was increased. If they veered to the left, the right correction factor was decreased. This is the best way to adjust the correction factor going forward but only one side can be adjusted to anchor the correction factors in experimental certainty. If the Left Correction Factor is kept the same, the findings from the ten rotations test hold and ensure that ten roller rotations are equal to about 10 meters of travel. When these correction factors are not correct, it is visually apparent if the rollers are also coupled. When the correction factors are wrong, the coupled wheelchair propulsion causes the wheelchair to veer to the left or right in the simulation when it should always be moving straight forward.

4.3.2 Roller Velocity Comparison

These correction factors were inputted into the *ConsoleErgometerRacing* program and three tests at three different speeds were completed. These tests were used to compare the velocity of the ergometer (m/s) and the velocity as shown on the video recording of the test session (m/s) (Figure 22 and Appendix J). When forced through 0, the relationship is almost 1:1. A paired t-test was completed, but before it was SPSS boxplots were used to check for significant outliers visually and none were found. Additionally, the Shapiro-Wilk test of normality found no significant differences between the samples. The ergometer velocity (M = 0.49 m/s, SD = 0.11 m/s) was not significantly different from the video velocity (M = 0.50 m/s, SD = 0.13 m/s), t(5) = -0.99, p = 0.37.

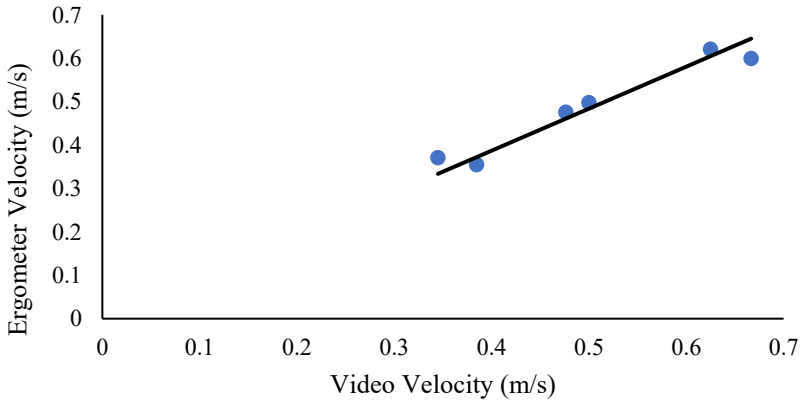

Figure 22. The velocity of the ergometer (m/s) plotted as a function of the video velocity (m/s). The equation of the line is 0.968x with an R^2 value of 0.927.

Along with the tests to confirm that the velocity of the rollers as shown by the ergometer program were correct, the *ConsoleErgometerRacing* program was run with different random wheelchair radiuses and different input weights. Both had no affect on the experienced velocity as shown by the *ConsoleErgometerRacing* program as an output. The weight of the individual and their height both become more important in maneuverability tasks as inertia is more influential and the magnetic brakes are employed. However, the magnetic brakes are not critical for straight-line propulsion, as in this study and outlined in Section 4.3.4. Also of note, the *ConsoleErgometer Racing* and the original *ConsoleErgometer*, used for the everyday four-wheeled wheelchair, programs both showed the same results.

4.3.3 Universiade Pavilion Distance

The Universiade Pavilion, or Butterdome, is a standard indoor 200 meter running track. From before the 60-meter start line to the end of the straight track is 83.5 meters (Figure 23). When measured with a tape measure, it was found to be 83.40 meters long for the same section. When Redliner on the racing wheelchair was used to measure the same RW section, it was 76.42 meters with the left Redliner and 75.96 meters with the right Redliner, or 76.19 meters overall. When Redliner on a regular four-wheeled wheelchair was used to measure the same RW section, it was 81.94 ± 0.89 meters with the left Redliner and 82.3 ± 0.65 meters with the right Redliner, or 82.09 ± 0.79 meters overall.

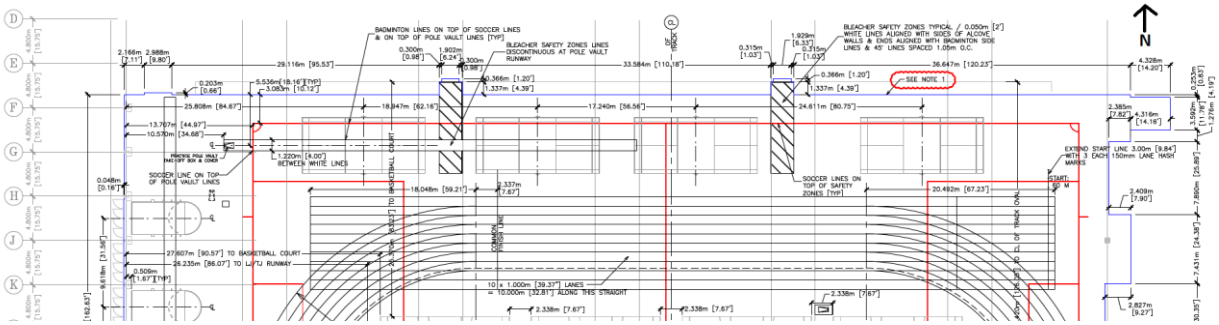

Figure 23. Diagram of the straight 80 m or 60 m running track in the Universiade Pavilion. The start line is on the right side of this image. A full-size version of the blueprint is available in Appendix K.

When the racing wheelchair was propelled in the VR environment after the ergometer was calibrated, the same section of track was 86.59 meters with the left Redliner and 85.2 meters with the right Redliner, or 85.90 meters overall. The EON simulation places the participant after the 60-meter start line on the track and from here the track is 80.35 meters

long. The wheelchair ergometer measured the distance traveled by the left roller to be 80.39 ± 0.60 meters and the right roller to be 80.28 ± 0.58 meters, an average of 80.29 ± 0.57 meters. Thus, both the VR and RW environments are about 80 meters on the straightaway.

In addition to confirming that the VR simulation is the correct size, these blueprints also ensure that any improvements made to the VR simulation will be accurate. For example, the straightaway lines on the North-west corner of the track in the VR simulation do not currently continue West as they do in the RW (Figure 23). This can now be fixed and along with any other noted discrepancies.

Next, it was determined how many laps the participant would need to complete to travel about 1500 meters in Lane 5. The EON simulation starts the racer off in Lane 5 in the VR environment. Additionally, beginning in Lane 5 in the RW is preferable because Lane 5 is always clear of obstructions, such as netting from the court separators. As per Table 2, the participants were asked to complete six laps beginning behind the 60-meter start-line. One lap is 42.51 meters + 42.51 meters + 71.97 meters + 71.97 meters + 20.492 meters = 249.46 meters. The two straightaways are 42.51 meters, the curves in Lane 5 are 71.97 meters, and the distance from the starting line to the beginning of the straightaway is 20.492 meters.

Table 2. Distance traveled with each lap in Lane 5 of the track.

	Distance Traveled with Addition of Start (m)
First Lap	249.46
Second Lap	478.43
Third Lap	707.40
Fourth Lap	936.36
Fifth Lap	1165.33
Sixth Lap	1434.47

4.3.4 Universiade Pavilion Rolling Resistance

To create a realistic simulation, the forces experienced by the participant in the VR environment must mimic those experienced in the RW. Thus, when simulating the Universiade Pavilion, the RR experienced by the racing wheelchair in the RW must be replicated. To do this, in the summer of 2019, Redliner was used to collect accelerometer data in the RW Universiade Pavilion for two consecutive pushes where, after the second push, the wheelchair was allowed to come to a complete stop on its own. This is called a rolldown test.

The velocity (m/s) as a function of time (s) was graphed for each wheel, or Redliner. After the two consecutive pushes and stop, the deceleration (m/s^2) of the wheelchair was determined by finding the slope of the line (Figure 24).

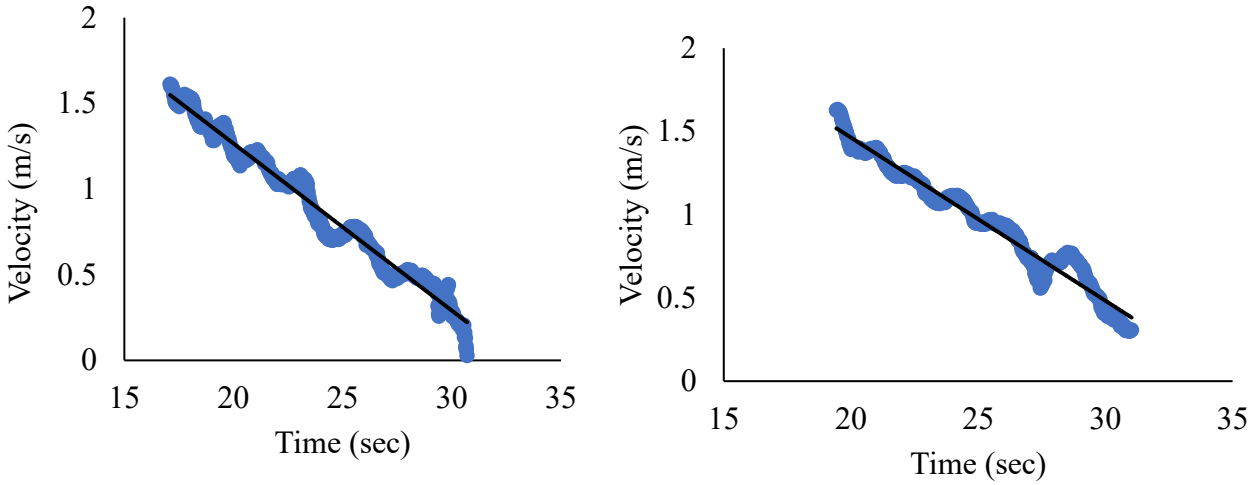

A. B.

Figure 24. Rolling resistance of the left wheel (A) and right wheel (B) in the RW for one trial. The equation of the line in A is y = -0.098 +3.22 and the R^2 value is 0.98. The equation of the line in B is y = -0.098x +3.42 and the R^2 value is 0.97.

The average RR for the RW for the left wheel was -0.094 m/s^2 and for the right wheel was -0.092 m/s^2 (Appendix L). The average RR for the RW is thus -0.093 m/s^2. The average RR for the VR environment for the left wheel was -0.18 m/s^2 and for the right wheel was -0.15 m/s^2 (Appendix L). The average RR for the VR environment is thus -0.16 m/s^2. When you work out the difference in RR between the two environments, -0.094 m/s^2 versus -0.16 m/s^2, it is minimal (Figure 25). A difference of 1.43 lbs of force more in the VR environment should not affect a participant's ability to propel.

$$Difference\ in\ RR\ B/w\ Worlds = (-0.1637) - (-0.0934) = -0.0703\ m/s^2$$

$$Force\ (N) = ma = -0.0703\ m/s^2 \times m_{participant+wheelchair}\ (90.3\ kg)$$
$$= -6.35N$$

$$-6.35N \times 0.224809\ lbs = -1.43\ lbs\ of\ Force$$

Figure 25. Calculations used for quantifying the difference in RR between the two environments.

Still, the VR RR is higher than the RW RR. Given this fact and that there is minimal turning in wheelchair racing, thus minimal rotational inertia, a voltage out to the rollers will not be applied to brake them magnetically. The manual ergometer braking control will be used

to apply a steady voltage of 0 V to both rollers' braking systems to ensure no current passes through them. The belt on the rollers will be removed to allow the rollers to roll move smoothly and stop a voltage from being applied to the rollers.

4.4 Racing Wheelchair Considerations in Virtual Reality

To mimic the straight-line propulsion experienced in the RW, the wheelchair must also be steered as it is in the RW, using a track compensator. To do this, the rollers of the wheelchair ergometer were coupled, to ensure straight-line wheelchair propulsion, and a digital indicator for the track compensator was built (Figure 26). This indicator digitally represents the activation and deactivation of the racing wheelchair's steering mechanism and interfaces with the VR simulation.

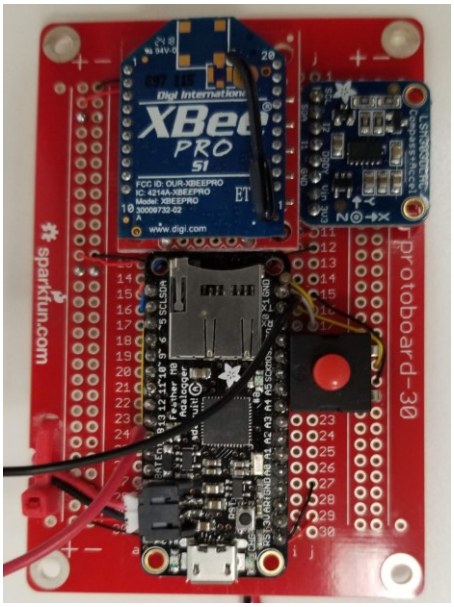

Figure 26. Track compensator indicator device with black microcontroller, blue XBee, and blue accelerometer + compass.

4.4.1 Digital Steering Devices

The track compensator indicator device sends the desktop computer a 360-degree heading in space, which the computer processes using the *ConsoleErgometerRacing* program to slow the apparent left roller velocity. Three different magnetic sensors were tried, but they appeared to be shielded by the building and/or the frame of the racing wheelchair. Any attempts at correcting the magnets by changing the origin of the sensor or recalibrating the magnets did not work. The sensor on the track compensator indicator device is a LSM303 Accelerometer + Compass Breakout unit from Adafruit. A remote desktop dial was also built so the VR simulation's technician can steer the wheelchair inside the EON ICube. This was written into the *ConsoleErgometerRacing* program so that both could be used at the same time. Both devices had XBees built into them so that the data could be streamed to the desktop computer in real-time. The XBees on the desktop computer side connect to the computer via a USB Explorer board. The track compensator indicator connects at COM4 and the dial at connects at COM3, this is written into the *ConsoleErgometerRacing* program (Figure 14).

The advantage to the remote desktop dial is that the technician for the EON ICube can assist the participating wheelchair user with steering when the track compensator indicator doesn't steer enough or when the wheelchair user over or understeers. In the RW when this happens, a MWU would wheelie or move their weight so that they can push harder on one wheelrim to correct and stay in their lane. This is currently not possible in the ICube and thus the remote desktop dial was required. The dial does not affect the roller velocity when set at "0", turns the wheelchair to the left when set at "1,2,3,4, or 5", and turns the wheelchair to the right when set at "-1 or -2".

When a wheelchair racing athlete propels around a curve on a track, the inside wheel travels less distance at a slightly slower speed than the right wheel. Once activated, the track compensator indicator had to be able to mimic this in VR. To do this, the difference in distance traveled in each lane was calculated (Table 3) and the *ConsoleErgometerRacing* program was modified to slow the left wheel velocity by this factor. The theoretically proposed value was 0.97; the left roller should appear to move at 0.97% of the right roller velocity.

Table 3. Table of the radius of the circle made by each wheel as the wheelchair user propels in each lane, the distance traveled by each wheel in each lane, and the ratio of each wheel's radius and distance to the other wheel.

Lane #	Left Wheel Radius of Circle (m)	Right Wheel Radius of Circle (m)	Distance Traveled Left (m)	Distance Traveled Right (m)	Ratio of Radius of Circle	Ratio of Distance Traveled
1.00	18.33	18.99	57.59	59.66	0.97	0.97
2.00	19.31	19.97	60.66	62.74	0.97	0.97
3.00	20.29	20.95	63.74	65.82	0.97	0.97
4.00	21.27	21.93	66.82	68.90	0.97	0.97
5.00	22.25	22.91	69.90	71.97	0.97	0.97
6.00	23.23	23.89	72.98	75.05	0.97	0.97
7.00	24.21	24.87	76.06	78.13	0.97	0.97
8.00	25.19	25.85	79.14	81.21	0.97	0.97

Upon start up, the track compensator indicator sends out an initial heading. The *ConsoleErgometerRacing* sets this value as a "0" and uses it to make the wheelchair travel straight in the VR environment. As the wheelchair user engages the track compensator more and more, by pushing on the track control device from the left (Figure 7), the heading value deviates more and more from the original value. The *ConsoleErgometerRacing* program reads this as a "1, 2, 3, 4, or 5" dependent on how large the deviation is. These values of "1, 2, 3, 4,

and 5" are matched to a left roller apparent velocity of "0.99%, 0.985%, 0.98%, 0.975% and 0.97%" of the right roller velocity (Appendix M), respectively. These velocities were experimentally confirmed to ensure that they would allow the wheelchair user to steer around the curve of lane 5 in a 200-meter track. The process outlined above instructs the EON simulation to turn to the left without physically having the left roller move at a slower velocity.

The ideal steering values for the track compensator indicator and the remote desktop dial were experimentally determined and found to work very well when participants engaged at the correct time. This correct time appeared to be at or near when a typical wheelchair racing athlete would engage or disengage. This can be confirmed in the coming months with an actual wheelchair racing athlete (Section 7.4). After a lap or two, many participants were able to engage the track compensator at the right time point going into and coming out of the curve such that they did not need any steering help from the technician. The correction ratio is not a constant 0.97 as theoretically thought and shown in Table 3. Instead, it is 0.99 to the left roller at "1", 0.985 to the left roller at "2", and so on, as shown in Appendix M.

The lines of code in Appendix M need to be modified if the track compensator indicator must be mounted underneath the track control device. The original code was written with the indicator sitting on top of the control device for use with the RRL's purple racing wheelchair. However, some larger participants do not fit in this smaller wheelchair and require a larger wheelchair. The larger red wheelchair used in this study, provided by the Para Athletics team at the Steadward Centre for Physical and Personal Achievement in Edmonton, only had room for the track compensator indicator to mount underneath the frame of the wheelchair. This required a few different lines of code to accommodate the track compensator indicator rotating through the opposite heading direction. Switching this code to the other version is a simple fix though and is outlined in Appendix M.

4.4.2 Increasing Device Performance

After the addition of the track compensator indicator device to assist with steering, the *ConsoleErgometerRacing* program would often crash. This was fixed by adding in a large buffer line of code. This issue came up again later in the study and was fixed by decreasing the baud rate from the track compensator indicator from 57600 bps to 38400 bps.

To decrease the experienced lag even further, the firmware was updated for the Redliners and track compensator indicator devices to make them process faster. As always, the devices set up their headers, give their battery voltage, and set up a loop. Previously, after each device had read all the values in the loop, it would print these items as data to the CSV file, close the loop and the CSV file, and then open them both again. This took extra time but meant that the data was constantly saved. Now, the CSV file is kept open all the time. A second button was installed, when pressed it closes the loop and the CSV file. Only once the button is pressed, will the data be saved to the CSV file. If the technician shuts the power to the device off before pressing the second button, no data is saved and the CSV that is created is entirely empty.

After the main study started, it was discovered that Redliners were not stable in their recordings and this led to the loss of three participants from the study. The lab had three microSD cards on hand that were 4 GB, 8 GB, and 32 GB in size. With the 4GB microSD card, the data streamed in every 28 microseconds, but periodically there was a drop out for greater than 40 ms and one drop out of almost 80 ms (Figure 27). The mean time interval was 27.36 ± 4.16 ms for the 4GB microSD card. A second, 8 GB microSD card used on the other Redliner, was more stable. It took in readings every 26 ms with intermittent samples at 30 ms, but it did have a long 170 ms drop out (Figure 28). The mean time interval was 26.45 ± 1.94 ms for the 8GB microSD card. The 32 GB microSD card was the most stable with data streaming in every 26 ms and no instances greater than 40 ms except for one, which was below 80 ms. The mean time interval was 26.42 ± 0.99 ms for the 32GB microSD card, the best of the set (Figure 29). Thus, it is critical that the Redliners use high-quality microSD cards to collect data as all computations that are done using the custom MATLAB program require consistent sampling rates, especially power (W). The data used in this test was collected on the desktop. Solving this sampling rate problem midway through the study led to better sample rates in the ten final study participants.

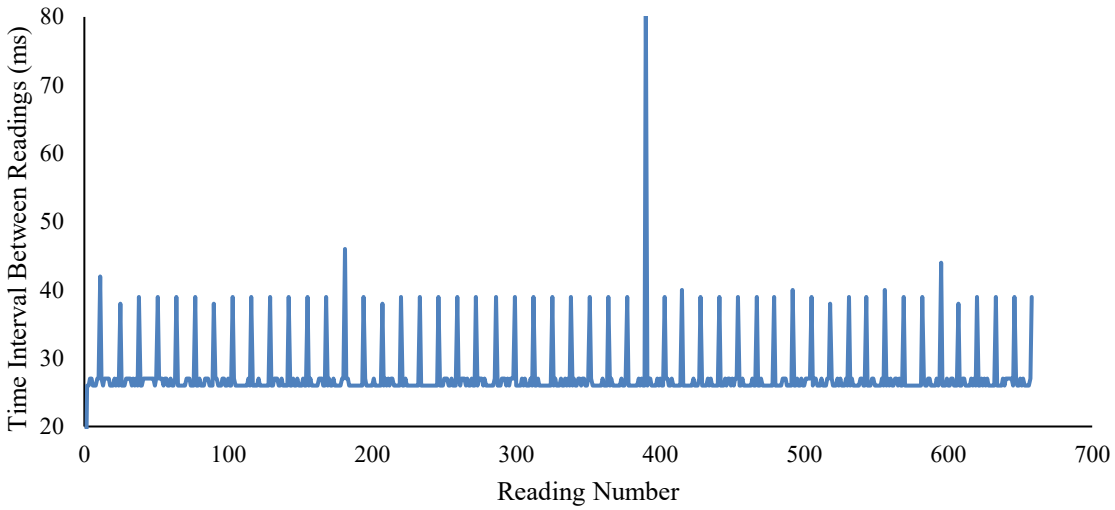

Figure 27. The time interval for each reading on the left Redliner (channel 1) while using a 4GB microSD card. The mean time interval was 27.36 ± 4.16.

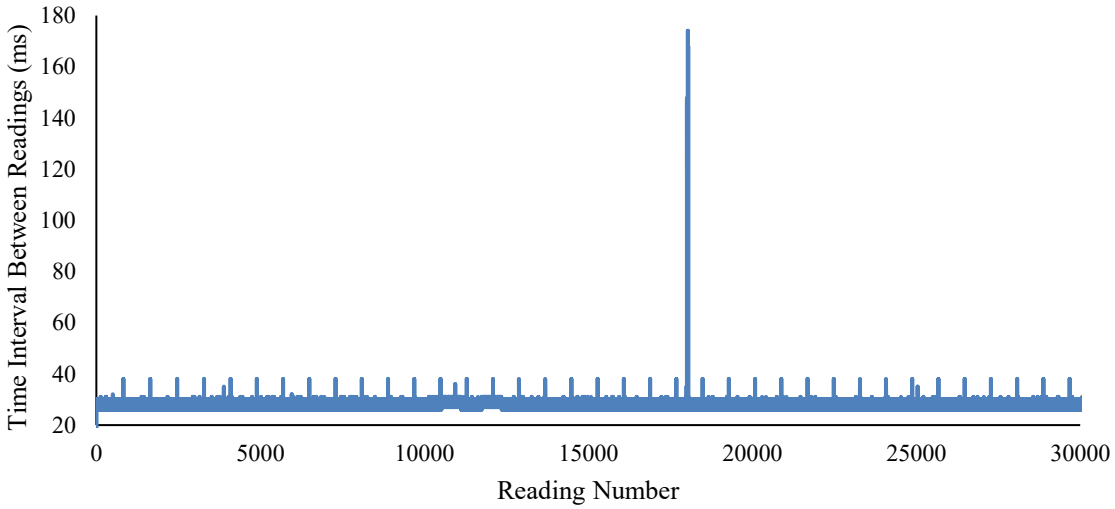

Figure 28. The time interval for each reading on the left Redliner (channel 1) while using an 8GB microSD card. The mean time interval was 26.45 ± 1.94.

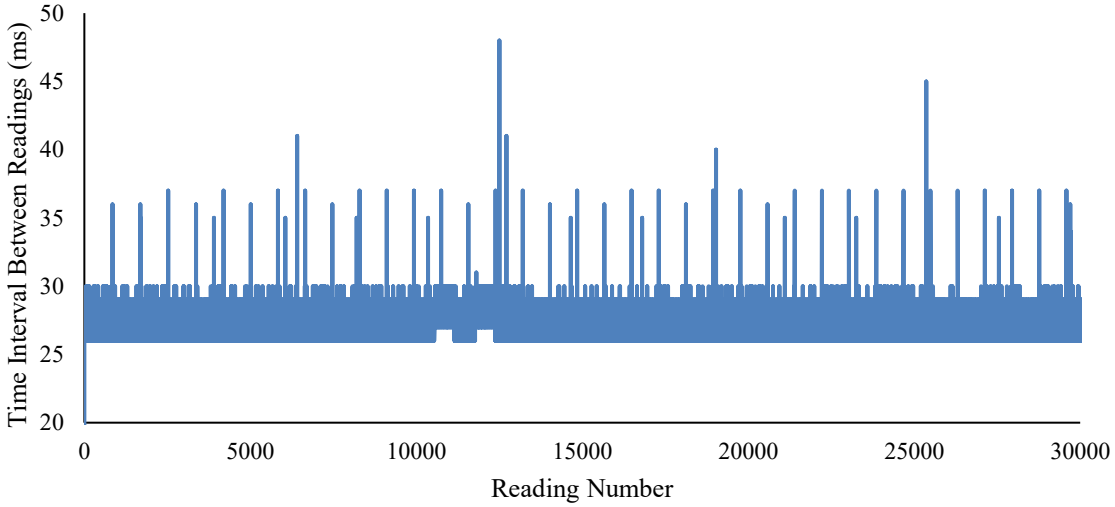

Figure 29. D. The time interval for each reading on the left Redliner (channel 1) while using a 32GB microSD card. The mean time interval was 26.42 ± 0.99.

4.5 Inertial Weight Calibration for Racing Wheelchairs

While propelling a manual wheelchair, the MWU feels the force of inertia slowing them down in the push phase (Section 2.1). This is because the MWU is working to accelerate their mass. During the recovery phase (Section 2.1), the MWU feels the force of RR slowing them down.

Participants in the pilot study told study coordinators that pushing in the VR environment was more difficult than in the RW. In the summer of 2019, the above-mentioned tests found that that the RR of the rollers in the VR environment was not significantly greater than the RR in the RW (Section 4.3.4). Thus, there existed the possibility that the inertial weights were too heavy and required more exertion from the participant in the VR environment. This is because inertial mass, I_m, was the only other variable at play in the VR environment: $F_{RW} = m_{participant+wheelchair}a + RR$, where m is mass and a is acceleration, and $F_{VR} = I_m\alpha + RR = \tau_{VR}$, where α is angular acceleration and τ is the resulting torque. In the VR environment, the inertia weight system replicates the RW mass of the participant+wheelchair through eight weights (Figure 13). The tests below were conducted to see if the inertia weights system installed by Dr. Zohreh Salimi was accurate for a coupled roller system and if a correct weighting scheme could be identified (Salimi & Ferguson-Pell, 2013).

4.5.1 Uncoupled Rollers Four-Wheeled Manual Wheelchair Test

To compare the RW and VR environments, a preliminary test was done where a 75.2 kg participant pushed a 15.1 kg racing wheelchair in the RW and VR. An examination was done on the resulting acceleration data. Before the t-test was completed for this experiment, SPSS boxplots were used to check for significant outliers visually and none were found. Additionally, the Shapiro-Wilk test of normality was completed and no significant differences were found. The accelerations for the 90.3 kg participant+wheelchair combination on the first straightaway of the test in VR (M = 2.52 rad/s^2; SD = 0.99 rad/s^2) were found to be significantly greater than in the RW (M = 1.53 rad/s^2; SD = 0.91 rad/s^2), t(41) = -3.30, p = 0.002. This

suggested that the two environments had different forces once the participant reached a steady state (SS). The SS phase in wheelchair racing can be defined as the period where the individual propels at a high but constant and submaximal velocity (Vanlandewijck et al., 2001

It is worth noting that these calculations were done by hand and this is a somewhat arbitrary method. For example, at one point two study coordinators calculated the RRs for RW and the VR environment for study participants Njl01 and LV3rT by hand. It was discovered that the two raters had different deceleration results and that choosing the peaks corresponding to pushes on the velocity traces was too subjective. It was at this point that the decision was made to automate data processing as much as possible to ensure accuracy. This was done using a custom MATLAB program. These results also meant that force measurements would be too subjective between raters without a more reliable way to collect acceleration.

To overcome the subjectivity, a test was completed where force was directly measured using the SMART^{wheel}. Dr. Salimi designed the inertia system for use with a four-wheeled everyday wheelchair and thus with the rollers uncoupled. To ensure that her calculations were accurate for the uncoupled rollers, the SMART^{wheel} was loaded on the left side of the lab's Quickie four-wheeled everyday wheelchair (Figure 10) with the rollers uncoupled. A Redliner was also attached to each of the wheels of the wheelchair. The recorded forces from the SMART^{wheel} and the inferred forces from Redliner were compared. The participant was asked to push on top of the rollers in the ICube, each time allowing the wheels to come to a full stop. The SMART^{wheel} recorded the force applied at the push rim and Redliner recorded the inferred force via acceleration. The results of these tests are outlined in Figure 30 and Table 4. The paint stick length (PSL) mentioned in the figure caption refers to the distance the inertia weights are away from the center hub of the inertia system (Figure 15). Paint sticks cut to different lengths were used as spacers to accurately set the location of the inertia adjustment weights. The paint stick is held between the center hub the outside of the disk.

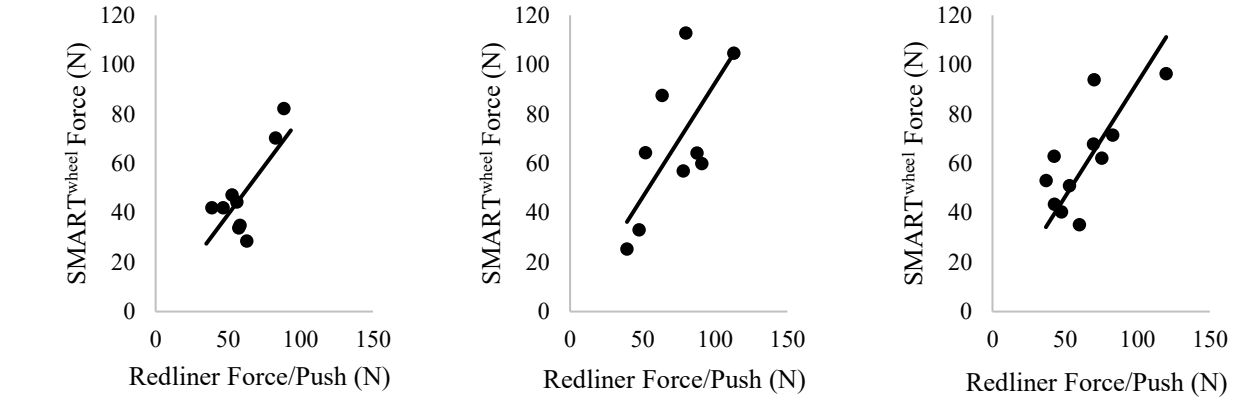

Figure 30. The SMART^{wheel} force (N) versus Redliner force (N) for uncoupled rollers with A) 10.1 cm paint stick, B) 13.1 cm paint stick, C) 16.7 cm paint stick. A) The equation of the line is y = 0.79x and the R^2 = 0.58. B) The equation of the line is y = 0.93x and the R^2 = 0.44. C) The equation of the line is y = 0.92x and the R^2 = 0.44.

Table 4. The slope of the line for each paint stick length with the 75.2 kg participant.

Paint Stick Length (cm)	**Slope of SW Force vs. est. Force +RR**
5.0	0.51
9.0	0.59
10.1	0.77
13.1	0.93
16.7	0.93

The tests showed that the forces were about 1:1 when the weights were set at Dr. Salimi's inertia weights settings for everyday four-wheeled manual wheelchairs when the rollers were uncoupled. The participant in this test weighed 75.2 kg and Dr. Salimi's calculations recommended that the paint stick be cut to 13.1 cm, this was without the added weight of the racing wheelchair (15.1 kg). With the added wheelchair weight, the suggested PSL was 16.7 cm.

These results mean that the inertia weights set at the distances calculated by Dr. Salimi's formula work well for four-wheeled everyday wheelchairs. An equation akin to the formula she used to set the inertia weights is $y = 17.016\ln(x) - 60.398$ and has an R of 1.000. Y is the length (cm) of the wooden paint stick that should be cut to set the inertia weights and X is the weight of the participant. For the 75.2 kg participant, this is equal to $17.016In(75.2\ kg) - 60.398 = 13.1$ cm.

4.5.2 Uncoupled and Coupled Rollers Test Using Acceleration

As the four-wheeled manual wheelchair seemed to have the correct inertial weight settings but the participants in the pilot study of the racing wheelchair study reported that it was much more difficult to push in the VR environment than in the RW, the coupled rollers might be increasing the forces or the inertia the participant experienced. Coupling the rollers might have led to doubling of the inertial mass experienced by the participant in the VR environment and the paint sticks might need to be shortened by half.

Since $F_{VR} = I_m\alpha + RR = \tau_{VR}$, the accelerations were compared for different PSLs. To test this, the same 75.2 kg participant propelled on top of the rollers with the 15.1 kg racing wheelchair and two Redliners but without the SMART^{wheel}. From this point on, the 75.2 kg participant had the mass of the purple racing wheelchair added to their mass, bringing the total mass of this participant to 90.3 kg. The participant was asked to push and then allow the wheels to come to a full stop. The test conditions were uncoupled rollers at a PSL of 13.1cm, coupled rollers at a PSL of 13.1cm, coupled rollers at a PSL of 6.5 cm, and coupled rollers at PSL 5.0 cm. Before the paired t-tests were completed for this experiment, SPSS boxplots were used to check for significant outliers visually and none were found. Additionally, the Shapiro-Wilk test of normality found no significant differences.

When comparing the accelerations for uncoupled 13.1cm (M=1.42 m/s^2, SD=0.38 m/s^2) and coupled 13.1cm (M=0.69 m/s^2, SD=0.35 m/s^2) the results were significantly different from each other, $t(25)=5.13$, $p<0.001$. When comparing the decelerations for uncoupled 13.1cm (M= -0.90 m/s^2, SD= -0.24 m/s^2) and coupled 13.1cm (M= -0.56 m/s^2, SD= -0.17 m/s^2) the results were significantly different from each other, $t(22)= -4.00$, $p<0.01$.

When comparing the accelerations for uncoupled 13.1cm (M=1.42 m/s^2, SD=0.38 m/s^2) and coupled 6.5cm (M=1.45 m/s^2, SD=0.45 m/s^2) the results were not significantly different from each other, $t(26)= -0.21$, $p=0.42$. When comparing the decelerations for uncoupled 13.1cm (M= -0.90 m/s^2, SD= -0.24 m/s^2) and coupled 6.5cm (M= -0.56 m/s^2, SD= -0.17 m/s^2) the results were not significantly different from each other, $t(24)= 1.43$, $p=0.08$.

When comparing the accelerations for uncoupled 13.1cm (M=1.42 m/s^2, SD=0.38 m/s^2) and coupled 5.0cm (M=1.22 m/s^2, SD=0.20 m/s^2) the results were significantly different from each other, $t(25)= 1.77$, $p=0.04$. When comparing the decelerations for uncoupled 13.1cm

(M= -0.90 m/s^2, SD= -0.24 m/s^2) and coupled 5.0cm (M= -0.78 m/s^2, SD= -0.16 m/s^2) the results were not significantly different from each other, t(24)= -1.44, p=0.08.

When comparing the accelerations for coupled 6.5cm (M=1.45 m/s^2, SD=0.45 m/s^2) and coupled 5.0cm (M=1.22 m/s^2, SD=0.20 m/s^2) the results were significantly different from each other, t(31)= 1.89, p=0.03. When comparing the decelerations for coupled 6.5cm (M= -0.56 m/s^2, SD= -0.17 m/s^2) and coupled 5.0cm (M= -0.78 m/s^2, SD= -0.16 m/s^2) the results were significantly different from each other, t(30)= -2.95, p<0.01.

The 13.1cm coupled and 13.1cm coupled accelerations and decelerations were different from each other, with the coupled acceleration being smaller. This suggests that coupling the rollers slows the participant down and increases the inertia of the system. The uncoupled 13.1cm and uncoupled 6.5cm PSLs were not significantly different from each other for accelerations and decelerations. This is of note because it might suggest that a correct setting can actually be found for the 90.3kg participant+wheelchair with the rollers coupled. The fact that the accelerations at these settings are so similar, with the uncoupled 6.5cm mean being just slightly higher, suggests that just under halving the original PSLs for participants might lead to the correct PSL. The decelerations at these settings are also not different from each other. The uncoupled 13.1cm PSL and coupled 5.0cm PSL accelerations were different from each other, but the decelerations at these settings were not. This might suggest that the RU phase is more important when discerning the difference between the two test environments. These results suggest that the ideal PSL for the coupled rollers is around half of the uncoupled rollers' setting.

4.5.3 Coupled Roller Tests Using Power

The accelerations for the uncoupled rollers at 13.1cm were not different from the uncoupled rollers at 6.5 cm. Thus, a new framework for detecting the differences between the two test environments at different PSLs needed to be developed. This framework is based on dynamics measurements and the power that exists during the period where the participant is getting up to their SS velocity.

To calculate power, first suppose that a wheelchair user pushes with a similar force pattern regardless of the study environment and system conditions. During wheelchair propulsion at a steady speed, there is a loss of energy due to RR with each push; however, this

is not significant when compared to the push forces imparted with each propulsion stroke. During the SS velocity, v_{ss}, the wheelchair user only puts in enough energy to overcome the RR in order to keep themselves at near constant velocity (Figure 31). Thus, the SS is the time section where the velocity is quite constant. It comes after the first major peak in velocity and ends once the velocity starts to decrease again past a set threshold. In the ramp up (RU) phase (A to B), larger pushes will be needed to overcome RR. The number of pushes to get to SS depends on the participant's selected v_{ss}, force applied, and how quickly the participant wants to get to SS. If the participant wants to get to SS faster, then the force applied to get to SS will likely be larger. The change in velocity from stationary to SS is the acceleration from stationary and is the result of a conglomerate of pushes. From the start of SS until deceleration (B to C), the force is an outcome of the RR and the wheelchair user's cadence (pushes/min), $F_{B\ to\ C} = m(a_{propulsion} + a_{RR})$.

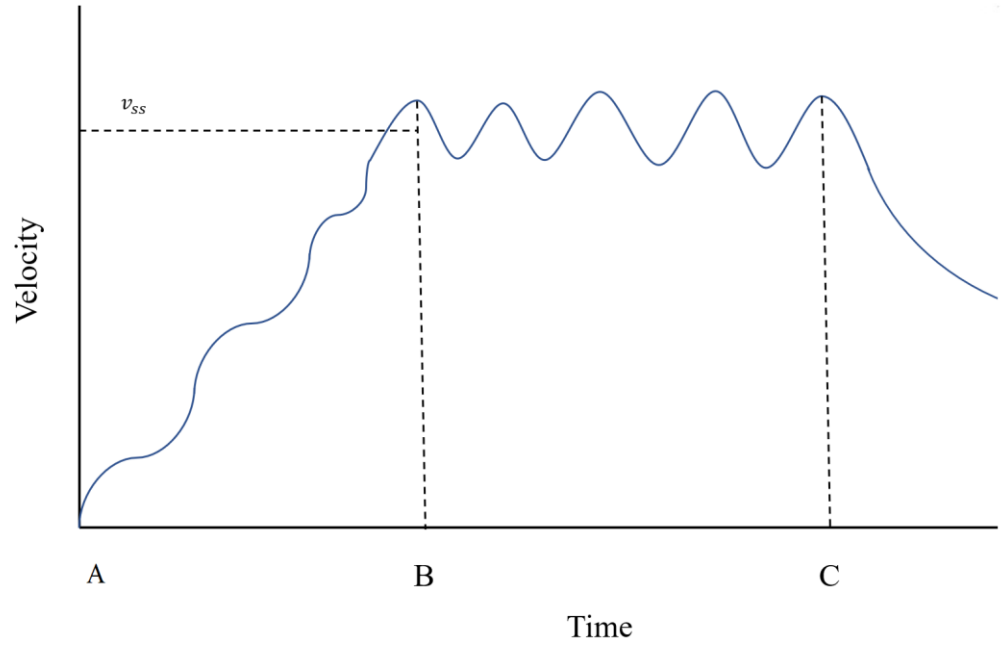

Figure 31. Idealized velocity profile for manual wheelchair propulsion.

In the SS, it was assumed that energy will be conserved and that $a_{propulsion} \approx -a_{RR}$ (Figure 32), $a_p = \frac{v_1 - v_0}{t_1 - t_0}$ and $a_{RR} = \frac{v_2 - v_1}{t_2 - t_1}$. This means that during the SS phase of regular propulsion, the MWU is mostly working to overcome the force of RR. Conversely, during the RU phase from A to B, the MWU is working to overcome the force of inertia. This is because the MWU is working to accelerate their mass from rest to a SS velocity.

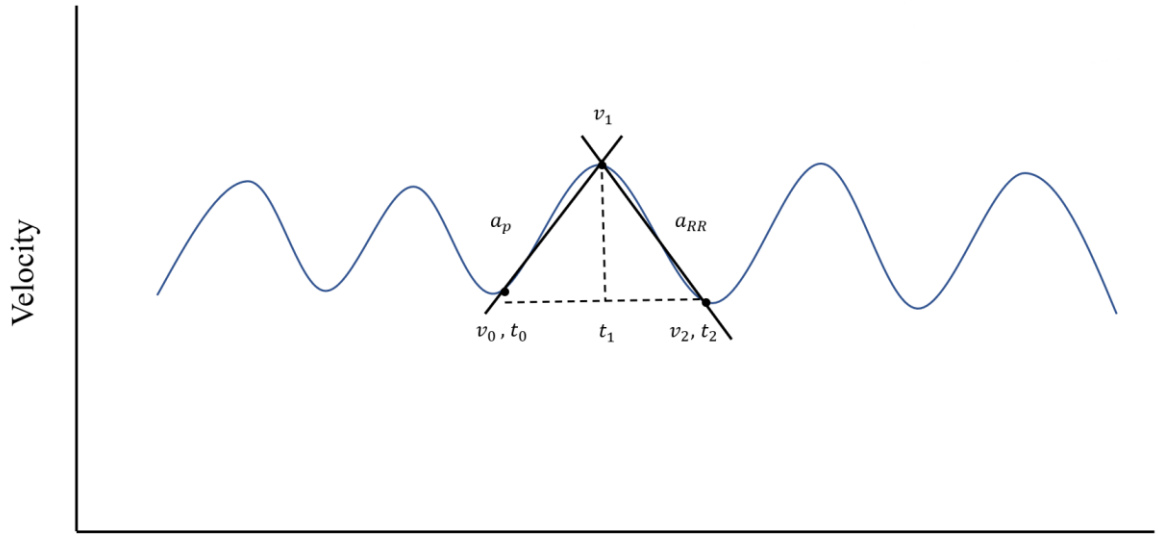

Figure 32. Idealized SS phase for manual wheelchair propulsion.

If the two environments are matched for inertia and RR, then the energy required to reach SS and maintain it should be similar between the two environments (Figure 33).

$$E_i = E_f, \qquad \Delta E = \frac{1}{2}m{v_1}^2 - \frac{1}{2}m{v_0}^2 = \frac{1}{2}m({v_1}^2 - {v_0}^2) = \frac{1}{2}m((v_1 - v_0)(v_1 + v_0))$$

$$\Delta E = \frac{1}{2}m{v_1}^2 - \frac{1}{2}m{v_0}^2 = \frac{1}{2}m({v_1}^2 - {v_0}^2) = \frac{1}{2}m((v_1 - v_0)(v_1 + v_0))$$

$$E_x = \int_{t_1}^{t_2} x(t)^2 \, dt$$

Figure 33. Matching the kinetic energy for the two environments.

Where,

E_i=energy initial,

E_f=energy final,

m=mass of the participant+wheelchair,

v_0=velocity initial,

v_1=velocity final,

t_0=start time, and

t_1=end time.

To determine the energy present in the linear velocity signal from the wheelchair, a power spectrum versus frequency plot was generated using a Fast Fourier transform (FFT) algorithm. Power (W, J/s) is the rate of work or the amount of energy consumed per unit of time. To calculate power, the FFT of the SS region of the linear velocity dataset was calculated

and then used to plot the power spectrum using the custom MATLAB program. The total power in the spectrum is the area under the curve of the power spectrum and is equal to:

$$Total\ Power\ (W) = \frac{1}{2} \times \left(m_{participant} + m_{wheelchair}\right) \times 10^{\frac{Powersum}{10}}$$

*Where the last factor in the equation is the power to sustain the SS and the Powersum is sum of the power vectors at each frequency vector. $Powersum = velocity^2$

All the inertia weight tests conducted below were done with power as the compared variable between the two test environments and with the 75.2 + 15.1 Kg participant+wheelchair combination. Still, all the below conducted tests had different RW and VR power values.

4.5.3.1 Four of the Original Set of Inertia Weights

To correct the inertia weights through a correction ratio, a participant of 75.2 + 15.1 kg was again asked to propel on coupled rollers. In this case, there were four of the original inertia weights attached to either roller at PSLs of 5.2 cm, 6.0 cm, 6.5 cm, 8.0 cm, and 9.0 cm. The participant propelled for one minute at a SS, or steady velocity.

A custom MATLAB program was used to calculate the total power (W) present in the velocity spectrum. The total power for the participant in the RW was divided by the total power for each PSL in the VR environment (Figure 34). This ratio was averaged across the PSLs and found to be 1.37 and then multiplied by the apparent weight of the person+ wheelchair (kg) for each PSL (14). The apparent weight of the person+ wheelchair for this run on this data was found using Dr. Salimi's trendline, even though it was known to be too heavy. For example, with Dr. Salimi's equation, a PSL of 5.2 equated to a person's weight of 47.3 kg. This was added to the 15.1 kg wheelchair weight and then entered into the custom MATLAB program to calculate power.

$$\frac{RW\ Total\ Power\ in\ Spectrum}{VR\ Total\ Power\ in\ Spectrum\ at\ 5.2\ cm} = \frac{46.998\ W}{32.364\ W} = 1.45 = Ratio\ at\ 5.2cm$$

$$m_{New\ of\ Person+wheelchair}\ (kg) = m_{Person\ at\ 5.2cm\ +wheelhair} \times 1.37 = 62.4\ kg\ \times 1.366 = 85.257\ kg$$

Figure 34. Process for correcting the weight of the person+wheelchair using the power ratio between the two environments.

The original PSL (cm) was graphed against the new weight of person+ wheelchair (kg) (Figure 35). The equation of the line was y = 0.24x - 14.92 and $R^2 = 1.00$, where Y is the PSL

(cm) and X is the weight of the person and their wheelchair (kg). As the minimum setting of the weights is 3 cm and the maximum setting is 18.8 cm (Figure 13), 75.6 kg is the minimum and 142.7 kg is the maximum weight of the person plus the wheelchair using the original set of inertia weights. Using the 15.1 kg wheelchair, this means that a person can weight a minimum of 60.5 kg and a maximum of 127.6 kg. The range is 67.1 kg. This is not an ideal range as the upper limit is much too heavy.

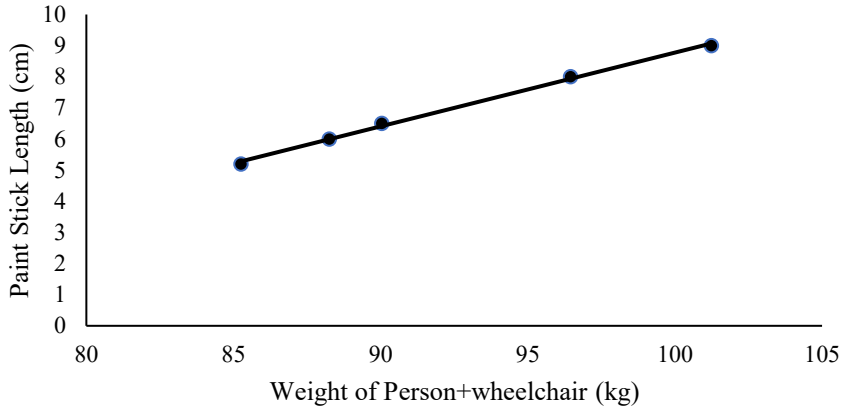

Figure 35. Original paint stick length (cm) as a function of the new weight of person+ wheelchair (kg). The equation of the line is y = 0.24x - 14.92 and R^2 = 1.00.

The new regression equation calculated above was used to rerun the experiment to adjust the weight to a shorter PSL. This would also lead to a smaller ratio value and closer power measurements between the two test environments. For example, Dr. Salimi's equation stated that a PSL of 5.2 should be used for a 47.3 kg person, while the equation shown in Figure 35 stated that it should be used for a 70 kg person.

Again, the 75.2 + 15.1 kg participant propelled on coupled rollers set with four of the original inertia weights attached to either roller at PSLs of 5.2 cm, 6.0 cm, 6.5 cm, 8.0 cm, and 9.0 cm. The apparent weight of the person+wheelchair for this run on this data was found using the equation y = 0.24x - 14.92. The RW/VR ratio used to correct was 0.97 and so the VR power was getting close to RW power. The data from this test is shown in Figure 36, where the equation of the line is y = 0.17x - 14.89 and R^2 = 1.00.

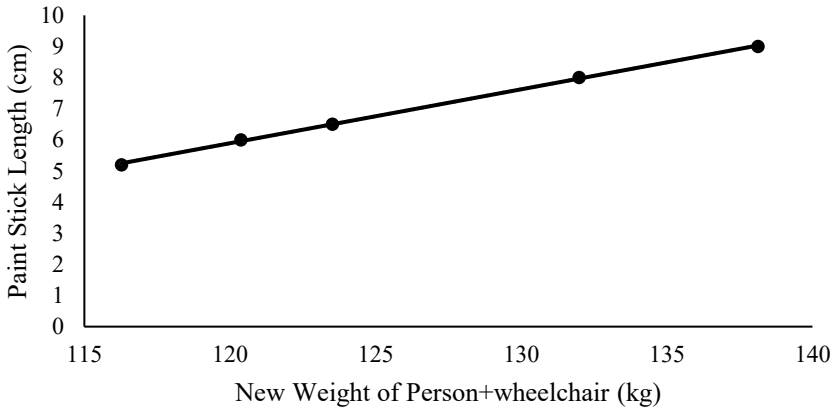

Figure 36. Paint stick length (cm) as a function of the weight of the person plus their wheelchair (kg). The equation of the line is y = 0.17x – 14.89 and the $R^2 = 1.00$.

Still though, participants stated that the inertia weights were too heavy. If the equation y = 0.17x - 14.89 was used to compute new PSLs for participants, they were outside of the range of our system. The new minimum and maximum weight of the person plus the wheelchair became 103.3 kg and 194.5 kg, respectively, a range of 91.2 kg. Using the 15.1 kg wheelchair, this means that a person can weigh a minimum of 88.2 kg and a maximum of 179.4 kg. It was very unlikely that we would get many participants above 88.2 kg, or 195 lbs, and that they would be able to fit in the seat of the smaller purple racing wheelchair belonging to the RRL. They would need to be quite tall and slim to fit and be over 88.2 kg. This might exclude many female participants. Thus, it was proposed that new weights be cut that were smaller than the original disks and weighed less.

4.5.3.2 Two of the Original Set of Inertia Weights

To be sure that the original set of inertia weights was too heavy, the same experiment was conducted with coupled rollers but with two weights on each roller instead of four. The PSLs we tested were 3 cm, 6.5 cm, 9.0 cm, 13.1 cm, 16.7 cm, and 18.8 cm. The apparent weight of the person+wheelchair for this run on this data was found using the equation y = 0.24x - 14.92. The RW/VR ratio was 1.22.

The equation of the line was y = 0.28x - 14.97 and $R^2 = 1$. This value led to PSLs that were within the range of the system, but the participants reported that pushing the wheelchair was still more difficult than the RW. This might be because the participant had to overcome the uneven inertial loading that was created with only two weights on either side. Four weights would help to keep the system in motion through inertia.

4.5.3.3 Four of the New Set of Inertia Weights

Thus, a new set of eight weights were made at half the thickness of the first set. Each disk in the original set was 5” in diameter, 1.5” thick, 3.77kg (8.3 lb), and made of AISI 1018 mild low-carbon steel. The second set were the same diameter and material but were 0.7” thick and weighed 1.8 kg (3.97lbs) each.

Two more test sessions were done with these light weights with the belt on and without the belt on by the 75.2 + 15.1 kg participant. The belt connects to the roller’s bearing and allows the rollers to be magnetically braked. For both test sessions, the apparent weight of the person+wheelchair was found using the equation y = 0.24x - 14.92. Although the magnetic braking was not activated, McKenzie (2018) has shown that they can add low level resistance due to inductive effects.

For the light weights with the belt on, the RW/VR ratio was 1.20. The equation of the trend line was y = 0.22x – 10.91, $R^2 = 0.98$. The minimum and maximum weight of the person plus the wheelchair for this equation are 64.1 kg and 137.0 kg, respectively. The range is 72.9 kg. Using the 15.1 kg wheelchair, this means that a person can weigh a minimum of 49 kg and a maximum of 121.9 kg. This could be further improved by doing this test again until the RW and VR power no longer differ.

For the light set of weights with the belt off, the RW to VR ratio was 1.10 and the equation of the line was y = 0.24x - 9.45, $R^2 = 0.99$. The minimum and maximum weight of the person plus the wheelchair for this equation are 51.6 kg and 117.0 kg, respectively. The range is 65.4 kg. Using the 15.1 kg wheelchair, this means that a person can weigh a minimum of 36.5 kg and a maximum of 101.9 kg. This could be further improved by doing this test again until the RW and VR power no longer differ.

4.5.4 Concluding Statement

Even though the equation of the line with the belt off still needed to be tested, a protocol for testing the validity of paint sticks had been developed. This will need to be refined though, as this protocol depends on knowing the correct weight of the participant plus their chair to input into the custom MATLAB program to calculate power. A new method to calibrate the inertia weights using the light set of weights is explored below in Section 5.4.

5. Results

5.1 Experimental Sample Size

Recruitment did not mirror the 3:1 male to female ratio that was expected. Out of the ten participants who had reliable data, 3 were male and 7 were female. The sample size also did not meet the expected 15 subjects that were proposed above. However, as in Figure 37, the power analysis of experimental values for this study suggested that the sample size be 12 subjects for velocity measurements and 7 subjects for distance measurements.

Velocity: **= 12.00 subjects**
Distance Traveled: **= 7.34 subjects**

Figure 37. Power analysis results. See Appendix A for calculations.

5.2 Real-World versus Virtual World Dynamics

5.2.1 Overview

A custom MATLAB program was used to calculate cadence (pushes/min), peak and average velocity of the SS and RU phase (m/s), average and peak acceleration of the SS (m/s^2), total distance traveled (m), and total power for the SS and whole test (W). These measurements, those collected with the ergometer, and those calculated by hand using the velocity trace (total time [sec], time interval [sec], and RU phase energy [J], power [W], force [N], and acceleration [m/s^2]) are compared below between the RW and VR environment. If no significant differences are found between the two environments, then the VR environment accurately represents the RW. However, any significant differences between the dependent variables will need to be examined, explained, and addressed for future testing.

One common problem with technology under development is a phase shift between dynamics plots due to time deviations and data smoothing techniques. To ensure this was not problematic with Redliner, the average difference in time between the velocity plots and acceleration plots, where velocity was constant and acceleration was zero, was examined. It was found that the average deviation between the two plots was 0.17 seconds ± 0.26 seconds (M ± SD). Thus, the phase shift experienced with Redliner is minimal.

The results from the dynamics test are shown in Table 5. These results are explained further in the following sections.

Table 5. The RW and VR mean and standard deviation for each test factor. The red values are significantly different between the two test environments. The green values are not significantly different between the two test environments. The two yellow values are the only values that are greater in VR than in the RW. The p-value for each test factor is also shown.

Test Factor	RW vs. VR	RW [M (SD)]	VR [M (SD)]	p-value
Pushes to SS	RW>VR	12.40 (2.57)	8.90 (2.69)	0.008
SS Cadence (pushes/min)	RW≈VR	66.33 (7.57)	58.02 (6.68)	0.073
Whole Test Cadence (pushes/min)	RW>VR	59.08 (2.33)	49.26 (5.64)	0.006
Average Velocity (m/s)	RW>VR	1.99 (0.47)	1.37 (0.40)	<0.0001
Peak Velocity (m/s)	RW>VR	2.67 (0.63)	2.27 (0.62)	0.011
RU Velocity (m/s)	RW>VR	2.08 (0.61)	1.67 (0.52)	0.002
Average Acceleration (m/s/s)	RW=VR	0.00 (0.00)	0.00 (0.00)	N/A
Peak Acceleration (m/s/s)	RW≈VR	1.07 (0.35)	0.96 (0.31)	0.58
RU Acceleration (m/s/s)	RW≈VR	0.29 (0.10)	0.27 (0.074)	0.58
Distance Traveled (m)	RW<VR	1268.76 (57.69)	1382.24 (70.51)	0.002
Time Taken for 6 Laps (s)	RW<VR	669.81 (137.43)	986.44 (228.86)	0.001
Time Interval (ms)	RW≈VR	30.60 (7.95)	30.63 (6.95)	0.75
Power RU Phase (W)	RW≈VR	36.97 (22.48)	27.49 (13.95)	0.083
Average Power (W)	RW≈VR	41.55 (7.66)	40.84 (6.71)	0.11
Total Energy (J)	RW>VR	303.32 (181.37)	201.01 (131.07)	0.003
Average Force (N)	RW≈VR	23.74 (9.09)	21.60 (5.92)	0.48

5.2.2 Ramp Up Phase Explanation

As the MATLAB code had not been written to get energy, power, force, and acceleration from the RU phase, these calculations were done by hand. The RU phase is the phase of the test where the participant propels up to the SS (Figure 31 A to B). It was evident in MATLAB that the velocity plot in the RW had more, smaller pushes in the RU phase than the VR environment (Figure 38 A). The VR environment's velocity plot appears as a straight inclined line with no bumps to correspond to pushes for a much longer period (Figure 38 B). For the dataset shown in Figure 39, the RW had 27 pushes while the VR environment had 13 pushes. There was more variation in the number of pushes in the VR environment as well (VR SD = 1.41 and 1/7 had a standard deviation of 0, RW SD = 1.11 and 4/7 samples had a standard deviation of 0). In the VR environment, the pushes were shadowed by vibrations without a low-pass filter applied. Additionally, in VR, small pushes appear to be masked and thus could not be counted. Speed often decreased greatly after the RU phase in the VR environment.

Pushes were also very close together, the spacing between the end of one and the beginning of another was very small. This made it difficult to pick peaks. Many participants got up to a set speed upon RU but then did not sustain this speed throughout the entirety of the test. Some participants never reached this peak velocity at the end of RU phase again. If the participant spent a longer time overcoming the inertia weights and trying to get up to SS velocity, pushes were greater in magnitude variation as well as closer together. Additionally, Redliner push data seemed clearer with the study's one, more experienced wheelchair user.

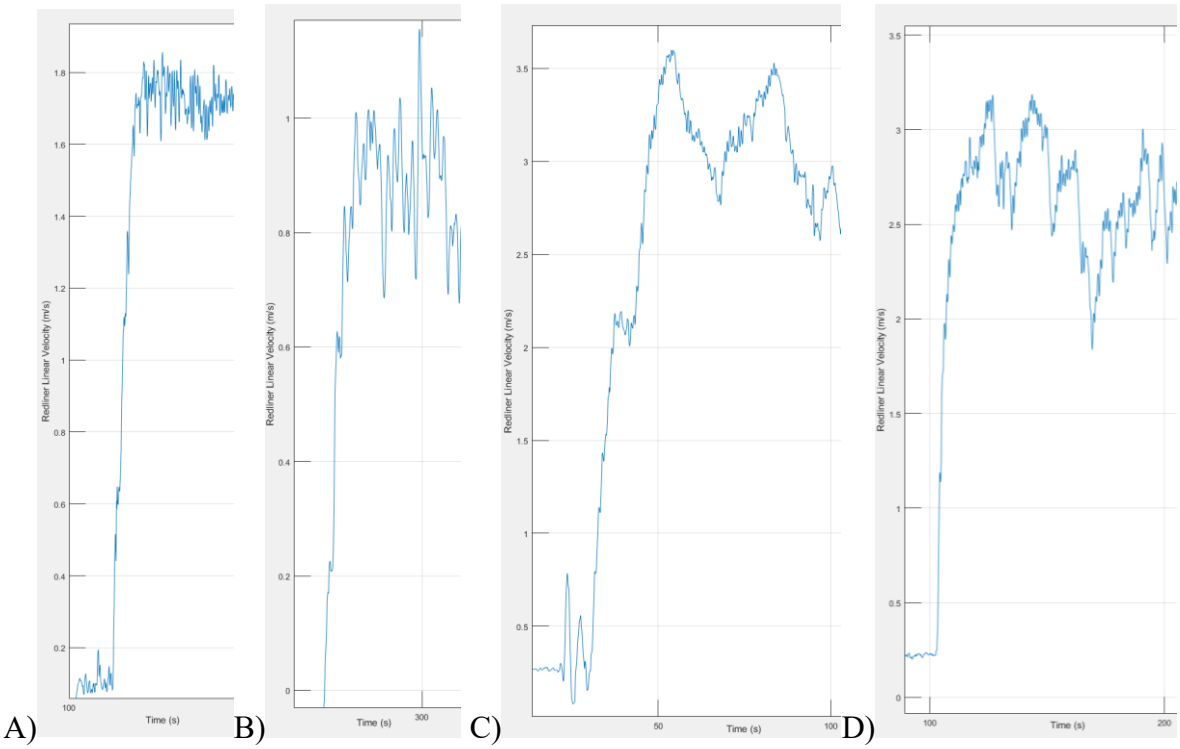

Figure 38. Sample velocity traces from participant EYr56 for the RW (A) and VR environment (B) and participant F for the RW (C) and VR environment (D).

Before the paired t-tests were completed on the entire test's push data, significant outliers were visually searched for using SPSS boxplots, none were found, and the Shapiro-Wilk test of normality was completed, no significant differences were found. In this study, the amount of pushes used by a participant in the RW to get up to SS (M = 12.40 pushes, SD = 2.57 pushes) was significantly larger than that of the VR environment (M = 8.90 pushes, SD = 2.69 pushes), $t(9) = 3.42$, $p = 0.008$).

5.2.3 Cadence

Cadence in manual wheelchair propulsion is the number of pushes applied to the wheelchair wheel per minute. Kwarciak et al. (2011) found that the average cadence for over-

ground pushing in a manual wheelchair was 50.6 ± 10.9 pushes/min, while Boninger et al. (2012) found that it could range from 38 to 55 pushes/min. Additionally, cadence in wheelchair racing athletes is often above 100 pushes per minute (Chow et al., 2000; Goosey et al., 1997; Wang et al., 1995; Cooper, 1990).

In theory, one could find the cadence of the individual using the power spectrum output from the custom MATLAB program, but this proved too unreliable. The data stream would need a filter applied to it before power was computed to clear outliers in the dataset that were characteristic of vibrations of Redliner and not actual pushes. This method will still be explored in the future, and then compared to the method below to ensure accuracy, but for now it was simpler to explore a different route.

Using MATLAB, cadence is calculated below by applying a low-pass filter to the linear velocity dataset before finding maximum and minimum peaks in the velocity trace. Once the maximum peaks are found, the time between peaks (sec) is computed and paired with the velocity of the peak (m/s). The original dataset of linear velocity had many short time interval maximum peaks (Figure 39). The usual time interval for a push to occur is 0.8 to 1.5 seconds. Peaks that are below 0.3 seconds in duration are characteristic of vibration noise and must be filtered out.

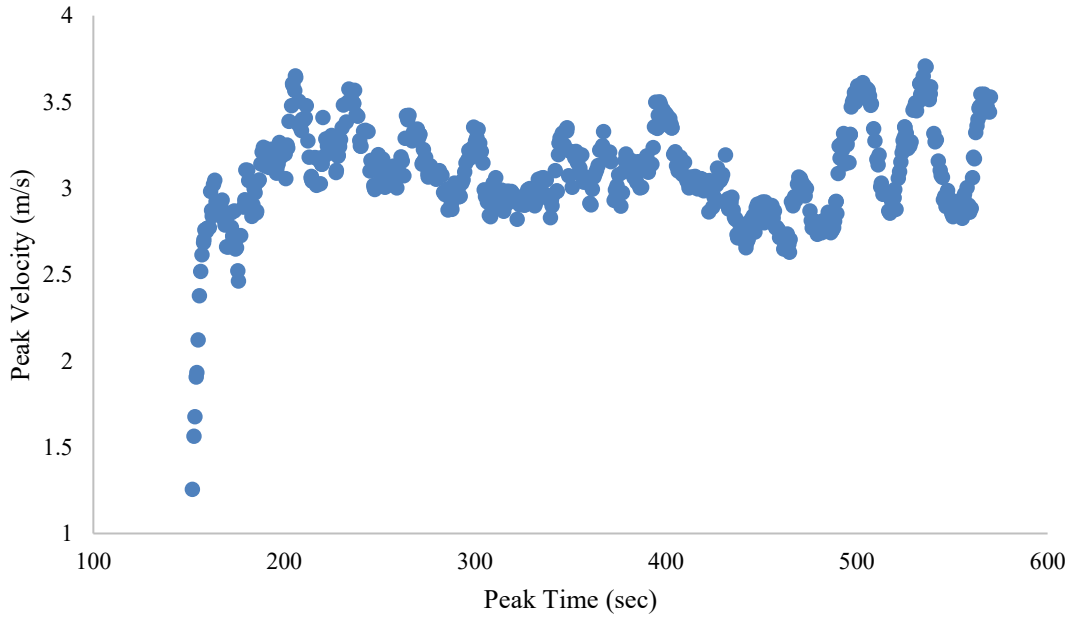

Figure 39. The velocity of each peak (m/s) plotted as a function of the time between peaks (sec) of the original dataset. No low-pass filter was applied to the velocity trace before computing the time between peaks.

The low-pass filter was set at 0.0125 Hz, as it was the optimum tested filter value. The following results were calculated using TwQ7b's dataset for the left wheel in the RW, as this was a robust and reliable dataset. For 0.0125 Hz, the % of samples below 0.4 sec was 0.91% and the % of samples below 0.3 sec was 0.23%. For a filter of 0.00625 Hz, the % of samples below 0.4 sec was 0.71% and the % of samples below 0.3 sec was 0.24%. However, the total number of data points for the 0.0125 Hz dataset was 438 while the 0.00625 Hz dataset was 423 data points in size, a difference of 15. The 0.025 Hz dataset was 465 data points long and the 0.003125 dataset was 412 data points long. The cadence for the RW trial with a 0.0125 Hz filter was 60.36 pushes per minute while the 0.00625 Hz cadence was 52.91 pushes per minute. Figure 40 shows the percentage of data points below 0.40 sec as a function of the low pass filter for participants TwQ7b and EVx2m.

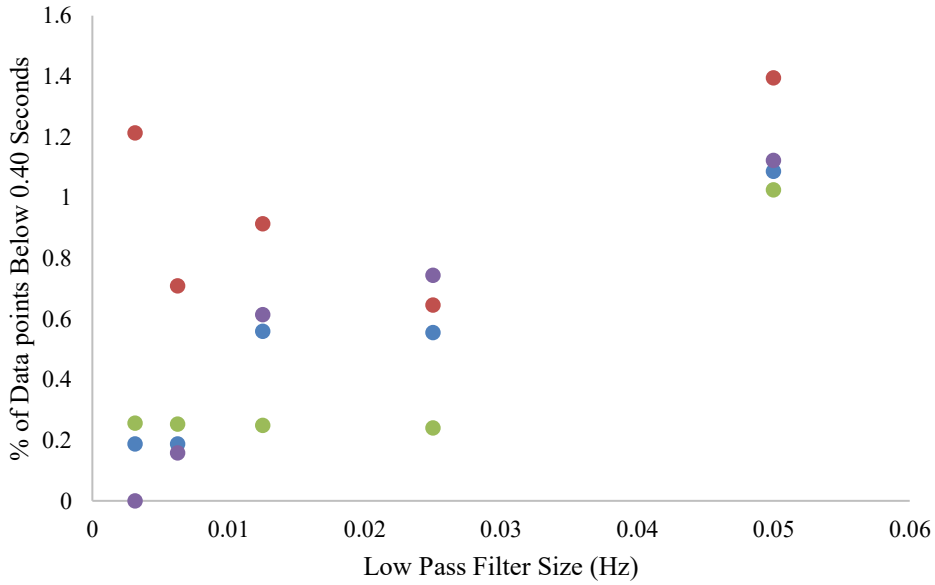

Figure 40. The percentage of data points below 0.40 seconds as a function of the low pass filter for participants TwQ7b and EVx2m. The red markers are from TwQ7b for the left wheel for the RW and the purple markers are for the left wheel for the VR environment. The blue markers are for EVx2m for the left wheel in the RW and the green markers are for the VR environment.

A frequency of 0.0125 Hz, or 0.079 rad/s, removed most of the small peaks that exist in the dataset due to vibrations of the Redliner but not too many so as to shift and disrupt the dataset. In Figure 41, the dataset is smoother and has fewer short time interval peaks. This dataset also has a robust number of samples. Employing a low-pass filter is incredibly useful

as any filter greater than 0.025 Hz created much larger cadence values, which were unrealistic for manual wheelchair propulsion (Table 6). The high frequency components were almost certainly due to system vibrations.

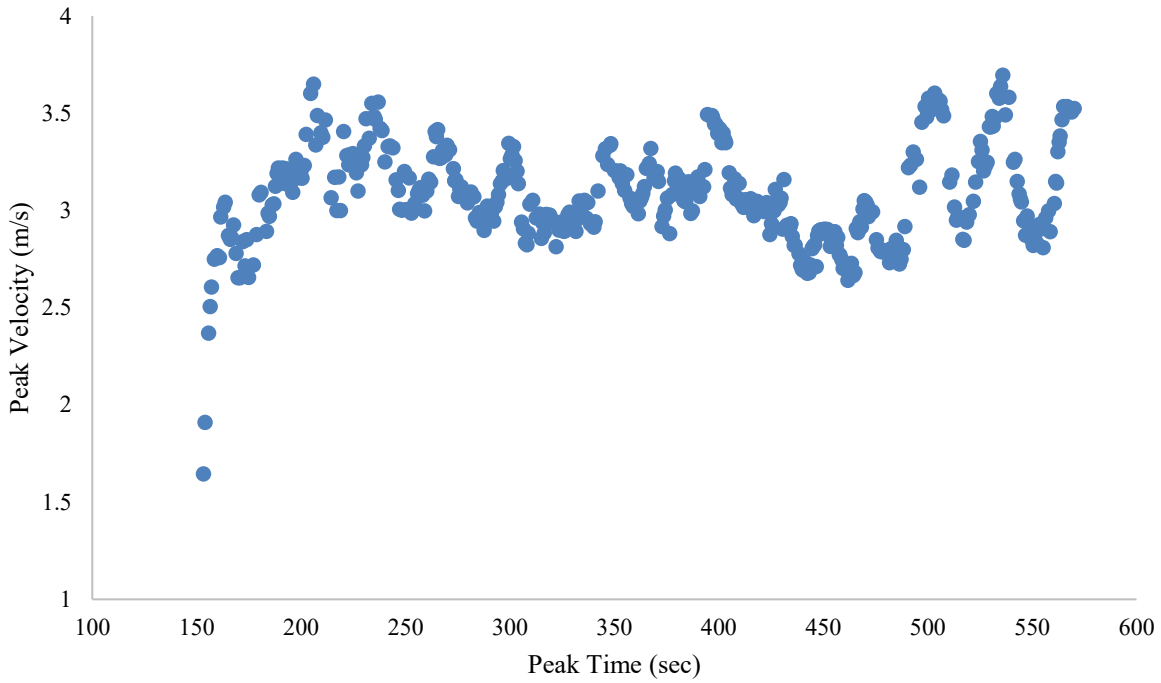

Figure 41. The velocity of each peak (m/s) plotted as a function of the time between peaks (sec) of the original dataset. A low-pass filter of 0.0125 Hz was applied to the velocity trace before computing the time between peaks.

Table 6. Average cadence for the four test sessions as a result of various low pass filters.

Low-pass Filter (Hz)	SS Cadence (pushes/min)	Whole Test Cadence (pushes/min)
0.003125	58.0892	55.9143
0.00625	59.6669	56.6416
0.0125	61.5334	57.8216
0.025	64.244	59.7656
0.05	68.846	62.9766

As stated above, the maximum peaks array with the low-pass filter applied was used to find the time between maximum peaks. The time between maximum peaks (sec) is the time taken to complete one push and can be divided from 60 to get the number of pushes in a minute.

Four of the participants were excluded from this test as three were missing wheel data on at least one side and the last participant had velocity traces that were inconsistent due to frequent stopping in VR. Before the paired t-tests were completed on the SS and whole test

cadence, significant outliers were visually searched for using SPSS boxplots, none were found, and the Shapiro-Wilk test of normality was completed, no significant differences were found.

The SS cadence in the RW (M = 66.33 pushes/min, SD = 7.57 pushes/min) was not significantly different from that of the VR environment (M = 58.02 pushes/min, SD = 6.68 pushes/min), t(5) = 2.26, p = 0.073. The cadence throughout the whole test in the RW (M = 59.08 pushes/min, SD = 2.33 pushes/min) was significantly different from that of the VR environment (M = 49.26 pushes/min, SD = 5.64 pushes/min), t(5) = 4.56, p = 0.006. The SS cadence had similar standard deviations between the two worlds while the whole test cadence had a standard deviation in the VR environment that was double that of the RW.

5.2.4 Distance, Velocity, Acceleration, and Time

Before the paired t-tests were completed on the average, peak, and RU velocity, SPSS boxplots were used to check for significant outliers visually and none were found. Additionally, the Shapiro-Wilk test of normality was completed and no significant differences were found. The experimentally collected velocity is smaller in the VR environment, as the ratio of VR velocity/RW velocity is 0.69 ± 0.18. The ratio of RW/VR for velocity, distance, and power in the SS was calculated and the velocity ratio was found to vary much more than the distance or power ratio. In line with this, the average RW velocity (M=1.99 m/s, SD=0.47 m/s) was significantly greater than the average VR velocity (M=1.37 m/s, SD=0.40 m/s) as captured using Redliner; t(9)=5.61, p<0.0001. The peak RW velocity (M=2.67 m/s, SD=0.63 m/s) and peak VR velocity (M=2.27 m/s, SD=0.62 m/s) as captured using Redliner were significantly different from each other; t(9)= 3.17, p=0.011. RU velocity could be determined as the velocity plot was being used to find power and energy. The average RU velocity in the RW (M = 2.08 m/s, SD = 0.61 m/s) was significantly greater than that of the VR environment (M = 1.67 m/s, SD = 0.52 m/s), t(9) = 4.18, p = 0.002. The standard deviations for these tests were all very similar between the two test environments.

When the velocity data was compared against the ergometer velocity data, outliers were present and the Shapiro-Wilk test of normality was significant. Thus, a paired-samples sign test was done instead as the distribution of differences between paired observations was not symmetrical. The RW average velocity (M =2.04 m/s, SD = 0.51 m/s) collected with Redliner was significantly larger than the VR average velocity (M = 1.49 m/s, SD = 0.45 m/s) collected by the wheelchair ergometer in all eight cases, p = 0.008. The VR average velocity (M = 1.41

m/s, SD = 0.40 m/s) collected with Redliner was less than the VR average velocity (M = 1.49 m/s, SD = 0.45 m/s) collected by the wheelchair ergometer in 7/8 cases but it was not significant, p = 0.070. Once again, the standard deviations for these tests were all very similar between the two environments. The ergometer only had data for eight of the ten participants, as two datasets did not save correctly.

Before the paired t-tests were completed on the peak and RU acceleration, SPSS boxplots were used to check for significant outliers visually and none were found in the RU dataset. Additionally, the Shapiro-Wilk test of normality was completed and no significant differences were found in the RU dataset. However, outliers were present and the Shapiro-Wilk test of normality was significant for the peak acceleration dataset. Thus, one participant was removed from the analysis as their RW acceleration was extremely large and VR acceleration was extremely small. After this, the peak RW acceleration (M=1.07 m/s^2, SD=0.35 m/s^2) and peak VR acceleration (M=0.96 m/s^2, SD=0.31 m/s^2) as captured using Redliner were found to be not significantly different from each other; t(8)=0.58, p=0.58. The average accelerations as shown by Redliner were not different from each other as both the RW and VR environment values were 0.000 m/s^2 for all participants. Acceleration could also be found in the RU phase from the same velocity trace that was being used to find power and energy. As such, the RU acceleration was also examined using a paired t-test to see if it was different between the two environments. The RU acceleration in the RW (M = 0.29 m/s^2, SD = 0.10 m/s^2) was not significantly different than that of the VR environment (M = 0.27 m/s^2, SD = 0.074 m/s^2), t(9) = 0.57, p = 0.58. Once again, the standard deviations for these tests were all very similar between the two environments.

SPSS boxplots were used to check for significant outliers visually in the Redliner distance data and none were found. Additionally, the Shapiro-Wilk test of normality was completed and no significant differences were found. The experimentally collected distance is bigger in the VR environment, as the ratio of VR distance/RW distance is 1.09 ± 0.068. The RW distance traveled (M = 1268.76 m, SD = 57.69 m) was significantly smaller than VR distance traveled (M = 1382.24 m, SD = 70.51 m) as captured using Redliner, t(9) = -4.47, p = 0.002. The standard deviations between the RW and VR environment for distance traveled collected by Redliner were also similar.

When the Redliner distance data was compared against the ergometer distance data, outliers were present in the dataset and the Shapiro-Wilk test of normality was significant. Thus, a paired-samples sign-test was done instead as the distribution of differences between the RW and VR environment was not symmetrical. The RW distance traveled (M = 1267.27 m, SD = 65.31 m) collected with Redliner was smaller than the VR distance traveled (M = 1399.50 m, SD = 476.13 m) collected by the wheelchair ergometer in 7/8 cases but it was not significant, $p = 0.070$. The VR distance traveled (M = 1407.37 m, SD = 52.39 m) collected with Redliner was larger than the VR distance traveled (M = 1399.50 m, SD = 476.13 m) collected by the wheelchair ergometer but it was also not significant, $p = 0.070$. In Section 4.3.3, the ergometer also measured the distance as being greater than that of Redliner. The ergometer distance traveled had a greater standard deviation than both Redliner datasets from both test environments.

Before the paired t-tests were completed on the time variables, SPSS boxplots were used to check for significant outliers visually and none were found in the Redliner time dataset. Additionally, the Shapiro-Wilk test of normality was completed and no significant differences were found. Using Redliner, the time taken to complete the six laps in the RW (M=669.81 seconds, SD=137.43 seconds) was significantly shorter than the time taken to complete the six laps in VR (M=986.44 seconds, SD = 228.86 seconds), $t(9)= -4.81$, $p= 0.001$. The time taken to complete the six laps in the RW (M = 619.80 seconds, SD = 124.42 seconds) using Redliner was also significantly smaller than the time taken in the VR environment (M = 827.06, SD = 195.13) as reported by the wheelchair ergometer, $t(6)= -2.76$, $p= 0.033$. The time taken to complete the six laps in the VR environment (M = 910.78 seconds, SD = 122.59 seconds) using Redliner was not significantly larger than time taken in the VR environment (M = 827.06, SD = 195.13) as reported by the wheelchair ergometer, $t(6)= 1.43$, $p= 0.20$. The standard deviations for the time taken to complete each test session were different between the two test environments and the two collection devices.

When the Redliner time interval was examined between the two environments, outliers were present in the dataset and the Shapiro-Wilk test of normality was significant. Thus, a paired-samples sign test was done instead as the distribution of differences between the RW and VR environment was not symmetrical. The time interval between data samples in the RW (M=30.60 ms, SD=7.95 ms) on Redliner was not significantly different from the time interval

between samples in the VR environment (M=30.63 ms, SD=6.95 ms), p=0.75, with 6/10 samples being greater in the RW and 4/10 in the VR environment. The standard deviations for these datasets were similar.

5.2.5 Power

Power was computed using the custom MATLAB program as outlined in Section 4.5.3 and used the RW weight of the participant and their wheelchair as the input. The experimentally collected power was slightly bigger in the RW, as the ratio of VR power/RW power is 0.98 ± 0.030. However, a paired t-test completed on the participants' power data found that this difference was not significant for the SS power in the RW (M=41.65, SD=7.61) and the SS power in the VR environment (M=40.84, SD=6.71); t(9)=1.75, p=0.11. The SS power standard deviations are similar between the two test environments.

In addition to the power of the SS, the RU phase was also examined. Before the paired t-tests were completed on the RU phase power, SPSS boxplots were used to check for significant outliers visually and none were found. Additionally, the Shapiro-Wilk test of normality was completed and a significant difference in the average RW RU phase power with Redliner was found (p=0.047). No other significant differences were found.

The average power per push to get to SS was calculated by hand from the MATLAB velocity plot as:

$$Power_{Average/push}(w) = \frac{\Delta Energy_{per\ push}}{\Delta time} = \frac{\frac{1}{2} \times m_{participant+wheelchair} \times ({v_2}^2 - {v_1}^2)}{t_2 - t_1}$$

The average power per push to get to SS in the RW (M = 36.97 W, SD = 22.48 W) was not significantly different than that of the VR environment (M = 27.49 W, SD = 13.95 W), t(9) = 1.95, p = 0.083. The standard deviation of the RW dataset appears to be twice that of the VR dataset.

5.2.6 Energy

Before the paired t-tests were completed on the total energy in the RU phase, SPSS boxplots were used to check for significant outliers visually and none were found. Additionally, the Shapiro-Wilk test of normality was completed and no significant differences were found. The sum of total energy to get to SS was calculated by hand from the MATLAB velocity plot as:

$$Total\ Energy\ (J) = \sum Energy_{per\ push} = \frac{1}{2} \times m_{participant+wheelchair} \times ({v_2}^2 - {v_1}^2)$$

* Where the velocity is taken at the beginning (v_1) and end (v_2) each of a push, which is seen as a local maximum and minimum on the velocity trace in the custom MATLAB code.

The energy to get to SS in the RW (M = 303.32 J, SD = 181.37 J) was significantly larger than the VR environment (M = 201.01 J, SD = 131.07 J), t(9) = 4.12, p = 0.003. The standard deviations in the RW dataset are larger than the VR environment.

5.2.7 Force

Before the paired t-tests were completed on the RU phase force, SPSS boxplots were used to check for significant outliers visually and none were found. Additionally, the Shapiro-Wilk test of normality was completed and no significant differences were found. The average force per push to get to SS was calculated by hand from the MATLAB velocity plot as:

$$Force_{Average/push}(N) = m_{participant+wheelchair} \times a = \frac{m_{participant+wheelchair} \times (v_2 - v_2)}{t_2 - t_1}$$

The average force per push to get to SS in the RW (M = 23.74 N, SD = 9.09 N) was not significantly different from that of the VR environment (M = 21.60 N, SD = 5.92 N), t(9) = 0.75, p = 0.48. The standard deviations are also similar.

5.2.8 Track Compensator and Steering Accuracy in Virtual World

In the VR environment only, steering was examined using the Track Compensator Value and Dial Value output to the ergometer CSV file by LabVIEW. The results are displayed in Table 7. A participant was classified as "turning" when the track compensator indicator device was displaying a value of 1, 2, 3, 4, or 5, but not 0. This meant that the participant was in the curve of the track and not the straightaway. A technician was classified as "steering" when the dial value was a -1, -2, 1, 2, 3, 4, or 5, but not 0.

The average percentage of the test session spent steering with the track compensator was 58.65% ± 3.74%. Of this active time, the remote desktop dial was used 20.76% ± 7.43% of the time. Of the entire test session, the remote desktop dial and track compensator indicator were used at the same time for 13.75% ± 5.60% of the time. Participant 5 was more accurate at steering in VR than Participant 2.

Table 7. The percentage of the test session spent steering with the track compensator and with the remoter desktop dial for each participant.

Participant ID	% of Time Both Devices Steering/Turning	% of Time Track Compensator Turning	% of Time Technician Steering
1	10.57	59.56	15.30
2	24.90	65.65	35.47
3	12.44	57.89	19.18
4	12.28	56.81	16.92
5	9.63	55.02	17.18
6	12.65	56.99	20.52
Average	13.75	58.65	20.76
Standard Deviation	5.60	3.74	7.43

After a lap or two, many participants were able to engage the track compensator at the right time point going into and coming out of the curve that they did not need as much steering help from the technician.

Four of the ten study participants could not be included in this test as two did not have ergometer data files (Participant Av60p and BL16e), one was complete before LabVIEW was updated to print the *TrackCompValue* and *DialValue* to the CSV file (Participant NjI01), and one came to a test session where the track compensator indicator broke before the test session (Participant Ef63t).

5.3 Qualitative Feedback and Improvements

5.3.1 Overview

A large goal of this study was to improve the VR immersion system. This was done through quantitative and qualitative feedback on perceived presence, perceived exertion, and reported pain. Any failures in the functionality of the VR ergometer system, such as improper RR, may be realized through a participant's reported outcomes.

Before the tests started, a study checklist was made. This checklist was improved throughout the test so that future study coordinators can use it. A list of tools to bring to the RW environment to troubleshoot wheelchair issues was created and a list of things to check before the participant arrives and before a test session begins was also made. These included, for example, wheelchair wheel tightness and track compensator indicator security.

5.3.2 IPQ

The average aggregated IPQ score was 60.00% ± 7.20% (M±SD). The score was summed across all 16 questions and totaled out of 104 possible points. This amounted to an average reported presence of 57.69% ± 6.92%. Figure 42 shows the average score and standard deviation for each question. Note that questions 1-14 were out of six possible points and questions 15 and 16 were out of ten possible points. The largest areas for potential improvement using the results of the IPQ are Questions 1, 2, 7, 11, and 12, as the scores for these questions were the lowest. See Appendix D for a list of the questions.

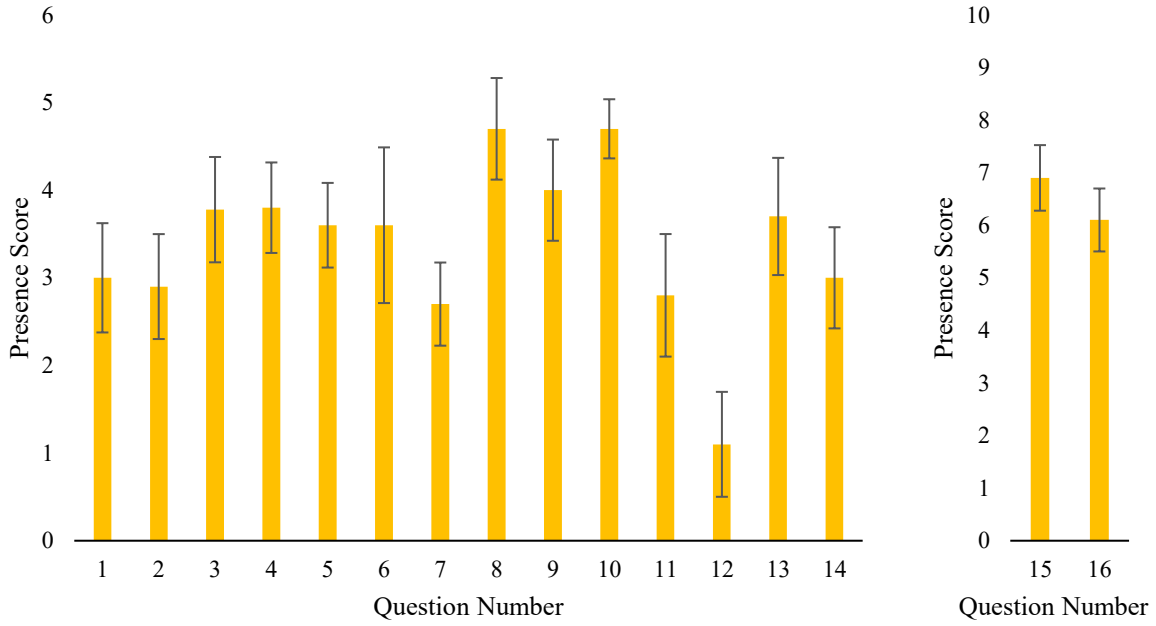

Figure 42. Mean response for each IPQ question with the corresponding standard deviation for each question. Questions 1-14 were out of six possible points and questions 15 and 16 were out of ten possible points (n=10).

The G subcategory had an average score of 3.00 ± 1.25. The SP subcategory had an average score of 3.54 ± 1.23. The INV subcategory had an average score of 0.98 ± 0.49. The SP subcategory had an average score of 2.65 ± 1.27. These questions were all out of 6 possible points and thus the average presence in each subcategory was: G 50.00%, SP 58.93%, INV 16.41%, and EU 44.17%.

Question 17 asked the participants to comment on what they felt was missing from the VR experience. The items included:

- straighter lines on the track,

- smaller, enclosed 3D glasses to increase immersion, [as one participant "*had to use right hand to adjust glasses frequently along with track compensator.*"],
- realistic (less) head tracking, [as "*faraway things moved too fast*"],
- the clock and banners on the walls in the Butterdome and more texture,
- other people in the Butterdome simulation as the Butterdome is usually very busy,
- ambient noise and people talking,
- a feeling of turning the racing wheelchair,
- a fan for wind speed, and
- lighter inertia weights, so it is easier to push in VR.

Many participants also noted that the VR simulation stopped on them, due to communication issues between the track compensator and desktop computer. The lags in communication meant that the steering mechanism in the VR environment would stop working and participants would be unable to steer. This issue was resolved halfway through the study, as outlined in Section 4.4.2. As well, many participants felt like they were moving too slow in the VR environment: "*I felt like I had to put in more effort to keep up my pace in the VR environment, it felt like I was dragging*." and "*Felt as though it was less momentum per push in virtual setting*."

5.3.3 MSAQ

The participants responded to the MSAQ with zeros on all the questions except questions 3, 4, 8, 10, 10A, 10B, and 12. This means that there was very little VIMS. The questions with responses were tied to regular exercise and wheelchair propulsion fatigue. See Appendix E for the exact wording of the MSAQ questions. Before the paired t-tests were completed for these 7 questions, SPSS boxplots were used to check for significant outliers visually and none were found in the Redliner time dataset. Additionally, the Shapiro-Wilk test of normality was completed and significant differences were found for VR Q3 (p=0.000), RW Q 3 (p= .), VR Q8 (p=0.000), RW Q8 (p=0.000), and RW Q10A (p=0.042). Thus, a paired-samples sign test was done instead on these questions.

The results are graphically represented in Figure 43 and Figure 44 for the RW and VR environments, respectively. The average score for question 3 was tied at 0 for all but one case where the VR environment was bigger [RW (M=0.00, SD=0.00) and VR environment (M=0.20, SD=0.63)]. The average score for question 4 was not significantly different in the

RW (M=2.20, SD=1.62) and the VR environment (M=3.60, SD=3.10), t(9)=1.41, p=0.191. The average score for question 8 was not significantly different in the RW (M=0.50, SD=0.97) and the VR environment (M=1.10, SD=2.13), t(9)=1.203, p=0.26. The average score for question 10 was not significantly different in the RW (M=3.60, SD=2.59) and the VR environment (M=2.20, SD=1.55), t(9)=1.71, p=0.12. The average score for question 10A was larger 5/10 times in RW and 5/10 times in VR [RW (M=2.60, SD=1.26) and VR (M=3.70, SD=2.21), p=1.00. The average score for question 10B was not significantly different in the RW (M=3.55, SD=1.01) and the VR environment (M=4.60, SD=2.27), t(9)=1.16, p=0.28. The average score for question 12 was not significantly different in the RW (M=2.60, SD=2.07) and the VR environment (M=3.4, SD=2.67), t(9)=1.00, p=0.34.

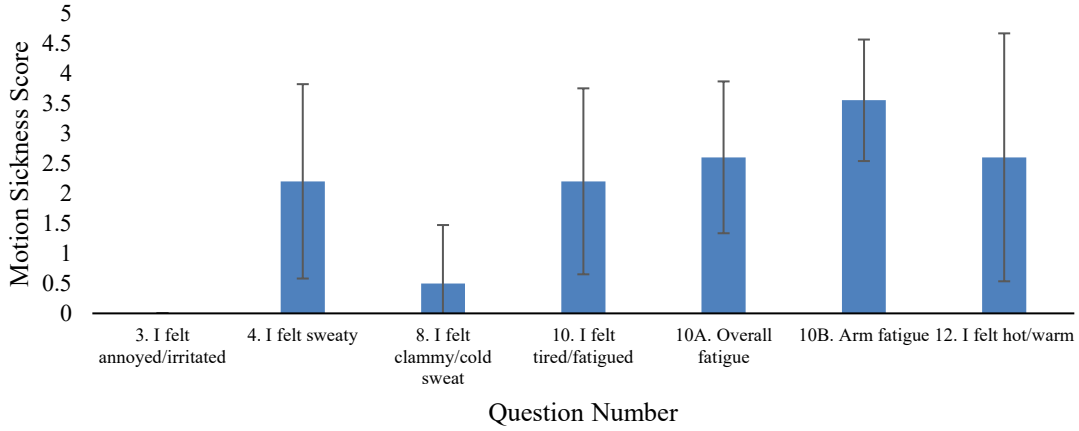

Figure 43. The average score and standard deviation for each question in the RW from the MSAQ (n=10).

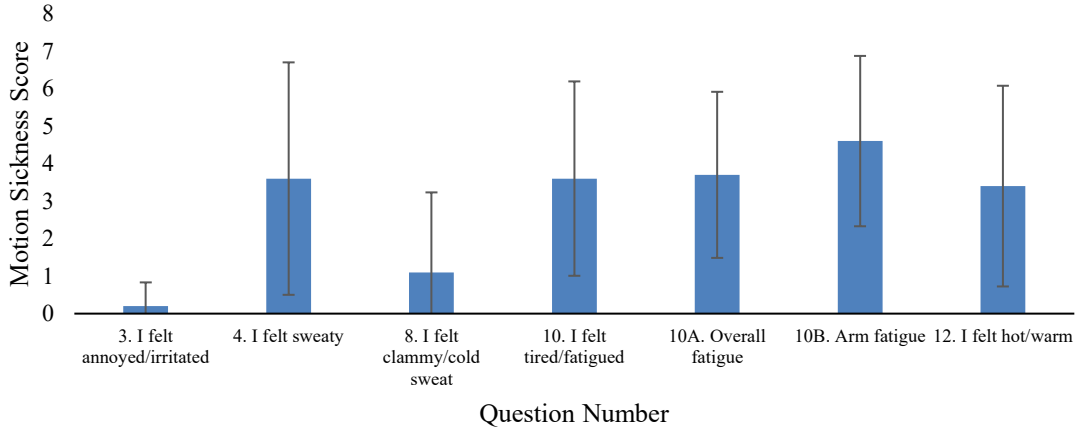

Figure 44. The average score and standard deviation for each question in the VR environment from the MSAQ (n=10).

The GI and C subcategories both had average scores of zero for both test environments. The P subcategory averaged 1.77 ± 1.12 in the RW and 2.70 ± 1.40 in VR environment. The S subcategory averaged 1.39 ± 1.59 in the RW and 2.02 ± 2.17 in VR environment. The T category, the overall score, averaged 0.76 ± 1.23 in the RW and 1.12 ± 1.73 in VR environment. The standard deviations for these categories are similar between the two test environments. The P subcategory data met the assumptions for a paired t-test while the S sub-category and T category did not. The average score for the P subcategory was not significantly different in the RW and the VR environment, $t(2)= -3.88$, $p=0.060$. In the S subcategory, a paired-samples sign test found no significant differences between the two test environments, with ties in 2/6 and the VR reported value being larger in 4/6 cases, $p = 0.13$. In the T category, the paired-samples sign test found a significant difference between the two test environments, with ties in 11/18 cases and the VR reported value being larger in 7/18 cases, $p = 0.016$.

5.3.4 Borg' RPE

The paired t-test or paired-samples sign test was used to compare RPE for each test area (shoulder [S], center [C], and reported overall [O]) by test environment (RW or VR). These tests were performed across the whole of the data series and within the three collection time points (750 meters into test [1], 1500 meters into test [2], and 5-minutes post-test [3]).

Additionally, to explore the relationship between perceived exertion, test environment, and collection time point, the Borg RPE results were also analysed using a linear mixed model. This model compared the means of RPE for each test area (Shoulder [S], Center [C], and Overall [O]) by test environment (RW and VR) and time point (750 meters into test [1], 1500 meters into test [2], and 5-minutes post-test [3]). The RPE values for RW and VR were collected from the same subject, which implies the data is not independent and that the correlation relationship from each group must be addressed. To deal with the existing correlation within participants, a linear mixed model was used to compare the mean difference for collection time point and test area as fixed effects. The p-value shows the significance of the overall mean comparison. Compound symmetry was used as the correlation structure and Satterthwaite df.

5.3.4.1 Paired Tests

The Borg RPE results were examined using a paired t-test and paired-samples sign test, as paired t-tests assume normality and some of the normality tests had p-values that were close

to the threshold. Normality tests for the dataset were approximately normally distributed in the Overall variable for the whole dataset, the Overall variable for the 750-meter dataset, and the entirety of the 1500-meter dataset. A paired t-test was conducted on these variables. Disagreement on normality occurred in the Shoulder and Center test area and in the 5-minutes post-test collection time point. Due to this, a paired-samples sign test was done on the Shoulder and Center variables for the whole dataset, the entirety of the 5-min post-test dataset, and the Shoulder and Center variables for the 750-meter dataset. Figure 45 displays the bar plots for two study participants. See Appendix F for the Borg RPE scale and questions.

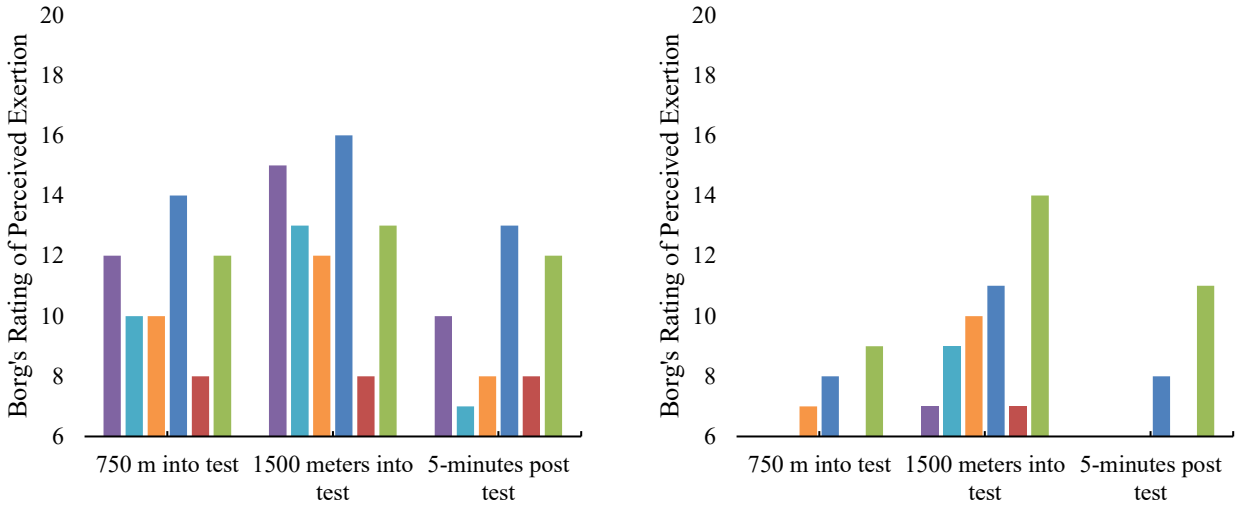

Figure 45. Left) RPE for participant LV3rT. Right) RPE for participant BL16e. RW Shoulders in purple, RW Center in light blue, RW Overall in orange, VR Shoulders in dark blue, VR Center in red, and VR Overall in green.

Across all three sampling times, the exertion reported by participants in their shoulders in the RW (M=9.95, SD=2.90) was significantly less than the exertion reported by participants in their shoulders in the VR environment (M=11.68, SD=3.29), $p < 0.0001$. Across all three sampling times, the exertion reported by participants in their center in the RW (M=7.48, SD=1.97) was not significantly different from the exertion reported by participants in their center in the VR environment (M=7.02, SD=1.12) with ties in 17/30 cases, p=0.27. Across all three sampling times, the exertion reported by participants overall in the RW (M=9.23, SD=2.45) was significantly smaller from the exertion reported by participants overall in the VR environment (M=10.91, SD=3.22), t(29)= -2.73, p=0.011). The standard deviations were similar for these tests. In the first two cases, the environment variables are correlated (S:

r=0.69, p<0.001; C: r=0.62, p<0.001) while in the overall category RW and VR are not correlated (O: r= 0.31, p=0.093).

At the 750 meter time point, the exertion reported by participants in their shoulders in the RW (M=10.10, SD=1.73) was significantly less than the exertion reported by participants in their shoulders in the VR environment (M=11.80, SD=2.15), p=0.017. At the 750 meter time point, the exertion reported by participants in their center in the RW (M=7.40, SD=1.35) was not significantly different from the exertion reported by participants in their center in the VR environment (M=7.00, SD=0.94), with ties in 6/10 cases, p=0.19. At the 750 meter time point, the exertion reported by participants overall in the RW (M=9.25, SD=1.51) was not significantly different from the exertion reported by participants overall in the VR environment (M=10.85, SD=2.29), t(9)= -1.74, p=0.12. In the first two cases, the environment variables are weakly and positively correlated (S: r=0.75, p=0.012; C: r=0.70, p=0.025) while in the overall category RW and VR are not correlated (O: r= -0.14, p=0.69).

At the 1500 meter time point, the exertion reported by participants in their shoulders in the RW (M=12.45, SD=2.63) was not significantly different from the exertion reported by participants in their shoulders in the VR environment (M=13.90, SD=2.38), t(9)= -1.57, p=0.15. At the 1500 meter time point, the exertion reported by participants in their center in the RW (M=8.85, SD=2.56) was not significantly different from the exertion reported by participants in their center in the VR environment (M=7.75, SD=1.23), t(9)= 1.47, p=0.18. At the 1500 meter time point, the exertion reported by participants overall in the RW (M=11.65, SD=1.70) was not significantly different from the exertion reported by participants overall in the VR environment (M=12.80, SD=2.57), t(9)= -0.95, p=0.37. In all cases, the two environment variables are not correlated (S: r=0.32, p=0.37; C: r=0.39, p=0.26; O: r=-0.60, p=0.073).

At the 5 minutes post-test time point, the exertion reported by participants in their shoulders in the RW (M=7.30, SD=1.57) was significantly less than the exertion reported by participants in their shoulders in the VR environment (M=9.35, SD=3.61) (8/10 cases), p=0.008. At the 5 minutes post-test time point, the exertion reported by participants in their center in the RW (M=6.20, SD=0.42) was not significantly different from the exertion reported by participants in their center in the VR environment (M=6.30, SD=0.67) (ties in 7/10 cases), p=1.00. At the 5 minutes post-test time point, the exertion reported by participants overall in

the RW (M=6.80, SD=1.03) was not significantly different from the exertion reported by participants overall in the VR environment (M=9.10, SD=3.73) (ties in 3/10 cases), p=0.13. In all cases, the two environment variables are not correlated (S: r=0.60, p=0.067; C: r=0.55, p=0.10; O: r=-0.27, p=0.46).

5.3.4.2 Linear Mixed Model

The RW and VR for each time point are shown in Figure 46, Figure 47, and Figure 48. It is worth noting again that the minimum value for this questionnaire is six. All three graphs show an increase in reported exertion at the 1500-meter time point but that the 5-min post-test time point had the lowest reported exertion. The linear mixed model showed that the test environments ($F = 31.78$, $p < 0.0001$) and collection time points ($F = 13.65$, $p = 0.001$) were significantly different from each other for reported exertion in the shoulder. For reported exertion in the participant's center, it showed that the test environments ($F = 2.26$, $p = 0.14$) were not significantly different but that the collection time points ($F = 13.65$, $p = 0.001$) were significantly different from each other. Finally, the test environments ($F = 19.07$, $p < 0.0001$) and collection time points ($F = 9.20$, $p = 0.004$) were significantly different from each other as reported by the participants overall.

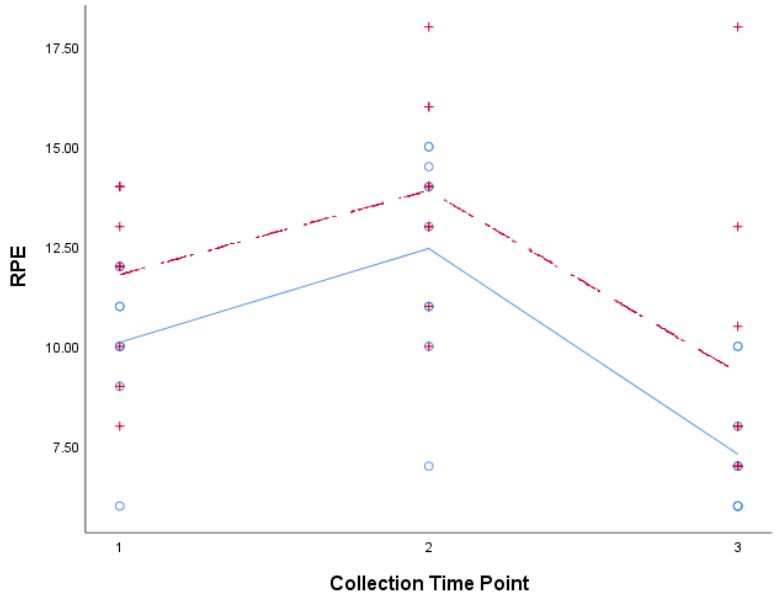

Figure 46. The RPE for all participants for their shoulders with RW data points being represented by blue circles and VR data points being represented by red crosses. The means for each time point (1, 2, and 3) are represented by blue lines for the RW test environment and red lines for the VR test environment.

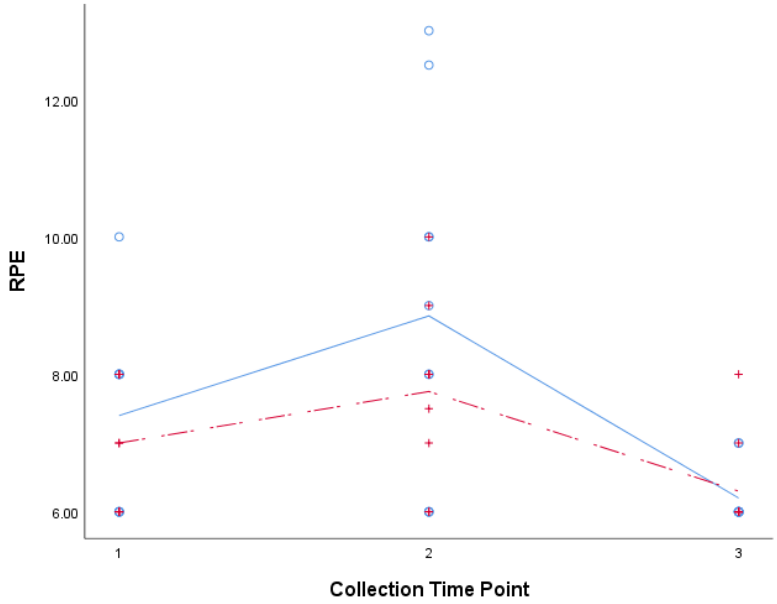

Figure 47. The RPE for all participants for their center with RW data points being represented by blue circles and VR data points being represented by red crosses. The means for each time point (1, 2, and 3) are represented by blue lines for the RW test environment and red lines for the VR test environment.

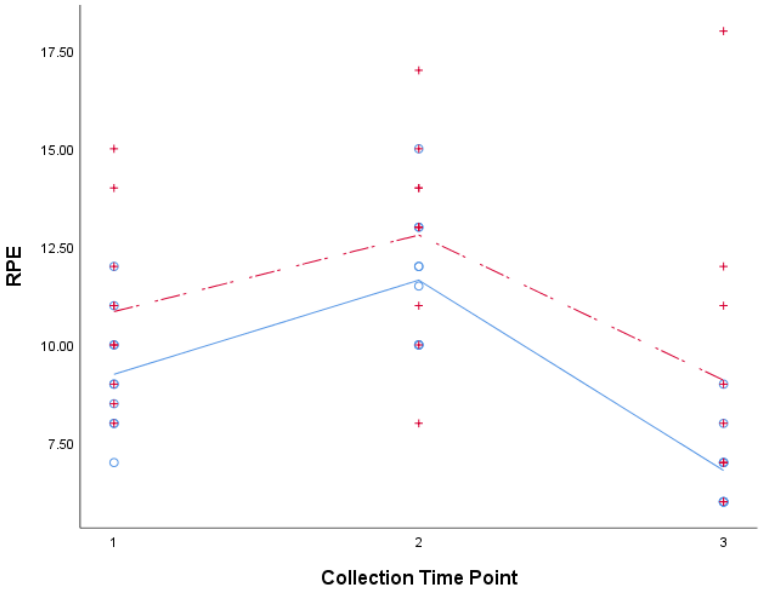

Figure 48. The RPE for all participants overall with RW data points being represented by blue circles and VR data points being represented by red crosses. The means for each time point (1, 2, and 3) are represented by the black lines with the bolder line being the VR test environment and the thinner line being the VR test environment.

5.3.4.3 Pearson's Product-Moment Correlation Coefficient

The final test conducted for this dataset was a Pearson's correlation as the shoulder and overall categories seemed to be correlated. There was a strong, positive correlation between shoulder perceived exertion and overall perceived exertion, which was statistically significant ($r = 0.85$, $n = 60$, $p < 0.0001$). There was also a weaker, positive correlation between center perceived exertion and shoulder perceived exertion and between center perceived exertion and overall perceived exertion, both of which were statistically significant ($r = 0.50$, $n = 60$, $p < 0.0001$; $r = 0.52$, $n = 60$, $p < 0.0001$).

5.3.4.4 Pearson's Chi-Square Test

For categorized outcome, McNemar's test or generalized McNemar's test (aka Stuart-Maxwell test) was considered to examine the association between RW and VR based on matched pair data. However, McNemar's test cannot be performed as the number of categories for RW and VR is not identical. A Pearson's Chi-square test was also considered but would have required combining many of the Borg RPE categories into larger blocks as many rows and columns summed to zero.

5.3.5 WUSPI

The participants responded to the WUSPI for questions 5, 7, 8, 9, 10, 11, 12, 13, 14, and 15. This was because many of the questions asked about tasks that the non-disabled participants had never performed. They were instructed to mark these as "Not Performed." Each question was out of ten. Only the questions that received responses were analyzed with a paired-samples sign test between the RW and VR environment. The average and standard deviation for these questions are presented graphically in Figure 49. One participant did not respond to any of the questions on this questionnaire and thus the sample size is 9 for this questionnaire. The participant missed responding to this questionnaire by accident, perhaps the questionnaire sheets of paper got stuck together, and the error was not noticed until after the participant had left the RRL. See Appendix G for the list of WUSPI questions in this study. The data was not normally distributed and had outliers because of many scores of zero and so a paired-samples sign test was done instead of a paired samples t-test.

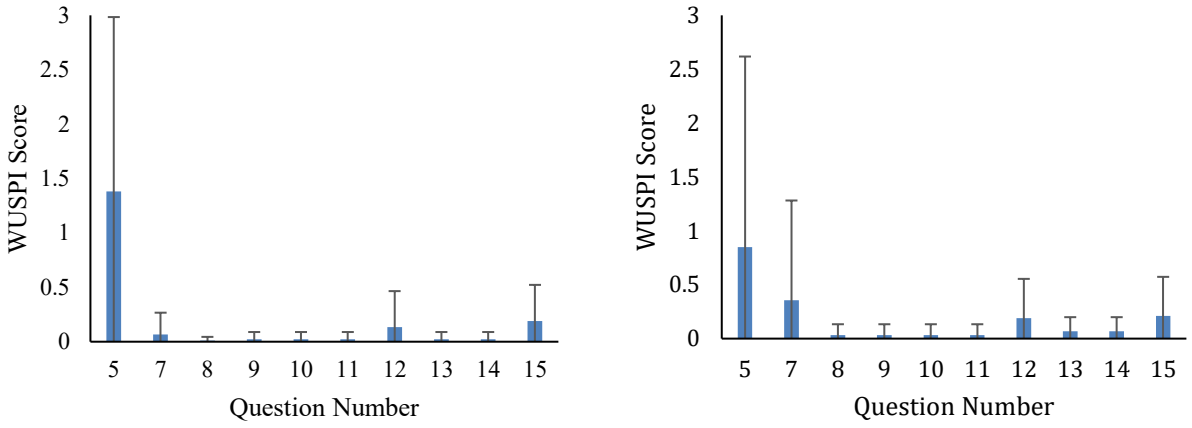

Figure 49. The WUSPI average score and standard deviation for each question in the RW from the WUSPI questionnaire (left). The average score and standard deviation for each question in the VR environment from the WUSPI questionnaire (right).

Most of the variation for this questionnaire was in question 5: "Pushing your wheelchair for 10 minutes or more?"; however, none of the results were significantly different from each other. The average score for question 5 in the RW (M=1.01, SD=1.17) was greater 5/9 times as compared to the VR environment (M=0.31, SD=0.50), p=0.074. The average score for question 7 was tied 6/9 times between environments [RW: M=0.07, SD=0.20; and VR: M=0.36, SD=0.93; p=0.59]. The average score for question 8 was tied 7/9 times between environments [RW: M=0.01, SD=0.03; and VR: M=0.03, SD=0.10; p=0.66]. The average score for question 9 was tied 7/9 times between the two environments [VR: M=0.02, SD=0.07; and VR: M=0.03, SD=0.10; p=0.66. The average score for question 10 was tied 7/9 times between the two environments [RW: M=0.02, SD=0.07; VR: M=0.03, SD=0.10; p=0.66]. The average score for question 11 was tied 7/9 times between the two environments [RW: M=0.02, SD=0.07; and VR: M=0.03, SD=0.10; p=0.66]. The average score for question 12 was tied 5/9 times between the two environments [RW: M=0.13, SD=0.33; VR: M=0.19, SD=0.37; p=0.72]. The average score for question 13 was tied 6/9 times between the two environments [RW: M=0.02, SD=0.07; VR: M=0.07, SD=0.13; p=0.28]. The average score for question 14 was tied 6/9 times between the two environments [RW: M=0.02, SD=0.07; VR: M=0.07, SD=0.13; p=0.28]. The average score for question 15 was tied 6/9 times between the two environments [RW: M=0.19, SD=0.33; VR: M=0.21, SD=0.36; p=0.60].

5.3.6 VAS

The questionnaire for the VAS is presented in Appendix H. The data was not normally distributed pretest in both test environments and had outliers pretest because of many scores of zero. A paired-samples sign test was done instead of a paired samples t-test. The differences between the scores met the assumptions of paired t-test.

The pretest shoulder pain (M=0.26, SD=0.72) was significantly smaller than the post-test shoulder pain (M=1.90, SD=2.03) reported by participants in the RW environment (6/10cases smaller, 4/10 cases were ties), p=0.031. The pretest shoulder pain (M=0.56, SD=1.14) was also significantly smaller from the post-test shoulder pain (M=2.32, SD=2.20) reported by participants in the VR environment (8/10 cases smaller, 2/10 ties), p=0.008. The pretest and post-test were not correlated either, r=0.57, p=0.85. However, the difference in post-test shoulder pain and pretest shoulder pain was not significantly different in the RW environment (M=1.64, SD=1.66) and the VR environment (M=1.76, SD=1.81), t(9)= -0.210, p=0.84. This dataset was normally distributed and did not have significant outliers.

A Friedman test was completed instead of a two-way ANOVA as the assumption of normality was violated. There was a statistically significant difference in shoulder pain in the two environments at the various test time points $\chi^2(2) = 16.94$, $p = 0.001$. The recommended post hoc test was a Wilcoxon signed-rank test. A Bonferroni adjustment on the results from the Wilcoxon tests leads to a new p-value of 0.025. There were no significant differences between the RW pretest and post-test trial (Z = -2.21, p = 0.027). There were significant differences between the VR pretest and post-test trial (Z = -2.52, p = 0.012) (Figure 50B).

Visually, the participant's reported shoulder pain did not differ much between the RW (M=1.08, SE=0.40) and the VR environment (M=1.44, SE=0.47) (Figure 50A). However, the participant's reported shoulder pain was lower at the pretest sample time (M=0.41, SE=0.21) as compared to the post-test sample time (M=2.11, SE=0.58) (Figure 50B).

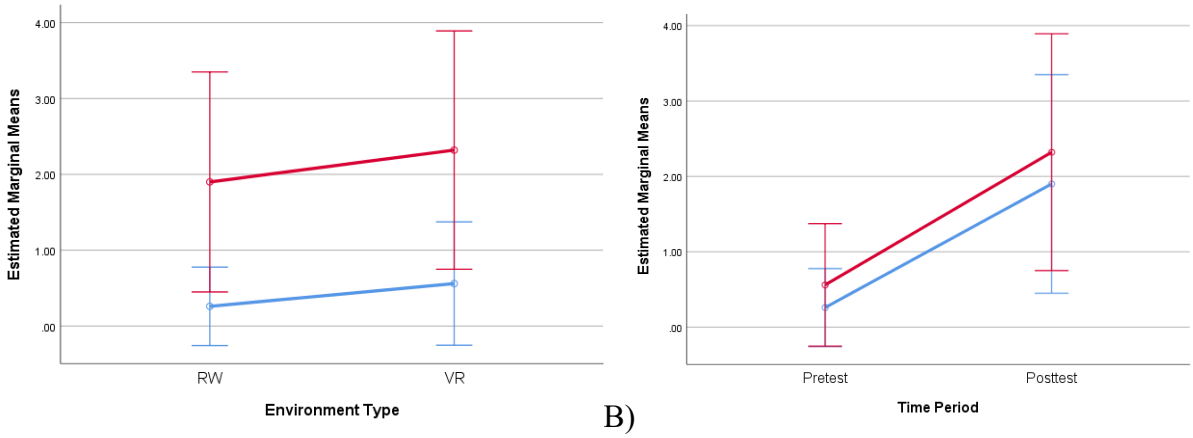

A) B)

Figure 50. A) The average reported shoulder pain as shown by environment type, with pretest in blue and post-test in red. B) The average reported shoulder pain at the two collection times, with RW in blue and VR in red.

5.4 Inertia Weights

The best approach to determine where the inertia weights should be set when the rollers were coupled was still uncertain. The settings will need to be confirmed in the full-scale study, but here the goal was to determine the best approach to matching the inertia of the rollers to the dynamic inertia of the RW. Several different parameters can be used to determine the best setting for this comparison.

5.4.1 Moment of Inertia Calculation

The moment of inertia for the rollers was mathematically calculated to confirm that the on-file value of 0.66 kgm^2 was accurate. Each roller is a cylinder with characteristic mass and inertia properties. The inertia was calculated as follows with Figure 51 as a reference roller/cylinder and Figure 52 showing the corresponding RW measurements. Note that each roller has two radiuses to be concerned with as they have an overhang.

$$I = \frac{1}{2} m\,(r_2{}^2 + r_1{}^2) = m r_2{}^2 (1 - t + \frac{t^2}{2})$$

Where $t = r_2 - r_1$ = thickness of tube.

First, the mass of the roller needed to be calculated.

$$m = area \times height \times \rho$$

Where ρ = density of the steel.

$$Area\ of\ Shell = \pi(2r_2t - t^2)$$

$$Mass\ of\ Roller = \pi\rho h(2r_2t - t^2)$$

$$= 15.86\ kg$$

Where, from Figure 52,

ρ = 7850 kg/m^3
h = 0.456 meters
t = 0.0045 meters
r_2 = 318mm ÷ 2 = 0.159 meters

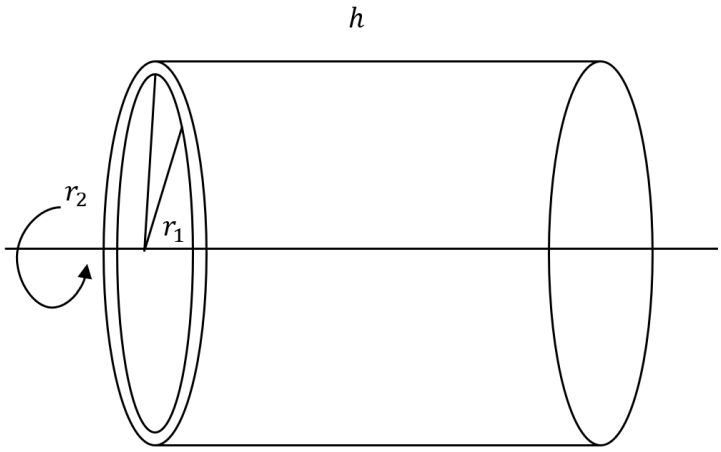

Figure 51. Diagram of one of the rollers to show the dimensions.

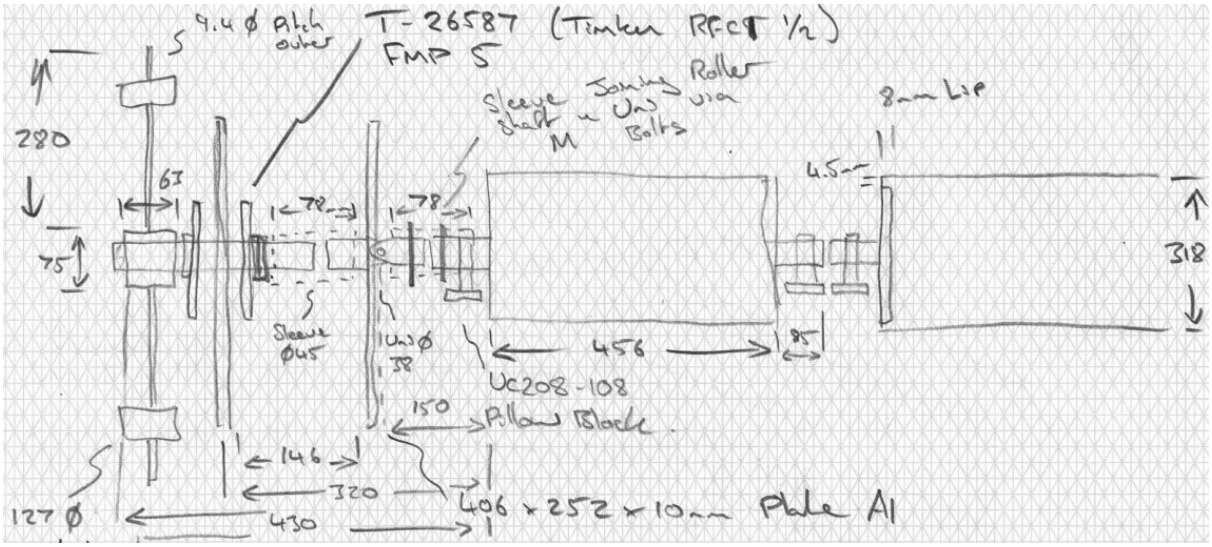

Figure 52. A hand drawn schematic of the wheelchair ergometer's rollers complete with dimensions in millimeters (McKenzie, 2018)

The endcap mass can be calculated as:

$$Mass\ of\ End\ Caps = \rho\pi t(r_2 - t)^2 = \rho\pi t{r_2}^2 = 2.81\ kg$$

$$Total\ Mass\ of\ Roller = 15.86 + 2.81 + 2.81 = 21.48\ kg$$

The inertia of the cylinder and disk can be written as

$$I_{cyl} = m{r_2}^2\left(1 - t + \frac{t^2}{2}\right) = m{r_2}^2 = 21.48 \times 0.159^2 = 0.54\ \text{kg}m^2$$

$$I_{disk} = \frac{1}{2}mr^2 = \frac{1}{2} \times 2.81 \times 0.159^2 = 0.035\ \text{kg}m^2$$

$$I_{Tot} = 0.54 + 0.035 + 0.035 = 0.61\ \text{kg}m^2$$

This calculated inertia was close enough to the on-file value of 0.66 kgm^2. The on-file value was used going forward.

5.4.2 Error Between the Two Environments

To indicate how to select the optimum PSL in the future, another protocol was developed which did not depend on the ratio of power between the two environments. Additionally, it was done using the velocity of the RU phase as this appeared to be the phase where the participants commented it was more difficult to push within than in the VR environment. The minimum error between the two test environments was calculated and used to indicate the best PSL for the 90.3 kg participant. The error between the two test environments was calculated by subtracting the RW average velocity value for the RU phase from the VR average velocity for the RU phase: $Error = RU\ v_{VR} - RU\ v_{RW}$. These errors were graphed as a function of the PSL they occurred at and are presented in Figure 53. The equation of the line is 0.34x – 1.045 and the $R^2 = 0.73$. Where the error is zero, the difference between the RU phase velocity in the two worlds is the smallest.

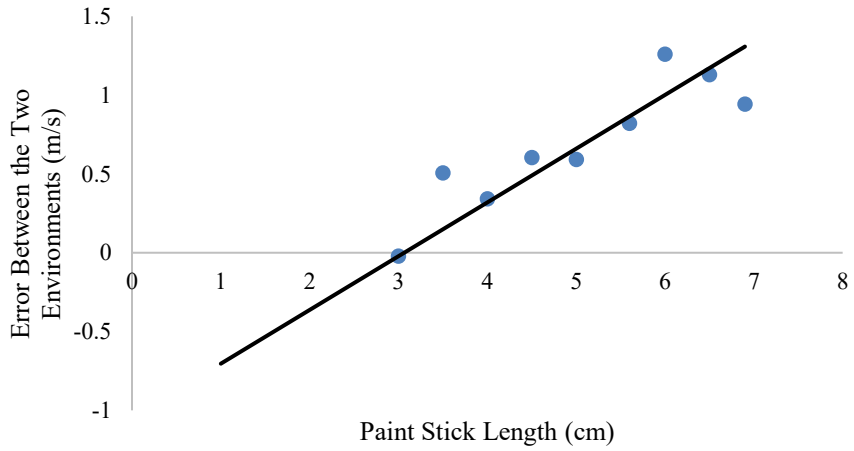

Figure 53. The error between the two environments for velocity (m/s) graphed as a function of PSL (cm). The equation of the line is 0.34x – 1.045 and the $R^2 = 0.73$.

The minimum error in RU phase velocity was selected as the power method had proved to be too subjective to the mass inputted into MATLAB (Section 4.5). RU phase energy was not used because it was dependent on the total number of pushes that the participant put in to get up to their SS velocity. The RU phase was chosen as it was the phase where the force of inertia plays more of a role (Section 4.5.3).

6. Discussion

The experimental sample size was 10 as the university shut down due to the COVID-19 crisis and was made up of 3 males and 7 females. From the experimental results of SS velocity and power, 12.00 subjects and 7.34 subjects (8 subjects) was recommended (Appendix A). The variability in each participants' chosen velocity contributes to this larger sample size from velocity. This sample size calculation was done with a comparison of means using the data from the seven participants who did not have missing wheel data.

There were clear differences in the velocity plots in the RW and the VR environment. From the standard deviations in the two environments, the RW is more consistent in the number of pushes as compared to the VR environment. The RW had more pushes to get to SS than the VR environment. It is logical that there would be fewer pushes to get to a SS if the SS phase begins at a lower relative velocity. The vibrations following the pushes on the velocity trace in the VR environment without the low-pass filter applied, could be the result of additional vibrations from the rollers. The technician can often hear the vibrations from the belt upon roller slow down during tests with the belts on. More vibrations would be seen if the participant had trouble overcoming the inertia weights. The participant would stay in the RU phase for longer and feel more vibrations, as the rollers vibrate more at the beginning of the test in the RU stage. It was noted that if the participant spent a longer time overcoming the inertia weights and trying to get up to SS velocity, the pushes were greater in their vertical magnitude of variation as well as closer together. This might be because the participant slows down faster, seen as a steep drop on the velocity trace. This is a clear example of the VR environment being more difficult to propel in than the RW.

6.1 Quantitative Measures

The low-pass filter was very effective at removing vibrations from the velocity trace and ensuring accurate calculations of cadence. The filter should remain below 0.025 Hz to ensure optimal usage and a robust number of samples. The cadence in the RW was larger when compared to the VR environment throughout the whole test. This might be the result of participants being unable to overcome the inertia weights. This decrease in cadence is tied to a decreased velocity in the VR environment. Once the participants got up to their SS velocity,

there was no significant difference in the cadence between the two environments. This supports the idea that SS propulsion between the two environments is the same.

The average velocity throughout the test, peak velocity, and the RU phase velocity were all greater in the RW. The participants traveled faster in the RW than in the VR environment overall. The smaller velocities for the test in VR might be due to greater resistive forces experienced in VR. Additionally, it could be due to the few cases where the track compensator indicator dropped out and the participant had to stop. At these points, the participant's speed dropped to zero or near-zero until the connection was restored. These instances would have lowered the average, peak, and RU phase velocities.

The paired-samples sign test found that the ergometer velocity was situated above the Redliner VR velocity and below the Redliner RW velocity. The ergometer velocity is significantly smaller than the Redliner RW velocity and larger than the VR Redliner velocity, but not significantly so. The ergometer velocity is the average velocity throughout the entire test, just like the Redliner velocity. This suggests that the VR Redliner velocity is underreporting. Perhaps the vibrations from the wheelchair ergometer lead to more interference in the velocity traces. Additionally, a Butterworth filter is applied before computing velocity with Redliner and this may decrease the overall velocity. Redliner is theoretical in how it measures dynamic quantities (Figure 19 and Figure 20); Redliner is an inferring measurement device while the ergometer directly measures velocity and acceleration. In the future, Redliner should be calibrated against the wheelchair ergometer. Additionally, the smaller average velocity for the test in VR might also be due to the few cases where the track compensator indicator dropped out and the participant had to stop. At these points, the participant's speed dropped to zero or near-zero until the connection was restored. Additionally, in the RW the participants can wheelie or shift their weight to steer. This creates noise in the Redliner linear velocity dataset as one wheel may be held stationary while the other moves or a wheel might move backwards in a wheelie maneuver.

Both the peak and RU phase accelerations were not different from each other in the two environments. As $Force = ma$, this is again suggestive that the force between the two environments is not different. However, it should be noted here that the accelerations in the VR environment were slightly smaller than in the RW environment. The average accelerations as shown by Redliner were not different from each other as both the RW and VR environment

values were 0.000 m/s^2 for all participants. It is also worth noting that the ergometer shows accelerations on the computer screen in LabVIEW, but it has not been clarified how LabVIEW sends this data out to the CSV file yet. If this could be clarified, then the ergometer accelerations could be compared to the Redliner accelerations.

The distance traveled was smaller than the expected 1434.47 meters outlined in Table 2. Using Redliner, the VR environment was smaller by 52.23 meters and the RW environment was smaller by 165.71 meters. The fact that the VR distance traveled was significantly greater, at 1382.24 ± 70.51 meters, could be due to the greater drifting done by participants in VR. It was more likely that participants would veer in the VR environment if they over or understeered, which would happen if they started turning too early or too late in the VR environment. Even though the technician had the desktop dial to set them back on course, this could still lead them to travel further overall. Participant LV3rT was adamant about staying in their lane throughout the entirety of the RW test and they traveled 1310.97 meters in their RW test. In the VR environment, they tried to be as precise, but they still traveled further in the VR environment, 1368.24 meters.

Again, the ergometer value was between the Redliner values. The ergometer distance traveled was larger than the RW distance traveled from Redliner but smaller than the VR distance traveled collected by Redliner, but not significantly in either case. This is the opposite of what occurred with the velocity data but is in line with the fact that velocity was smaller and distance traveled was larger in the VR environment. Interestingly, the participants went further in VR even though they started a few meters back on the track in RW. The wheelieing might create a larger effect in the RW than anticipated and the VR Redliner distance traveled might be more accurate.

In line with the distance traveled being greater and the velocity overall being smaller, the time taken to complete the VR test was greater. It took 1.67 times longer to complete the trial in VR than in the RW. The Redliner RW time reported was significantly smaller than the ergometer time. The Redliner VR time reported was larger than the wheelchair ergometer time reported but not significantly. This finding is in line with the distance data. The longer time for the test in VR might also be due to the few cases where the track compensator indicator dropped out and the participant had to stop.

The time interval being not significantly different between the two test environments shows that the Redliner devices measured time equally and consistently between the two environments. There was one participant in the RW and another participant in the VR environment where the average time interval between samples was >45 microseconds. This should be avoided and improved in future studies to make comparing between datasets of participants more reliable.

The SS phase power was not different between the two test environments. This result, in addition to the acceleration above, implies that the RR is the same between the two environments and suggests that overcoming the inertia weights is the problem. This is because the power required to propel the wheelchair once at a SS is the power required to overcome the RR (Figure 32). This result is also in line with the findings in Section 4.3.4 where the difference in the force of RR was found to be -1.43 lbs. Interestingly as well, the RU phase power was not different, which implies that overall the power does not differ between the two environments.

The amount of energy used in the RU phase was different between the two environments though, higher in the RW environment. This seemed to be somewhat the result of the number of pushes that were used to get to SS in both environments. If the participant does not get to a relatively larger SS velocity, there are likely less pushes to sum over to result in a higher total energy. In this study, the number of pushes used by a participant in the RW to get up to SS was significantly larger than that of the VR environment. The correlation between the total energy and number of pushes to get to SS should be examined going forward with research studies.

Not surprisingly, given that the accelerations were not different between the two test environments, the force in the RU stage was not different between the two environments. This suggests that the inertia weights are the factor that is causing study participants to complain that the VR environment is more difficult to propel in than the RW. The VR RU phase forces were slightly lower; this may be the result of slightly smaller accelerations being output by participants in VR because it is more difficult to propel here.

The average percentage of the test session spent steering with the track compensator was 58.65% ± 3.74%. The participants turned for more than half of the test session in all participant cases. This should be compared to the RW environment in the future. Of this active

time, the remote desktop dial was used for 20.76% ± 7.43% of the time. Both the track compensator indicator and the remote desktop dial were used at the same time for 13.75% ± 5.60% of the test. The % of time that both steering devices were used at the same time varied more than the % of time that the track compensator indicator was actively turning. This could point to variation in participants' steering skills. Thus, some participants needed more or less help from the technician with steering in the VR environment.

Overall, the standard deviations between the two test environments were similar. Differences occurred in whole test cadence, ergometer distance traveled, time taken to complete each test session, RW RU phase power, and energy to get to SS. The SS cadence had similar standard deviations between the two worlds, while the whole test cadence had a standard deviation in the VR environment that was double that of the RW. The ergometer distance traveled had a greater standard deviation than both Redliner datasets from both test environments. The standard deviations for the time taken to complete each test session were different between the two test environments and the two collection devices. The standard deviation of the RW RU phase power dataset appears to be twice that of the VR dataset. The standard deviations in the RW for the RU phase energy are larger than the VR environment.

6.2 Qualitative Measures

The IPQ was not as high as necessary to report high quality immersion in VR. The average presence in each subcategory was: G 50.00%, SP 58.93%, INV 16.41%, and EU 44.17%. An average reported presence of 57.69% ± 6.92% overall is mediocre but this should be improved by implementing some of the participants' suggested changes. The 3D software can be used to make the lines on the track appear more congruent on the straightaways and this will ensure that the lines appear straighter. Additionally, ensuring optimal alignment of the projector grid alignment and EON Studios gird alignment programs will also help. The 3D simulation is also being improved through work with EON Virtual Reality, the supplier of the ICube. They have supplied the RRL with another 3D glasses print file, but it is proving to be difficult to print on the RRL's 3D printer and this needs to be explored further. Note that this design supplied by EON might not fit every participant and so this issue might need to be examined again going forward. The head tracking issue was resolved by recalibrating the

Vicon motion capture system used to track the participant's head inside the ICube. The VR simulation can be improved by the RRL's 3D graphic design team in the coming months by adding the clock and banners to the walls in the Butterdome, creating more texture and details in the environment, and adding avatars to the simulation. Ambient sound recordings taken from the actual Butterdome have already been implemented. The inertia weights will need to be further examined in a subsequent study using the techniques outlined above. The greatest areas of improvement using the results of the IPQ are Questions 1, 2, 7, 11, and 12. The participants were too aware of the RW while in VR and felt that the VR environment was not as realistic as the RW. The awareness of the RW should be decreased through the addition of a fan for windspeed, a soundtrack playing audio of the Butterdome and track noises associated with wheelchair propulsion at levels consistent with the participant's speed, enclosure of the ICube with the curtain while also allowing the observation camera to see inside, and the addition of an earpiece microphone system for communication with the participant. Each of these suggestions touches on noticeable deviation from the RW. For example, in cycling on level ground at speeds above 8 m/s with no wind, air resistance accounts for over 80% of the total resistance (Hedrick et al., 1990). Therefore, aerodynamics and the accurate representation of windspeed are a necessary component of developing an immersive VR experience.

The fact that many of the MSAQ questions were answered with zeros supports the idea that straight-line wheelchair propulsion in the ICube does not create as much VIMS as maneuverability tasks do. While using the ICube with four-wheeled wheelchair and maneuverability tests, Salimi (2012) found that a maximum of four acclimatization sessions held on different days before the experimental trial was enough to resolve motion sickness or reduce it to a tolerable level and ensure that the results were not impacted by VIMS. None of the questions in MSAQ were different between the two environments and thus the participants did not experience a debilitating event of VIMS without a full-scale acclimatization protocol. The GI and C subcategories both had average scores of zero for both test environments and thus were not different between the two test environments. The differences in the P and S subcategories were not significantly different. In the T category, a paired-samples sign test found a significant difference between the two test environments, with ties in 11/18 cases and the VR reported value being larger in 7/18 cases, $p = 0.016$.

The Borg RPE differed between the two environments in a few instances. First, the exertion reported by participants in their shoulders and overall, across all three sampling periods, was significantly larger in VR than in the RW. To further examine this, the sessions were broken up into 750-meters into the test, 1500-meters into the test, and 5-minutes post-test. In the 750-meter session, the exertion reported by participants in their shoulders was again significantly smaller in the RW than in the VR environment. At the 1500-meter session, none of the test areas were significantly different between the two test environments; however, they were the highest average reported exertions of the three test sessions. After the 5-minute post-test session, the exertion reported by participants in their shoulders was again significantly less in the RW environment than the VR environment. All other cases not mentioned were not significantly different. Thus, the shoulder exertion was less in the RW than in the VR environment except at the stage where the greatest exertion would be expected, the 1500-meter time point. Figure 46, Figure 47, and Figure 48 all show an increase in reported exertion at the 1500-meter time point but that the 5-min post-test time point has the lowest reported exertion. It is possible that, because most of the participants did the VR session after the RW session, some residual exertion was experienced by the participants upon beginning their VR session. However, it is also possible that the increase was due to an increased exertion needed to propel in the VR environment. Given the fact that the pretest pain with the VAS was zero in 9/10 participants, the latter explanation is more likely.

The linear mixed model showed that the overall mean score was different between the two test environments and collection time points for the shoulder test area. For the center test area, the test environment was not but the collection time point was significantly different for reported exertion. For the overall test area, the reported exertion was different for both the test environment and collection time point. From this test, the collection time point has a greater influence on the reported exertion than the test environment did. Thus, the immersion and accuracy of the VR system should still be improved. The shoulder perceived exertion and overall perceived exertion were correlated. This might be because the overall feeling of exertion that participants felt was more tied to the higher exertion they felt in their arms and shoulders as muscle fatigue (Qi et al., 2015). Wheelchair propulsion demands a relatively low cardiovascular response and this might have led to a lower center perceived exertion level. When participants were asked how they felt overall, they might have been more drawn to

higher exertion level they felt in their shoulders and may have been skewed upwards rather than report a balanced score over their whole body.

Many of the responses to the WUSPI were zeros or "Not Performed." It was not expected that the healthy, young population used in this study would have a history of shoulder pain. Shoulder pain is a critical metric in MWUs as many MWUs have pre-existing shoulder or upper extremity pain and pathology. From the WUSPI questionnaire taken in both test environments, none of the results were significantly different from each other and every question had 3–7 zeros out of 9 responses.

The VAS paired-samples sign-tests showed, unsurprisingly, that the post-test shoulder pain was always larger than the pretest shoulder pain. The pretest shoulder pain was significantly smaller than the post-test shoulder pain in both test environments. A Friedman test found a statistically significant difference in shoulder pain in the two environments at the various test time points. There were no significant differences between the RW pretest and post-test trials, but there were significant differences between the VR pretest and post-test trials. Since these individuals do not have a history of shoulder pain, they would not be exasperating any existing issues by propelling. Additionally, the difficulty that the participants had propelling in the VR environment might not be classified by the participants as pain. Since the RW did not have significant differences in shoulder pain pre and post-test but the VR environment had larger post-test reported shoulder pain, the VR environment might require more energy expenditure than the RW. It is possible that RPE and shoulder pain through the VAS are correlated with this relatively low exertion task and low preexisting shoulder pain population. In the future, these should be examined to improve these questionnaires in this population.

6.3 Inertia Weights

The inertia for the 75.2 kg participant should be replicated with uncoupled rollers at 13.1 cm. The inertia represented by this is 0.85 kgm^2. It is worth noting that this calculation does not consider the weight of the wheelchair, which is needed going forward. The inertia for the 90.3 kg combination should be 1.02 kgm^2. The roller inertia of 1.32 kmg^2 for the coupled

rollers presents a problem. The coupled roller inertia can never get below 1.32 kgm^2 as inertia is summed with the addition of new bodies and the inertia of one roller is 0.66 kgm^2.

However, it is worth noting that, with the light set of weights, participant Ef63t was supposed to have been given a PSL of 3.6 cm, according to the regression line y = 0.24x – 10.91, but that they were given a PSL of 3.0 cm instead. They commented that propelling was much easier than the first time they had propelled in the VR system at the setting provided by Dr. Salimi's equation for uncoupled rollers. Section 4.5.2 suggests that just under halving the original PSLs for participants might lead to the correct PSL as the uncoupled 13.1 cm PSL and coupled 6.5 cm PSL did not have significantly different accelerations and decelerations. Additionally, the uncoupled 13.1 cm PSL and coupled 5.0 cm PSLs were different from each other, but the decelerations at these settings were not. This might further suggest that the RU phase is more important when discerning the difference between the two test environments.

Furthermore, the SS cadence and SS power are not different between the two test environments. This implies that the SS phase is not responsible for creating the forces that are not representative of the RW. The power required to propel the wheelchair once at a SS is the power required to overcome the RR (Figure 32).

A protocol for testing the next set of inertia weights was developed. The next inertia weight tests should be done with the light set of inertia weights cut to half the thickness again (0.01778 meters / 2 = 0.0089 meters). This is because the error in Figure 53 was zero at 3.0 cm, which is the lower limit of the system. It should have the participant+wheelchair combination of 90.3 kg propel in the RW to SS a variety of times to get a very reliable RU RW velocity value. Then the participant should try propelling at a range of ~10 PSLs varying by 0.2 – 0.3 cm each time. If the light weights are thinned by half, I recommend that the settings be from ~3.5 cm to ~5.5 cm. The error between the two environments can then be graphed against PSL to find where the trend line crosses the x-axis. Where the error is zero, will be nearest the ideal PSL. This experiment can be repeated with different individuals until a participant+wheelchair mass versus PSL trendline can be created. The equation of this line should then be experimentally validated.

7. Conclusion

7.1 Hypotheses

Due to clear differences in RU phase push number, whole test cadence, RU and average velocity, distance traveled, time taken to complete the test, and RU energy, Ho 1 must be rejected. The RU phase push number was less in the VR environment, cadence throughout the whole test was lower, average and RU phase velocity were smaller, distance traveled was larger, time taken to complete the test was larger, and RU phase energy was smaller. The RW velocity was significantly smaller than the ergometer reported velocity while the distance traveled was smaller but not significantly. Also, the RW time was significantly shorter than the ergometer reported time. The ergometer was more accurate than the Redliner dynamics device. Some participants needed more or less help from the technician with steering. The % of time that both steering devices were used at the same time varied more than the % of time that the track compensator indicator was actively turning. There were noticeable and observable differences in dynamics measures when a manual wheelchair user propelled their racing wheelchair in VR and the RW.

Overall, the standard deviations between the two test environments were similar. Furthermore, the standard deviations were not similar in the variables that differed between the two environments: whole test cadence, ergometer distance traveled, time taken to complete each test, and RU phase energy. However, the standard deviation of the RW RU phase power dataset appears to be twice that of the VR dataset even though the RU phase power was not significantly different between the two test environments. Thus, the earlier assumption, that the standard deviations between the two worlds would be similar, was incorrect but it appears that this assumption could be met in the future if the inertia weights are calibrated correctly.

All the hypotheses under Ho 2 represent hypotheses that are secondary to the purpose of this study. The long-term goal is to improve performance of wheelchair racing athletes rather than create fully immersive VR experiences, train individuals to report exertion, or manage shoulder pain; however, all of these can help support the long-term goal. For example, reporting exertion might be a great skill to train a wheelchair athlete to have so they can quickly and reliably report exertion on race day to themselves during the race or to others. Doing so may help them manage their energy such that they reach the end of the race having put in all

they can but not having overexerted. In this study, there were differences in perceived presence, supported by a relatively low average reported presence of 57.69% ± 6.92%. However, straight-line wheelchair propulsion in the ICube does not appear to lead to VIMS like maneuverability tasks do, as the GI, C, P, and S subcategories of the MSAQ were not different between the two test environments. Still, the null hypothesis that there is no difference in perceived presence while completing an exercise test in the two environments is rejected. The perceived exertion was different between the two environments, specifically in the shoulder and overall test area. The test environments and collection time points had different levels of RPE, except for the center category. Thus, Ho 2.2 must be rejected. The WUSPI questions were answered as zeros or "not performed" and, for the responses that were given that were meaningful, there were no significant differences in the responses between the two test environments. A Friedman test found a difference in shoulder pain in the two environments at the two test time points. No significant differences between the RW pretest and post-test trials existed, but there were significant differences between the VR pretest and post-test trials. However, for the healthy, young population with essentially a single exposure used in this study, it is not expected that shoulder pain would be anything other than fatigue from activity. Thus, the Ho 2.3 hypothesis is rejected.

The above results are summarized below in Figure 54 as a comparison of the RW to the VR environment.

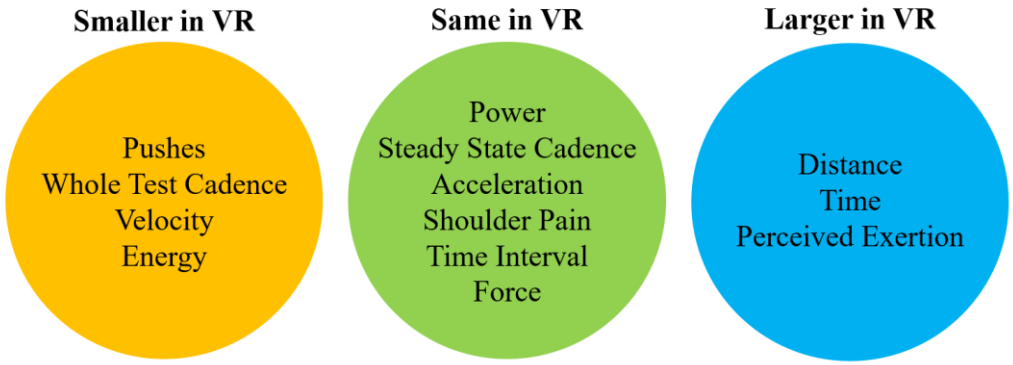

- Presence and immersion in VR can be improved.
- VIMS was not experienced by study participants.
- SS propulsion is similar between environments and overcoming inertia is the issue.

Figure 54. Visual summary of the results of the study.

7.2 General Takeaways

The VR simulation was improved, and can be further improved, by implementing the recommendations outlined above. A big part of creating a more realistic simulation will be the through implementing the qualitative feedback received in the questionnaires. In addition to the recommendations made by the participants, the ability to wheelie the wheelchair should be further explored. Even though it is a difficult maneuver to replicate in the VR environment, it is a crucial part of racing wheelchair propulsion in the VR environment.

This study had the participants go at their own selected speed. This should be reconsidered in the future as the many different speeds resulted in inconsistent pushing. The next study coordinator should consider whether they want more consistency within and between subjects for better comparability.

The RRL is currently developing a new version of Redliner, which uses gyros and should produce more reliable datasets. The new device will measure velocity directly and thus the error may be smaller. However, gyros are also characteristically known to drift with short periods of time and so this method will also need to be explored experimentally.

7.3 Improvements to the Study Design

Due to time constraints, trunk swing could not be measured between the two environments. In the future, it can be looked at using an inertial measurement unit and motion capture system. Salimi and Ferguson-Pell (2013) used an inertial measurement unit to detect trunk swing in this way. The unit could be validated in the VR environment with motion capture for use in the RW. This will also demonstrate the feasibility of using motion capture in a VR environment.

Future study coordinators should consider asking participants to push more consistently. All study participants could push at a consistent speed or they could all have a consistent RU to SS phase and then be asked to stay at that SS velocity for the entirety of the test. Doing so is better for the MATLAB detection system and has been proposed to lead to an increased understanding of the differences between the two test environments (Koontz et al., 2012). The biggest issue with the custom MATLAB program and consistency of detection between the two environments is if the participant stops halfway through a test. Additionally,

data streaming problems should be minimized as drops in data affect the custom MATLAB program's ability to calculate dynamics quantities accurately. The technician should be wary that the low-pass filter they select does not decrease velocity substantially. They could compare the Redliner velocity to the ergometer velocity for calibration before the study begins. Additionally, automating the RU detection phase with the velocity trace would make these measures more objective, any error would be consistent across participants. An attempt should be made to clarify how LabVIEW sends accelerations out to the CSV file so these can be compared to the RW.

There exists the possibility of detecting individual wheelchair propulsion style characteristics from the velocity plots for each person. When examining the velocity trace in depth, individual differences in style become apparent. It would be interesting to see if this exists in experienced manual wheelchair users and in wheelchair racing athletes.

The participants steered in the VR environment for more than half of the test session in all participant cases. This should be compared to the RW environment in the future. For this study, the track compensator indicator was used to gather heading data in the RW environment but the MATLAB code to analyze this was not written. The track compensator indicator should be used in the RW environment to monitor steering and create a biomechanical model of the race. Since the dimensions of the indoor track and each lane are known, it may be possible to create a 3D render of the athlete's race. It is an opportunity to create "post-game footage" for wheelchair racing athletes to look at to improve their steering accuracy as this is one of the more difficult parts of wheelchair racing (Sierra Roth, Personal communication, May 16, 2020). Additionally, it will allow researchers to comment on wheelchair steering accuracy, which is a novel field of study with very little current research, in the hopes that guidelines for steering in racing wheelchairs can be created. This study shows that some study participants were more or less accurate at steering as the standard deviation for the % of Time Both Devices Steering/Turning was 5.60%, with Participant 5 being the most accurate at steering in VR.

The questions on the IPQ should be changed to continuous data using a visual-analog scale and a 10 cm line. Additionally, questions 15 and 16 should be in the same format as questions 1-14 and the same scale. If additional weight is desired on questions 15 and 16, then they could stay out of ten, but if this was not the goal when designing the questionnaire, this should be changed. Questions 15 could also be clarified, in contrast to Question 14, to ensure

that the participant scores how challenging the VR environment is relative to the RW environment. The MSAQ should be kept as is, but the use of it should be reconsidered after a few studies using it with straight-line propulsion. It might become unnecessary if straight-line propulsion is found to not generate VIMS. The questions on the Borg RPE might be changed to just have the participant report on shoulders, or even arms/biceps, and center. Then the study coordinator could average across the two to get an overall reading. The WUSPI should only be used with full-time manual wheelchair users. The form should also be updated to include a 10 cm line to create continuous data. The VAS for shoulder pain was very useful; however, it was difficult to analyze with so many zeros in the dataset. If shoulder pain is not a good indicator of the difficulty of propelling a manual wheelchair, a different metric should be employed. It is possible that RPE and shoulder pain through the VAS are correlated with this relatively low exertion task and low preexisting shoulder pain population. In the future, these should be examined to improve these questionnaires in this population.

7.4 Case Study on One Wheelchair Racing Athlete

One wheelchair racing athlete is currently scheduled to be part of a case study using this wheelchair ergometer. If the issues outlined above can be resolved, this participant has indicated that they will be able to conduct this test in the summer of 2020, when they are back in Edmonton from their university studies in a separate province. Thus, connections have been made in the community to allow full-time manual wheelchair users to partake in these studies. The biggest issue thus far in completing research studies in the RRL with manual wheelchair users has been participant recruitment.

7.5 Study Limitations

The results from this study cannot be generalized to comment on manual wheelchair propulsion in MWUs as the study participants were not full-time MWUs. Considerable differences exist between experienced MWUs and study participants who do not regularly propel a manual wheelchair (Veeger et al., 1998; Vanlandewijck et al., 2001). For example,

the net mechanical efficiency of recruited full-time MWUs was found to be significantly higher than that of the recruited non-disabled participants (Vanlandewijck et al., 2001). Thus, this pilot study exists as a calibration study to get the RRL's wheelchair ergometer system to a place where it can accurately represent RW racing wheelchair propulsion. Once this is completed, studies with members from the small population of wheelchair racing athletes in Alberta can be completed.

Data points were missing for four of twenty wheels in this study: Av60p Left wheel in RW and VR, LV3rT Left in RW, and Ef63t Left in VR. This is a limitation of this study as sometimes these three participants had to be removed to conduct reliable statistical analysis. The loss in data might be due to participants hitting the device and turning if off. It might also be due to transmission lags that were too lengthy. In one instance, it was due to technician error as the black button was not pressed before turning the device off, see Section 4.4.2 for details.

A total of 18 subjects were recruited for this study, but 8 were lost. Three were due to microSD card failure. Two were due to microcontroller coding errors that corrupted the data. This data could not be salvaged and these participants could not be recruited to come back due to scheduling conflicts and then the fact that the University of Alberta shut down due to the COVID-19 pandemic. Three additional loses were due to scheduling conflicts and the university shutdown that caused them to not be able to complete their VR trial.

Additionally, the smaller average velocity for the test in VR might also be due to the few cases where the track compensator indicator dropped out and the participant had to stop. At these points, the participant's speed dropped to zero or near-zero until the connection was restored. These decreased velocity values would have lowered the average velocity value. Furthermore, in the RW, the velocity and distance traveled would have been affected by the participant's wheelieing to steer. This action cannot currently be performed in the VR environment but would lead to jostles in the accelerometer readings as the wheels of the wheelchair would not always be moving forward. Perhaps this is part of the reason why the RW distance traveled is smaller.

Another limitation was that the remote desktop dial needed to be used if the correction factor was not perfect. If a test began and the participant drifted left or right before they reached the curve in the track, they were not made to begin the test again. Instead, they continued on

and the technician helped to keep them straight. This could have led to a slightly higher reported % of Time Technician Steering and % of Time Both Devices Steering/Turning.

Finally, the time between RW test sessions and VR test sessions was not consistent. Some participants had to come back to the RRL on a separate occasion to complete the VR test session. Some participants came back to redo their VR test session at a different day. Going forward, this time period should be more consistent so that the questionnaires from the two test environments can be compared against each other with more confidence. For example, this could be part of the reason why the participants reported higher RPE and shoulder pain in VR.

7.6 Summary Statement

In conclusion, SS cadence, peak and RU phase acceleration, SS and RU phase power, RU phase force, and time interval were not different between the two test environments. From these results, it is implied that overall power and the RR were not different between the two environments and that SS phase propulsion between the two environments was similar. Thus, the inertia weight system still needs to be calibrated for the coupled roller system. The correct coupled inertia weight setting appears to be just below half of the uncoupled inertia weight settings. Whole test cadence, RU, peak, and average velocity, distance traveled, ergometer velocity and distance traveled, time taken to complete the test, RU energy, and RU push number were all different between the two test environments. The ergometer measurements were more in line with the VR Redliner data than the RW Redliner data but were in between the RW Redliner data and VR Redliner data overall. Differences in steering accuracy were detected between participants in VR. Presence and immersion in VR can still be improved, supported by a relatively low average reported presence. VIMS was not experienced by study participants. The WUSPI questions were answered overall with zeroes or "not performed". No significant differences between the RW pretest and post-test shoulder pain, but there were significant differences between the VR pretest and post-test shoulder pain. The shoulder and overall test areas had different levels of reported exertion between the two test environments. 1500-meters was the most similar test time point between the two test environments and showed an increase in reported exertion.

The RRL aims to understand the methods that will optimize a wheelchair athlete's performance and enable them to propel themselves with a more efficient and competitive

propulsion technique that also reduces their likelihood of injury. This is in line with the final recommendation from the Consortium for Spinal Cord Medicine (2005), which was that researchers must establish the most effective method of preserving upper limb function in MWUs. In this study, dynamics measurements and questionnaires on perceived experience in VR were used to validate the RRL's VR wheelchair ergometer system.

Findings from this study have the potential to allow for novel usage of the wheelchair ergometer system for training and further research into motion capture and sEMG to characterize propulsion technique. Dynamics, joint angle, and muscle recruitment must be studied together to characterize the push (van der Woude et al., 2001) and help foster strength balance in the upper extremities of MWUs. This may be possible under simulated RW conditions in the future. The long-term goal of this study is to allow a participant to propel their wheelchair in VR on a wheelchair ergometer as they normally would in the RW. Once a VR wheelchair ergometer can confidently be used to conduct performance testing, a whole host of new research around wheelchair propulsion can be explored.

Bibliography

Alberta Health Services [AHS]. (2012). Rehabilitation conceptual framework. Retrieved from http://rehabcarealliance.ca/uploads/File/knowledgeexchange/Alberta_ Health_Services-Rehabilitation-Conceptual-Framework.pdf.

Allen, M., Cripps, A., Rayment, M., & O'Connor, K. (2008). Shoulder injuries in paraplegic wheelchair users: A clinician handbook.

Ambrosio, F., Boninger, M.D., Souza, A.S., Fitzgerald, S.G., Koontz, A.M., Cooper, R.A. (2005). Biomechanics and strength of manual wheelchair users. *The Journal of Spinal Cord Medicine*, 28(5), 407-414.

Boninger, M. L., Souza, A. L., Cooper, R. A., Fitzgerald, S. G., Koontz, A. M., & Fay, B. T. (2002). Propulsion patterns and push rim biomechanics in manual wheelchair propulsion. *Archives of Physical Medicine and Rehabilitation*, *83*(5), 718–723. https://doi.org/10.1053/ apmr. 2002.32455

Borg, G. (1998). Borg's perceived exertion and pain scales. Champaign (IL): Human Kinetics.

Burnham, R.S., Steadward, R.D. (1994). Upper extremity peripheral nerve entrapments among wheelchair athletes: prevalence, location, and risk factors. *Archives of Physical Medicine and Rehabilitation*, 75(5), 519-524.

Chow, J. W., Millikan, T. A., Carlton, L. G., Chae, W., & Morse, M. I. (2000). Effect of resistance load on biomechanical characteristics of racing wheelchair propulsion over a roller system. *Journal of Biomechanics*, 33(5), 601-608.

Consortium for Spinal Cord Medicine. (2005). Preservation of upper limb function following spinal cord injury: A clinical practice guideline for health-care professionals. *The*

Journal of Spinal Cord Medicine, *28*(5), 434–470. https://doi.org/10.1080/10790268. 2005. 11753844

Cooper, R. A., Koontz, A. M., Ding, D., Kelleher, A., Rice, I., & Cooper, R. (2010). Manual wheeled mobility – current and future developments from the human engineering research laboratories. *Disability and Rehabilitation*, *32*(26), 2210–2221. https://doi.org/10.3109/ 09638288.2010.517599

Cooper, R.A. (1990). An exploratory study of racing wheelchair propulsion dynamics. *Adapted Physical Activity Quarterly*, 7(1), 74-85.

Cooper, R. A., Robertson, R. N., & Boninger, M. L. (1998). Repetitive strain injury among manual wheelchair users. *Team Rehab Report*, *9*(2), 35–38.

Cowan, R. E., Boninger, M. L., Sawatzky, B. J., Mazoyer, B. D., & Cooper, R. A. (2008). Preliminary outcomes of the SMART^{wheel} users' group database: a proposed framework for clinicians to objectively evaluate manual wheelchair propulsion. *Archives of Physical Medicine and Rehabilitation*, *89*(2), 260–268. https://doi.org/10.1016/j.apmr.2007.08.141

Curtis, K. A., Roach, K. E., Brooks Applegate, E., Amar, T., Benbow, C. S., Genecco, T. D., & Gualano, J. (1995a). Development of the Wheelchair User's Shoulder Pain Index (WUSPI). *Spinal Cord*, *33*(5), 290–293. https://doi.org/10.1038/sc.1995.65

Curtis, K. A., Roach, K. E., Applegate, E. B., Amar, T., Benbow, C. S., Genecco, T. D., & Gualano, J. (1995b). Reliability and validity of the Wheelchair User's Shoulder Pain Index (WUSPI). *Spinal Cord*, *33*(10), 595–601. https://doi.org/10.1038/sc.1995.126

de Klerk, R., Vegter, R. J. K., Goosey-Tolfrey, V. L., Mason, B. S., Lenton, J. P., Veeger, D. H. E. J., & van der Woude, L. H. V. (2020). Measuring handrim wheelchair propulsion

in the lab: A critical analysis of stationary ergometers. *IEEE Reviews in Biomedical Engineering*, *13*, 199–211. https://doi.org/10.1109/RBME.2019.2942763

Derman, W., Schwellnus, M.P., Jordaan, E., Runciman, P., Van de Vliet, P., Blauwet, C., Webborn, N., Willick, N., Stomphorst, J. (2016). High incidence of injury at the Sochi 2014 Winter Paralympic Games: a prospective cohort study of 6564 athlete days. *British Journal of Sports Medicine*, 50, 1069-1074.

DiGiovine, C. P., Cooper, R. A., & Boninger, M. (2001). Dynamic calibration of a wheelchair dynamometer. *Journal of Rehabilitation Research and Development*, 38(1), 17.

Engel, J. M., Kartin, D., Carter, G. T., Jensen, M. P., & Jaffe, K. M. (2009). Pain in youths with neuromuscular disease. *American Journal of Hospice and Palliative Medicine®*, *26*(5), 405–412. https://doi.org/10.1177/1049909109346165

Executive Committee for the International SCI Data Sets Committees, DeVivo, M., Biering-Sørensen, F., Charlifue, S., Noonan, V., Post, M., Stripling, T., & Wing, P. (2006). International spinal cord injury core data set. *Spinal Cord*, 44(9), 535–540. https://doi.org/10.1038/ sj.sc.3101958

Finley, M. A., & Rodgers, M. M. (2004). Prevalence and identification of shoulder pathology in athletic and nonathletic wheelchair users with shoulder pain: A pilot study. *The Journal of Rehabilitation Research and Development*, *41*(3b), 395. https://doi.org/10.1682/JRRD. 2003.02.0022

Gellman, H., Sie, I., & Water, R. L. (1988). Late complications of the weight-bearing upper extremity in the paraplegic patient. *Clinical Orthopaedics and Related Research*, *233*, 132–135.

Gianaros, P. J., Muth, E. R., Mordkoff, J. T., Levine, M. E., & Stern, R. M. (2001). A questionnaire for the assessment of the multiple dimensions of motion sickness. *Aviation, Space, and Environmental Medicine*, *72*(2), 115–119.

Goosey-Tolfrey, V. L., West, M., Lenton, J. P., & Tolfrey, K. (2011). Influence of varied tempo music on wheelchair mechanical efficiency following 3-week practice. *International Journal of Sports Medicine*, *32*(02), 126–131. https://doi.org/10.1055/s-0030-1268439

Goosey, V. L., Fowler, N. E., Campbell, I. G. (1997). A kinematic analysis of wheelchair propulsion techniques in senior male, senior female, and junior male athletes. *Adapted Physical Activity Quarterly*, 14(2), 156-165.

Haefeli, M., & Elfering, A. (2006). Pain assessment. *European Spine Journal*, *15*(S1), S17–S24. https://doi.org/10.1007/s00586-005-1044-x

Harburn, K.L., Spaulding, S.J. (1986). Muscle activity in the spinal cord-injured during wheelchair ambulation. *American Journal of Occupational Therapy*, 40, 629-636

Hedrick, B., Wang, Y. T., Moeinzadeh, M., Adrian, M. (1990). Aerodynamic positioning and performance in wheelchair racing. *Adapted Physical Activity Quarterly*, 7(1), 41-51.

Heyward, O. W., Vegter, R. J. K., de Groot, S., & van der Woude, L. H. V. (2017). Shoulder complaints in wheelchair athletes: A systematic review. *PLOS ONE*, *12*(11), e0188410. https://doi.org/10.1371/journal.pone.0188410

Hills, L. (2011). Every push matters. Thesis submitted to University College London, 1-141

HowiRollSports. (2019). *Racing wheelchair steering compensator*. Retrieved January 30, 2019 from https://howirollsports.com/shop/top-end-steering-compensator/

HowiRollSports. (2019). *Top end eliminator NRG racing wheelchair*. Retrieved January 30, 2019 from https://howirollsports.com/shop/top-end-eliminator-nrg-racing-wheelchair/

Kentar, Y., Zastrow, R., Bradley, H., Brunner, M., Pepke, W., Bruckner, T., Raiss, P., Hug, A., Almansour, H., & Akbar, M. (2018). Prevalence of upper extremity pain in a population of people with paraplegia. *Spinal Cord*, *56*(7), 695–703. https://doi.org/10.1038/ s41393-018-0062-6

Kobayashi, D., Watanabe, T., Tyler, N., & Suzuki, T. (2017). A validation test of using shoulder joint moment in evaluation of load in wheelchair propulsion. In *2017 IEEE Life Sciences Conference (LSC)* (pp. 242–245). Sydney, NSW: IEEE. https://doi.org/10.1109/ LSC.2017.8268188

Koontz, A. M., Worobey, L. A., Rice, I. M., Collinger, J. L., & Boninger, M. L. (2012). Comparison Between Overground and Dynamometer Manual Wheelchair Propulsion. *Journal of Applied Biomechanics*, *28*(4), 412–419. https://doi.org/10.1123/jab.28.4.412

Krahn, G. L., Walker, D. K., & Correa-De-Araujo, R. (2015). Persons With Disabilities as an Unrecognized Health Disparity Population. *American Journal of Public Health*, *105*(S2), S198–S206. https://doi.org/10.2105/AJPH.2014.302182

Kwarciak, A. M., Turner, J. T., Guo, L., & Richter, W. M. (2011). Comparing handrim biomechanics for treadmill and overground wheelchair propulsion. *Spinal Cord*, *49*(3), 457–462. https://doi.org/10.1038/sc.2010.149

McKenzie, M. (2018). *Virtual reality wheelchair ergometer*. [International placement program final report, University of Alberta].

Martin Ginis, K. A., van der Scheer, J. W., Latimer-Cheung, A. E., Barrow, A., Bourne, C., Carruthers, P., Bernardi, M., Ditor, D. S., Gaudet, S., de Groot, S., Hayes, K. C., Hicks,

A. L., Leicht, C. A., Lexell, J., Macaluso, S., Manns, P. J., McBride, C. B., Noonan, V. K., Pomerleau, P., … Goosey-Tolfrey, V. L. (2018). Evidence-based scientific exercise guidelines for adults with spinal cord injury: An update and a new guideline. *Spinal Cord*, *56*(4), 308–321. https://doi.org/10.1038/s41393-017-0017-3

Mercer, J.L., Boninger, M., Koontz, A., Ren, D., Dyson-Hudson, T., Cooper, R. (2006). Shoulder joint kinetics and pathology in manual wheelchair users. *Clinical Biomechanics*, 21, 781-785.

Morse, M., Millikan, T., & Hedrick, B. (1994, May/June). The para-backhand pushing technique. *Sports 'N Spokes*, 58-60.

Mulroy, S. J., Gronley, J. K., Newsam, C. J., & Perry, J. (1996). Electromyographic activity of shoulder muscles during wheelchair propulsion by paraplegic persons. *Archives of Physical Medicine & Rehabilitation, 77*(2), 187-193.

National Institute of Health. (n.d.). Can physical activity improve the health of wheelchair users? Retrieved April 17, 2020, from https://prevention.nih.gov/research-priorities/research-needs-and-gaps/pathways-prevention/can-physical-activity-improve-health-wheelchair-users?utm_source=NCMRR+Rehab+News&utm_campaign=c42ac06dee-EMAIL_CAMPAIGN_2020_01_22_02_45&utm_medium=email&utm_term=0_04b8758f89-c42ac06dee-149840357

Qi, L., Ferguson-Pell, M.W., Salimi, Z., Haennel, R., Ramadi, A. (2015). Wheelchair users' perceived exertion during mobility activities. *Spinal Cord*, 53, 687-691.

Qi, L., Wakeling, J., Grange, S., Ferguson-Pell, M.W. (2014). Patterns of shoulder muscle coordination vary between wheelchair propulsion techniques. *IEEE Transactions on Neural Systems and Rehabilitation Engineering*, 22(3), 559-566.

Qi, L., Wakeling, J., Grange, S., & Ferguson-Pell, M. (2012). Changes in surface electromyography signals and kinetics associated with progression of fatigue at two speeds during wheelchair propulsion. *The Journal of Rehabilitation Research and Development*, *49*(1), 23. https://doi.org/10.1682/JRRD.2011.01.0009

Ramirez Herrera, R., Momahed Heravi, B., Barbareschi, G., Carlson, T., & Holloway, C. (2018). Towards a wearable wheelchair monitor: Classification of push style based on inertial sensors at multiple upper limb locations. In *2018 IEEE International Conference on Systems, Man, and Cybernetics (SMC)* (pp. 1535–1540). Miyazaki, Japan: IEEE. https://doi.org/10.1109/SMC.2018.00266

Reid, D., Angus, J., McKeever, P., & Miller, K.-L. (2003). Home is where their wheels are: Experiences of women wheelchair users. *American Journal of Occupational Therapy*, 57(2), 186–195. https://doi.org/10.5014/ajot.57.2.186

Rice, I., Gagnon, D., Gallagher, J., & Boninger, M. (2010). Hand rim wheelchair propulsion training using biomechanical real-time visual feedback based on motor learning theory principles. *The Journal of Spinal Cord Medicine*, *33*(1), 33–42. https://doi.org/10.1080/10790268.2010.11689672

Richter, W. M., Kwarciak, A. M., Guo, L., & Turner, J. T. (2011). Effects of single-variable biofeedback on wheelchair handrim biomechanics. *Archives of Physical Medicine and Rehabilitation*, *92*(4), 572–577. https://doi.org/10.1016/j.apmr.2010.11.001

Rodgers, M.M., Keyser, R.E., Rasch, E.K., Gorman, P.H., Russell, P.J. (2000). Influence of training on biomechanics of wheelchair propulsion. *Journal of Rehabilitation Research & Development*., 38(5), 505-511.

Salimi, Z., & Ferguson-Pell, M. (2018). Development of three versions of a wheelchair ergometer for curvilinear manual wheelchair propulsion using virtual reality. *IEEE Transactions on Neural Systems and Rehabilitation Engineering*, *26*(6), 1215–1222. https://doi.org/10.1109/ TNSRE.2018.2835509

Salimi, Z. (2017). *Can an ergometer based virtual reality environment reproduce typical real-world wheelchair manoeuvring?* [Doctoral dissertation, University of Alberta].

Salimi, Z., & Ferguson-Pell, M. W. (2013). Ergometers can now biomechanically replicate straight-line floor wheelchair propulsion: three models are presented. *Volume 3A: Biomedical and Biotechnology Engineering*, V03AT03A045. https://doi.org/10.1115/ IMECE2013-62327

Salimi, Z. & Ferguson-Pell, M.W. (2012, Oct. 19-21). "Ergometer model for representing straight-line floor wheelchair propulsion", in 13th Annual Alberta Biomedical Engineering Conference (BME) Program and Proceedings, Banff, Alberta, Canada, P.79.

Sauret, C., Couetard, Y., & Vaslin, P. (2011). Dynamic calibration of a wheelchair six-component wheel dynamometer rolling on the floor. *Computer Methods in Biomechanics and Biomedical Engineering*, *14*(sup1), 67–69. https://doi.org/10.1080/10255842. 2011.592366

Schubert, T., & Regenbrecht, H. (2002). Wer hat angst vor virtueller realität? phobie, therapie und präsenz in virtuellen welten [Who is afraid of virtual reality? Phobia, therapy and presence and virtual worlds]. Bente, G. (Hrsg.), *Virtuelle Realitäten [Virtual Realities]*, 255-274.

the SCIRE Research Team, Sawatzky, B., Bishop, C. M., & Miller, W. C. (2008). Classification and measurement of pain in the spinal cord-injured population. *Spinal Cord*, *46*(1), 2–10. https://doi.org/10.1038/sj.sc.3102137

Shimada, S. D., Robertson, R. N., Boninger, M., & Cooper, R. A. (1998). Kinematic characterization of wheelchair propulsion. *Journal of Rehabilitation Research & Development*, *35*(2), 210–218.

Shimada, S.D., Cooper, R.A., Lawrence, B., Robertson, R.N. (1995). Computer controlled wheelchair dynamometer. *Engineering in Medicine and Biology Society 1995. Proceedings of 17th International Conference of the Engineering in Medicine and Biology Society*. 5, 1177-1178

Sonenblum, S. E., Sprigle, S., & Lopez, R. A. (2012). Manual wheelchair use: bouts of mobility in everyday life. *Rehabilitation Research and Practice*, *2012*, 1–7. https://doi.org/10.1155/2012/753165

Stephens, C. L., & Engsberg, J. R. (2010). Comparison of overground and treadmill propulsion patterns of manual wheelchair users with tetraplegia. *Disability and Rehabilitation: Assistive Technology*, *5*(6), 420–427. https://doi.org/10.3109/17483101003793420

Stillman, M. D., Bertocci, G., Smalley, C., Williams, S., & Frost, K. L. (2017). Healthcare utilization and associated barriers experienced by wheelchair users: A pilot study. *Disability and Health Journal*, *10*(4), 502–508. https://doi.org/10.1016/j.dhjo.2017.02.003

Stone S. 2017 Jul 13. Track tech explained – racing wheelchairs. The Telegraph. London (UK): The Telegraph; [accessed 2019 Jan 30]. https://www.telegraph.co.uk/world-paraathletics-championships/2017/07/13/track-tech-explained-racing-wheelchairs/

Symonds, A., Holloway, C., Suzuki, T., Smitham, P., Gall, A., & Taylor, S. J. (2016). Identifying key experience-related differences in over-ground manual wheelchair propulsion biomechanics. *Journal of Rehabilitation and Assistive Technologies Engineering*, *3*, 205566831667836. https://doi.org/10.1177/2055668316678362

Troy, B. S., & Cooper, R. A. (1997). An analysis of work postures of manual wheelchair users in the office environment. *Journal of Rehabilitation Research & Development*, 34(2), 151.

University of Sheffield Learning Media Unit. (2005). Anatomy of the shoulder [DVD]. New York, N.Y.: Films Media Group.

Vanlandewijck, Y., Theisen, D., & Daly, D. (2001). Wheelchair propulsion biomechanics: implications for wheelchair sports. *Sports Medicine*, *31*(5), 339–367. https://doi.org/ 10.2165/00007256-200131050-00005

van der Helm, F. C. T., & Veeger, H. E. J. (1996). Quasi-static analysis of muscle forces in the shoulder mechanism during wheelchair propulsion. *Journal of Biomechanics*, *29*(1), 39 52. https://doi.org/10.1016/0021-9290(95)00026-7

van der Woude, L.H.V., Hendrich, K.E., Veeger, H.E.J., van Igen Schenau, G.J., Rozendal, R.H., De Groot, G., & Hollander, A.P. (1998a). Manual wheelchair propulsion: Effects of power output on physiology and technique. Medicine and Science in Sports and Exercise, 20(1), 70–78.

van der Woude, L.H.V., Veeger, H.E.J., Rozendal, R.H., van Ingen Schenau, G.J., Rooth, F., & van Nierop, P. (1998b). Wheelchair racing: effect of rim diameter and speed on physiology and technique. Medicine and Science in Sports and Exercise, 20(5), 492–500.

van der Woude, L.H.V., Veeger, H.E.J., Dallmeijer, A.J., Janssen, T.W.J., Rozendaal, L.A. (2001). Biomechanics and physiology in active manual wheelchair propulsion. *Medical Engineering & Physics*, 23(10), 713-733.

van der Woude, L.H.V., de Groot, S., Janssen, T.W.J. (2006). Manual wheelchairs: Research and innovation in rehabilitation, sports, daily life and health. *Medical Engineering & Physics*, 28, 905-915.

Veeger, H. E. J., Rozendaal, L. A., & van der Helm, F. C. (2002). Load on the shoulder in low intensity wheelchair propulsion. *Clinical Biomechanics (Bristol, Avon), 17*(3), 211-218.

Veeger, D. H. E. J., Meershoek, L. S., van der Woude, L. H. V., & Langenhoff, J. M. (1998). Wrist motion in handrim wheelchair propulsion. *Journal of Rehabilitation Research & Development*, *35*(3), 305.

Viger A. 1988. Wheelchair design. Presented at the national symposium on wheelchair track and road racing; 1988 Jun 7; p. 6-10.

Wan, J., Qin, Z., Wang, P., Sun, Y., & Liu, X. (2017). Muscle fatigue: General understanding and treatment. *Experimental & Molecular Medicine*, *49*(10), e384. https://doi.org/10.1038/ emm.2017.194

Wang, Y.T., Deutsch, H., Morse, M., Hedrick, B., & Millikan, T. (1995). Three-dimensional kinematics of wheelchair propulsion across racing speeds. *Adapted Physical Activity Quarterly*, 12(1), 78-89.

World Heath Organization [WHO]. Fact sheet on wheelchairs [Report on the Internet]. New Delphi: WHO; 2010 [cited 2019 April 4]. 4 p. Available from: http://www.searo. who.int/ entity/disabilities_injury_rehabilitation/wheelchair_factsheet.pdf

World Health Organization [WHO]. (2011). Chapter 4, Rehabilitation. In World report on disability 2011. Retrieved from https://www.ncbi.nlm.nih.gov/books/NBK304081/.

Wu, J. (2012). Comparison of manual wheelchair propulsion in "real-world" and computer simulated environments. [Master's thesis, University of Alberta].

Appendices

Appendix A: Sample Size Calculations

Employing comparison of means:

$$\text{Sample Size} = \frac{(u + v)^2.(\sigma_1^2 + \sigma_0^2)}{(\mu_1 - \mu_0)^2}$$

Where:

u = one-sided % point of normal distribution corresponding to 100% - power (power for this study = 90% therefore u = 1.28)

v = percentage point of the normal distribution corresponding to the 2-sided significance level (significance level for this study = 5% therefore v = 1.96)

σ = standard deviation of samples

μ = means for samples

The dependent variables to be tested in this study are:

Distance (m), Force (N), Speed (m/s), Acceleration (m/s^2), Distance (m), and Time (s).

Aggregated Score out of the Total Number of Points for each questionnaire.

In the following estimates we have set the conditions of:

90% probability of achieving significance at $p<0.05$.

Based on a study done in the RRL (Qi, 2015):

Heart rate during wheelchair push session at 60% VO_{2peak} [Mean (SD)]**:**

114.0 (15.5)

% VO_{2peak} at 1.6m/sec [Mean (SD)]**:**

71.6 (11.6)

Heart Rate:

Number participants for HR (bpm) effect due to training =

$$\frac{(1.28 + 1.96)^2 . (15.5^2 + 15.5^2)}{(0.1 * 114.0)^2}$$

= 9.7 subject

% VO_{2peak}:

Number participants for % VO_{2peak} effect due to training =

$$\frac{(1.28 + 1.96)^2 . (11.6^2 + 11.6^2)}{(0.1 * 71.6)^2}$$

= 55.1 subjects *estimation is high

Based on a study done in the RRL (Qi et al., 2014):

sEMG [Mean (SD)]**:**

0.9 (0.075)

sEMG:

Number participants for sEMG (anterior deltoid)

effect due to training = $\frac{(1.28 + 1.96)^2 \cdot (.075^2 + .075^2)}{(.1 * 0.9)^2}$

= 14.6 subjects

2018/2019 Pilot Study:

Dynamic Measures: **= 14.55 subjects average**

Velocity: $\frac{(1.28 + 1.96)^2 \cdot (0.46^2 + 0.65^2)}{(2.13 - 1.43)^2}$

= 13.71 subjects

Force: $\frac{(1.28 + 1.96)^2 \cdot (4.59^2 + 3.10^2)}{(21.25 - 17.05)^2}$

= 18.26 subjects

Distance: $\frac{(1.28 + 1.96)^2 \cdot (89.14^2 + 88.89^2)}{(228.41 – 108.97)^2}$

= 11.66 subjects

Metabolic Measures: **= 26.04 subjects**

Heart Rate: $\frac{(1.28 + 1.96)^2 \cdot (1.57^2 + 1.82^2)}{(6.91-5.43)^2}$

= 27.99 subjects

% VO_2 peak: $(1.28 + 1.96)^2 \cdot (309.76^2 + 346.64^2)$

$(1374.83-1068.04)^2$

= 24.10 subjects

2019/2020 Experimental Study*:

= 9.38 subjects average

Velocity: $\frac{(1.28 + 1.96)^2 \cdot (0.50^2 + 0.22^2)}{(2.11 – 1.60)^2}$

= 12.00 subjects

Distance: $\frac{(1.28 + 1.96)^2 \cdot (57.69^2 + 70.51^2)}{(1268.76 – 1382.238)^2}$

= 6.78 subjects

*Completed with the data from the 7 participants with complete datasets.

Appendix B: Ethics Approval

Health Research Ethics Board

308 Campus Tower
University of Alberta, Edmonton, AB T6G 1K8
p. 780.492.9724 (Biomedical Panel)
p. 780.492.0302 (Health Panel)
p. 780.492.0459
p. 780.492.0839
f. 780.492.9429

Approval Form

Date:	January 4, 2018
Study ID:	Pro00075648
Principal Investigator:	Martin Ferguson-Pell
Study Title:	Wheelchair athlete training using immersive virtual reality ergometer
Approval Expiry Date:	Thursday, January 3, 2019
Approved Consent Form:	Approval Date: 1/4/2018 — Approved Document: General Consent Form
Sponsor/Funding Agency:	Spinal Cord Injury Treatment Centre (Northern Alberta) Society

RSO-Managed Funding:

	Project ID	Project Title	Speed Code	Other Information
View	RES0034976	Laboratory Research Account for Research on the Prevention of Injury related to Wheelchair Propulsion	ZH553	Spinal Cord Injury Treatment Centre (Northern Alberta) Society

Thank you for submitting the above study to the Health Research Ethics Board - Health Panel. Your application, including the following, has been reviewed and approved on behalf of the committee;

- Information Sheet - Experimental Group (12/20/2017)
- Information Sheet - Pilot Group (12/20/2017)
- Study Protocol (11/18/2017)
- Motion Sickness Assessment Questionnaire (12/4/2017)
- Motion Sickness Assessment Questionnaire - For Training Sessions (12/4/2017)
- IGroup Presence Questionnaire (12/4/2017)
- ParQ+ (12/4/2017)
- Wheelchair User's Shoulder Pain Index (12/4/2017)
- Borg's RPE - Training Form (12/4/2017)
- Borg's Rating of Perceived Exertion (12/4/2017)

A renewal report must be submitted next year prior to the expiry of this approval if your study still requires ethics approval. If you do not renew on or before the renewal expiry date, you will have to re-submit an ethics application.

Approval by the Health Research Ethics Board does not encompass authorization to access the patients, staff or resources of Alberta Health Services or other local health care institutions for the purposes of the research. Enquiries regarding Alberta Health Services approvals should be directed to (780) 407-6041. Enquiries regarding Covenant Health should be directed to (780) 735-2274.

Sincerely,

Anthony S. Joyce, PhD.
Chair, Health Research Ethics Board - Health Panel

Note: This correspondence includes an electronic signature (validation and approval via an online system).

Appendix C: Custom MATLAB Program Code

```
%%%%%%%%%%%%%%%%%%%%%%%%%%%%%%%%%%%%%%%%%%%%%%%%%%%%%%%%%%%%%%%%%%%%%%%%%%
%%%%%%%%%
%% Use this program to extract the arrays you need to Analyze Redliner
data
%%
%%%%%%%%%%%%%%%%%%%%%%%%%%%%%%%%%%%%%%%%%%%%%%%%%%%%%%%%%%%%%%%%%%%%%%%%%%
%%%%%%%%%

%% ---------------------- GETTING STARTED ------------------------------
%%
%%
%% Edit the program to provide the correct file names at lines 32-34

%% Select either 56 or 57 depending on whether you blank columns

%% Run the program and select the trunction values to align data

%% If you get an error message showing your array is too long, shorten it
%% using a smaller End_Truncate value in lines 88 - 92
%% ---------------------------------------------------------------------
%%

%%%%%%%%%%%%%%%%%%% SETTING UP THE FILE AND PATH VARIABLES
%%%%%%%%%%%%%%%%%%%%%%%%
% Note: firstly you will need to launch the .csv files in Excel and save
% them as an xls file.  Make sure you close Excel afterwards or you will
get an
% error running this program.

% It easier to have these programs in folder with two other folders, one
% for the data called Redliner Data  and the other for Smart Wheel data.
% Results for the plots to be stored in a Plots folder.

clc;
clear all %NMedit -> clear workspace memory
RL_pathname = 'C:\Users\hamps\Desktop\Take 6 - Light Interia Weights 2 -
Longer SS/';

Plots_pathname = 'C:\Users\hamps\Desktop\Take 6 - Light Interia Weights 2
- Longer SS/';

RL_filename_no_ext = '6.5cm Light Weights Right 3';

Generic_filename_no_ext = 'VR';

%File Name for the peaks file
filenameglobal=RL_filename_no_ext;
filenameall=strcat(filenameglobal,' Velocity Peaks','.xlsx');

extname = '.xls';
RL_filename = strcat(RL_pathname,RL_filename_no_ext,extname);
```

```
RL_path_filename_no_ext = strcat(RL_pathname,RL_filename_no_ext);

Omega_Plot_filename =
strcat(Plots_pathname,'Omega','_',Generic_filename_no_ext);
Alpha_Plot_filename =
strcat(Plots_pathname,'Alpha','_',Generic_filename_no_ext);

Omega_Plot_Sync_filename =
strcat(Plots_pathname,'Omega_Sync','_',Generic_filename_no_ext);
Alpha_Plot_Sync_filename =
strcat(Plots_pathname,'Alpha_Sync','_',Generic_filename_no_ext);

% You need to include the full path here or
% make sure that the file is in the same directory as this program
% before you save the csv as an xlsx

%%%%%%%% DATA FORMAT FOR DIFFERENT REDLINER CHART CONFIGURATIONS
%%%%%%%%%%%
% Note: This program is designed for running one Redliner
% Depending on how you run Chart you may have a blank block of
% columns that MAY throw off this program and give an error that you
% have exceeded the dimensions of the data.  When Excel converts from CSV
% the blank spaces may not be counted as columnnS, but often are.

%% ------------------  READ IN THE DATA  ------------------------

RL_file = xlsread(RL_filename);


%% ---- RARELY YOU MAY NEED TO EDIT THIS TO MATCH EXCEL DATA COLUMN FORMAT
---- %%

% USUALLY MATLAB WILL IGNORE BLANK COLS IN EXCEL BUT IF THERE IS AN ISSUE
% EDIT THESE LINES
RL_data_format = 1;         % Select this option if data is in cols 3-8
%RL_data_format = 2;        % Select this option if data is in cols 11-16


%% ***********************************c****************************** %%


%% ---------------  SET UP THE CONSTANTS --------------------------- %%

%%%%%%%%%%%%%%% THESE VALUES DO NOT NORMALLY NEED TO BE EDITED
% Note you may also need to provide values for other parameters
% You can do this by editing the following values for the parameters

sensor_distance = 0.184;     %  This value is fixed for the Redliner
wheel_radius = 0.33;        % Change this value if you use non-standard
wheels
min_push_time = .1;          %  This seems to work but change it if you
miss a lot of pushes
```

```
max_capacity = 2.5;          % Revise this once you have done the capacity
measurement

mass_part_chair = 90.3;    % Mass of participant plus chair in Kg


RL_sampfr = 50;              % Approx Sampling frequency of Redliner in Hz
                             % Data provides average of about 20ms between
                             % samples = 50 Hz
RL_Fnyq = RL_sampfr/2;       % The Nyquist frequency is half sampling
frequency
                             % Since sampling interval is sometimes longer
                             % not sure what this means in terms of Nyquist

%%%%%%%%%%%%%%%%%%%%%%%%%%%%%% Redliner Equations
%%%%%%%%%%%%%%%%%%%%%%%%%%%%%%%%%%%%%%%%


%%%%%%%%%%%%%%%%%%%%%%%%%%%%%%%%%%%%%%%%%%%%%%%%%%%%%%%%%%%%%%%%%%%%%%%%%%
%%%%
%%% This is the calculation we use to estimated Redliner Tangential Force
%%%%
%%%%%%%%%%%%%%%%%%%%%%%%%%%%%%%%%%%%%%%%%%%%%%%%%%%%%%%%%%%%%%%%%%%%%%%%%%
%%%%
% Let r1 and r2 be the distance of each accelerometer from the hub of
% wheel
% Let a1 and a2 be the acceleration values from the top and bottom
accelerometers in m/s/s
% Centripletal force sensor 1 = a1 = w^2r1  where w = angular velocity
% Centripletal force sensor 2 = a2 = w^2r2
% So a1-a2 = w^2(r1 - r2) = w^2(sensor_separation)
% Therefore w = sqrt((a1 - a2)/r1-r2))
% If we wish to convert angular velocity w to linear velocity v
% v= 2*pi*w where pi = 22/7

%%%%%%%%%%%%%%%%%%%%%%%%%%%%%%%%%%%%%%%%%%%%%%%%%%%%%%%%%%%%%%%%%%%%%%%%%%
%%%%

RL_data = RL_file(5:end,:);  % Takes all columns starts at row 5 to avoid
headers

% We extract the values we need from the Redliner data array

%%  Case where RL Values are in columns 3-8
if RL_data_format == 1
TopX1_Unit=RL_data(1:end,3);
BotX1_Unit=RL_data(1:end,6);
TopY1_Unit=RL_data(1:end,4);
BotY1_Unit=RL_data(1:end,7);
TopZ1_Unit=RL_data(1:end,5);
BotZ1_Unit=RL_data(1:end,8);
RL_time = RL_data(1:end,2);         % The RL time elapsed is in column 2
RL_time2 = RL_data(1:end,2);        % Needed to find the beginning of the
ss
```

```
%RL_time = RL_time - RL_time(1); % Determines the run time resetting to
zero at start
RL_interval = RL_data(1:end,1); % Interval between samples
end
%% Case where RL Values are in columns 11-16
if RL_data_format == 2
TopX1_Unit=RL_data(1:end,11);
BotX1_Unit=RL_data(1:end,14);
TopY1_Unit=RL_data(1:end,12);
BotY1_Unit=RL_data(1:end,15);
TopZ1_Unit=RL_data(1:end,13);
BotZ1_Unit=RL_data(1:end,16);
RL_time = RL_data(1:end,10);        % The RL time elapsed is in column 10
RL_time2 = RL_data(1:end,2);        % Needed to find the beginning of the
ss
RL_interval = RL_data(1:end,9);  % Interval between samples
%RL_time = RL_time - RL_time(1); % Determines the run time resetting to
zero at start
end


% We calculate the angular velocity according to equation above
% and make sure the values are positive before attempting square root.
% We also change blanks in the Velocity data from the Excel sheet to "0"s
%so that MATLAB does not assign them as 'NaN"
X_Distance = TopX1_Unit - BotX1_Unit;
Omega_RL = zeros(size(X_Distance));

[numRows,numCols] = size(X_Distance);

for row = 1 : numRows
    if isnan(X_Distance(row, 1))
        Omega_RL(row, 1) = 0;
    else
        Omega_RL(row, 1) = sqrt(abs(X_Distance(row,
1))/(sensor_distance));
    end
end

% We must smooth the data before taking the differential
% Here we use a 2nd order Butterworth low pass filter cut off 1Hz

fco_Omega = 1;    % Edit to setup the cutoff frequency in Hz depending on
detail required

[Omega_RL_b,Omega_RL_a]=butter(2,fco_Omega/RL_Fnyq);
OmegaSmooth_RL=filter(Omega_RL_b,Omega_RL_a,Omega_RL);

%To determine acceleration from difference in tangential acceleration
%component as this avoids differentiation noise.
%We also change blanks in the Acceleration data from the Excel sheet to
"0"s
%so that MATLAB does not assign them as 'NaN"
Y_Distance = TopY1_Unit - BotY1_Unit;
Alpha = zeros(size(Y_Distance));
```

```
[numRows2,numCols2] = size(Y_Distance);

for row2 = 2 : numRows2 %**NMedit -> 2 : numRows2 changed from 1
    if isnan(Y_Distance(row2, 1))
        Alpha(row2, 1) = 0;
    else
        %Alpha(row2, 1) = sqrt(abs(Y_(row2, 1))/(sensor_distance));  %
Tangential method
        %NMedit -> this seems to give better accel plot, but still does
not
        %reflect velocity plot, check against angular velocity plots
        Alpha(row2, 1) = (OmegaSmooth_RL(row2) - OmegaSmooth_RL(row2-
1))./(RL_interval(row2)./1000);
    end
end


%% Filtering the RL signal
% Due to small alignment issues a radial component is inevitable.  This
can
% be subtly seen in the raw data signal for  Alpha.  To remove this appy a
% low pass filter well below the cadence.  Cadence is in the range 0.5 -
% 3.0 Hz and so we will apply a high pass at 0.5 Hz
% First apply the high pass

RL_fco_Alpha_HP = 0.1;

[RL_b_hp,RL_a_hp]=butter(2,RL_fco_Alpha_HP/RL_Fnyq,'High');
AlphaSmooth_HP=filter(RL_b_hp,RL_a_hp,Alpha);

% Edit to setup the secondary filter cutoff frequency in Hz
% For Redliner depending on detail required
RL_fco_Alpha = 1.0;
[RL_b,RL_a]=butter(2,RL_fco_Alpha/RL_Fnyq,'Low');
AlphaSmooth=filter(RL_b,RL_a,AlphaSmooth_HP);

% Need to make sure the matrices are the same size
Omega_size=size(OmegaSmooth_RL);  % For debugging
RL_time_size=size(RL_time); % For debugging
Alpha_size=size(Alpha);% For debugging
AlphaSmooth_size=size(AlphaSmooth); % For debugging

%%%%%%%%%%%%%%%%%%%% PLOT THE COMPLETE DATASETS
%%%%%%%%%%%%%%%%%%%%%%%%%%

%%%%%%%  Plot the Velocity %%%%%%%

%Remove the offset from the RL Omega data by averaging first 10 readings
% This offset is mainly due to sensor setup orientation on wheel.

OmegaSmooth_RL_offset_10 = abs(OmegaSmooth_RL (1:10,1));

OmegaSmooth_RL_offset = mean(OmegaSmooth_RL_offset_10, 1);
```

```
OmegaSmooth_RL_zeroed = OmegaSmooth_RL - OmegaSmooth_RL_offset;

Linear_Velocity = OmegaSmooth_RL_zeroed.*wheel_radius;

Linear_Acceleration = AlphaSmooth * wheel_radius;

%% integrate the velocity to estimate the distance and assign dt.
%This changes blanks in the dt/Time Interval data from the Excel sheet
%to "0"s so that MATLAB does not assign them as 'NaN"
dt = zeros(size(RL_interval));
[numRows3,numCols3] = size(RL_interval);

for row3 = 1 : numRows2
    if isnan(RL_interval(row3, 1))
        dt(row3, 1) = 0;
    else
        dt(row3, 1) = RL_interval(row3, 1)/1000;
    end
end

%This changes blanks in the Distance data from the Excel sheet
%to "0"s so that MATLAB does not assign them as 'NaN"
Distance = zeros(size(RL_interval));
[numRows4,numCols4] = size(RL_interval);

for row4 = 1 : numRows2
    if isnan(RL_interval(row4, 1))
        Distance(row4, 1) = 0;
    else
        Distance(row4, 1) = (abs(Linear_Velocity(row4, 1))).*dt(row4, 1);
    end
end

%Lowpass filter to filter out mall pushes that are vibrations.
Linear_Velocity_Low = lowpass(Linear_Velocity, 0.0125);

% Find the peaks. Create peaks and locs arrays for maximums
[Vpks,locs] = findpeaks(Linear_Velocity_Low,'MinPeakDistance', 1,
'MinPeakHeight',1);
% Find the time that corresponds to the maximum locs
Vlocs = RL_time(locs);
Vpeaks = (Vpks);

%Find the time between each max/peak
[numRows5,numCols5] = (size(Vlocs)); %find the size of the array
[numRows5] = [numRows5] - 1; %one less data point in the array as we are
subtracting
TimeBwMax = zeros(size(Vpeaks)-1); %one less data point as we are
subtracting
count = 1;
for row5 = 1 : numRows5
    TimeBwMax(row5, 1) = (Vlocs(count + 1, 1)) - (Vlocs(count, 1));
    count = count + 1;
end
```

```
% Find the minimums. Create peaks and locs arrays for minimums
%Inverse the velocity plot
Inverse_Vel = (-(Linear_Velocity_Low));
[Vpks2,locs2] = findpeaks(Inverse_Vel,'MinPeakDistance', 1); %Note that
this leads to
%very small peak values in the output document that should be deleted if
%the velocity is below 1. Later can add in code to delete these very small
%velocities
Vlocs2 = RL_time(abs(locs2)); % Find the time that corresponds to the
minimum locs
Vpeaks2 = (abs(Vpks2));

%write to excel the data
col_header={'Peak Time (s)','Peak Velocity (m/s)', 'Min Time (s)', 'Min
Velocity (m/s)'};     %Row cell array (for column labels)
xlswrite(filenameall,col_header,1);     %Write column header
xlswrite(filenameall,Vlocs,'Sheet1','A2'); %Write the time for the peaks
to the excel sheet
xlswrite(filenameall,Vpeaks,'Sheet1','B2'); %Write the velocity value of
the peaks to the excel sheet
xlswrite(filenameall,Vlocs2,'Sheet1','C2'); %Write the time for the
minimums to the excel sheet
xlswrite(filenameall,Vpeaks2,'Sheet1','D2'); %Write the velocity at the
minimums to the excel sheet

figure(1)

plot(RL_time,Linear_Velocity);
title('Redliner Wheel Linear Velocity (m/s)');
grid on;
xlabel('Time (s)'); ylabel('Redliner Linear Velocity (m/s)')
% axis([0 100 -1 5]);
xlim auto
ylim auto
print ('-dpng',Omega_Plot_filename);

figure(2)

plot(RL_time,((AlphaSmooth * wheel_radius)),'b');
title('Redliner Linear Acceleration (m/s/s)');
grid on;
xlabel('Time (s)'); ylabel('Redliner Linear Acceleration (m/s/s)')
xlim auto
ylim auto
%output the graph as a png and name it with Redliner file identifier
print ('-dpng',Alpha_Plot_filename);

figure(3) % Get the last figure

% CALCULATE THE FFT OF THE STEADY STATE REGION AND THEN AND PLOT
% THE POWER SPECTRUM

% We need to only use the steady state value which come after the first
% major peak and end once the velocity starts to decrease
```

```
%%%%%%%%%%%%%%%%%%%%%%%%%%%%%%%%%%%%%%%%%%%%%%%%%%%%%%%%%%%%%%%%%%%%%%%%
% Auto-detection of ss
%%%%%%%%%%%%%%%%%%%%%%%%%%%%%%%%%%%%%%%%%%%%%%%%%%%%%%%%%%%%%%%%%%%%%%%%
delta_LV=Linear_Velocity(2:end)-Linear_Velocity(1:end-1); %difference
between consecutive values of linear velocity
% i.e. an indicator of acceleration
length_dLV=length(delta_LV);
ss_num=0; % this is an indexer for the ##_arr arrays
state_ind=0; % index that tracks peaks in the linear velocity
reset_flag=false; % flag that detects when we're no longer at steady-state
ss_time_duration=4; %seconds of ss duration****set this value
ss_LV_diff=0.1; % if greater than this, then reset the ss counter
for ii = 1:length(delta_LV)-1 % go through the array
    if ((delta_LV(ii)>0)&&(delta_LV(ii+1)<0)) % check if we are at a peak
in the linear velocity
        % i.e. accel changes from positive to negative
        state_ind=state_ind+1; % increment for the state array
        state(state_ind)=ii; % store the index (i.e. related to time-
point) at the peak
        if (state_ind>2) % If we've detected/stored three peaks, find
means and determine if we're at steady-state
            mean_LV_1=mean(Linear_Velocity(state(state_ind-
2):state(state_ind-1)));
            mean_LV_2=mean(Linear_Velocity(state(state_ind-
1):state(state_ind)));
            if (abs(mean_LV_2-mean_LV_1)>0.1) % check if the mean between
two consecutive waves is steady-state
                %i.e. within 0.1 m/s
                %reset
                reset_flag=true; % set the flag if greater than 0.1 m/s -
means we're out of steady-state
            end
        end
    end
    if (reset_flag) % if we're out of steady state, check duration of
steady-state
        if ((RL_time(state(end))-RL_time(state(1)))>ss_time_duration)
            % store steady-state parameters if steady-state is long enough
            ss_num=ss_num+1; % increment to the end of the arrays
            sss_arr(ss_num)=state(1); % store beginning index i.e. time
start of steady-state
            sse_arr(ss_num)=state(end-1); % store end index i.e. time end
of steady-state
            % store steady state value as the mean over the entire
            % steady-state time

ss_LV(ss_num)=mean(Linear_Velocity(sss_arr(ss_num):sse_arr(ss_num)));
        else
            % if steady-state time length is too short, don't record and
            % reset the state variables for next steady-state detection
            state_old=state;
            clear state
            % BUT may still be more legit steady-state waves, so reset the
            % state back to the latest wave
            state(1)=state_old(state_ind-1);
            state(2)=state_old(state_ind);
```

```
            state_ind=2;
        end
        % reset flags and index for next steady-state
        reset_flag=false;
        clear state
        state_ind=0;
    end
end
% We now have three arrays: steady state start, end, and mean velocity
% They may have detected more than one steady state point in the data set
% So we now determine which steady state point to keep for determining
% power, which I believe is the maximum velocity value in this array

% max() finds max steady-state value in the array, and find() determines
% the index in the array at which this occurs. If you're unsure what this
% means, set a breakpoint here and look at the ss_LV, sss_arr, and sse_arr
% in the Workspace
ss_ind=find(ss_LV == max(ss_LV)); %record the index corresponding with the
maximum ss_LV,
% to get the indexes from the sss_arr and sse_arr arrays
 sss=sss_arr(ss_ind); % steady-state start index in the Linear_Velocity
array
 sse=sse_arr(ss_ind); % steady-state end index in the Lineary_Velocity
array

%sss=0; % steady-state start index in the Linear_Velocity array
%sse=sss_arr(ss_ind); % steady-state end index in the Lineary_Velocity
array

%%%%%%%%%%%%%%%%%%%%%%%%%%%%%%%%%%%%%%%%%%%%%%%%%%%%%%%%%%%%%%%%%%%%%%%%%%%
%%%%%%%%%%%%%%%%%%%%%%%%%%%%%%%%%%%%%%%%%%%%%%%%%%%%%%%%%%%%%%%%%%%%%%%%%%%

% For now I am putting in these values by hand
%sss=322; % Vector element at start of steady state epoch
%sse=422; % Vector elemnet at end of steady state epoch

N = length(Linear_Velocity(sss:sse));

% We need to subtract the stead state velocity to see what is being
% put in to maintain steady state.

SSvel = mean(Linear_Velocity(sss:sse));% must fix
% getting the vectors the same lenght.

Vel_ss = Linear_Velocity(sss:sse+1)-SSvel; % Remove the ss velocity to
% determine the energy to sustain steady state

RL_sampfr; % This is the estimated sampling frequency

ssdur = N/RL_sampfr; % Duration of steady state epoch
Fs=RL_sampfr; %NMedit -> set the Fs, I believe it is the same as RL_sampfr
tps = (0:1/Fs:N/RL_sampfr)'; % create time vector for the steady state
segment

len_tps =  length(tps);
```

```
len_Vel_ss = length(Vel_ss);

[Vel_ss,RL_time]=resample(Vel_ss,RL_time(sss:sse+1),Fs); %NMedit ->
resample to a consistent rate

%xTable = timetable(seconds(tps),Vel_ss);
xTable = timetable(seconds(RL_time),Vel_ss); %NMedit -> adjustment for the
resample, could be wrong

[pxx,f] = pspectrum(xTable); %***FFT occurs here I think as part of this
function for calculating the power spectrum
% pxx is the vector of the power in each frequency bucket of f
% So to get the total power simply sum pxx

Powersum = sum(pxx); %nominally in watts when mass has been included
% NOTE ALSO THAT THE VELOCITY HAS TO BE IN m/s FOR THIS TO BE TRUE

pspectrum(xTable,'FrequencyResolution',1) % Plot power spectrum over the
% available frequency range defined by Nyquist.  Use 2 Hz resolution
% which means determine the power in 2 Hz chunks of frequency domain

%% Calculate Distance by summing over the entire peroid and velocity and
acceleration
% by averaging over the entire period or finding the max value.
sum1 = sum(Distance);
mean1 = mean(Linear_Velocity);
mean2 = mean(Linear_Acceleration);
M1 = max(Linear_Velocity);
M2 = max(Linear_Acceleration);

% The following lines are used to average time between the maximum peaks
%once in steady state
StartPk = RL_time2(sss); %Find start time in steady state
EndPk = RL_time2(sse); %Find end time of steady state

%Create an array of the difference b/w sss and Vlocs
DifferenceStart = zeros(size(Vpeaks) - 1);
c=1;
for row5 = 1 : numRows5
    DifferenceStart(row5, 1) = abs(StartPk - Vlocs(c, 1));
    c = c + 1;
end

%Create an array of the difference b/w sse and Vlocs
DifferenceEnd = zeros(size(Vpeaks) - 1);
c=1;
for row5 = 1 : numRows5
    DifferenceEnd(row5, 1) = abs(EndPk - Vlocs(c, 1));
    c = c + 1;
end

%Find the minimum distance between the sse and see and the times in the
max
%peaks array
MinSt = min(DifferenceStart);
```

```
MinEd = min(DifferenceEnd);
% Find the cell location that min distances from sss and sse occur at
TimeSt = find(DifferenceStart==MinSt);
TimeEd = find(DifferenceEnd==MinEd);
%Find the actual time in the data series they occur at
SSStart = Vlocs(TimeSt);
SSEnd = Vlocs(TimeEd);

[numRows6,numCols6] = (size(Vlocs)); %find the size of the array
for row6 = (TimeSt-1) : (TimeEd-1)
    mean3 = mean(TimeBwMax(TimeSt-1:TimeEd-1)); %Average the array across
these specific times
end
%Average the Time Between Maximum peaks across whole test
mean4=mean(TimeBwMax);

%% print our results
fprintf('Estimated distance travelled: %.3f m\n', sum1);
fprintf('Average moving velocity: %0.3f m/s\n', mean1);
fprintf('Peak velocity: %0.3f m/s\n', M1);
fprintf('Average acceleration: %0.3f m/s/s\n', mean2);
fprintf('Peak acceleration: %0.3f m/s/s\n', M2);

Powerwatts = 0.5*mass_part_chair*(10^(Powersum/10)); % 0.5 * mass * power
to sustain ss
fprintf('Total power in spectrum: %.4f Watts\n', Powerwatts);
fprintf('Average SS TimeBwMax: %0.3f s\n', mean3);
fprintf('Average TimeBwMax for Whole Test: %0.3f s\n', mean4);
```

Appendix D: IGROUP PRESENCE QUESTIONAIRE (IPQ)

Please answer the questions by choosing the number that best describes your experience.

1. How aware were you of the real world surrounding you while navigating in the virtual world? (i.e. sounds, room temperature, other people, etc.)?

Extremely aware — Not aware at all

0	1	2	3	4	5	6

2. How real did the virtual world seem to you?

About as real as an imagined world — Indistinguishable from real world

0	1	2	3	4	5	6

3. I had a sense of acting in the virtual space, rather than operating something from outside.

Fully disagree — Fully agree

0	1	2	3	4	5	6

4. How much did your experience in the virtual environment seem consistent with your real-world experience?

Not consistent — Very consistent

0	1	2	3	4	5	6

5. How real did the virtual world seem to you?

Not real at all — Completely real

0	1	2	3	4	5	6

6. I did not feel present in the virtual space.

Did not feel present — Felt present

0	1	2	3	4	5	6

7. I was not aware of the real environment.

Extremely aware Not aware at all

0	1	2	3	4	5	6

8. In the computer-generated world I had a sense of "being there".

Fully disagree Fully agree

0	1	2	3	4	5	6

9. Somehow, I felt that the virtual world surrounded me.

Fully disagree Fully agree

0	1	2	3	4	5	6

10. I felt present in the virtual space.

Fully disagree Fully agree

0	1	2	3	4	5	6

11. I still paid attention to the real environment.

Fully agree Fully disagree

0	1	2	3	4	5	6

12. The virtual world seemed more realistic than the real world.

Fully disagree Fully agree

0	1	2	3	4	5	6

13. I felt like I was just seeing pictures.

Fully agree Fully disagree

0	1	2	3	4	5	6

14. I was completely captivated by the virtual world.

Fully disagree Fully agree

0	1	2	3	4	5	6

15. How do you rate your trials in real world relative to your trials in virtual world?

Virtual reality was much easier the same Virtual reality was much harder

0 ----------5---------- 10

16. How much similar were the forces you needed to apply to turn a given angle, i.e. 45 deg?

Virtual reality needed much less force the same Virtual reality needed much more force

0 ----------5---------- 10

17. Please comment on what you felt was missing from the virtual world experience?

_____

_____

_____

_____

Appendix E: MOTION SICKNESS ASSESSMENT QUESTIONNAIRE (MSAQ)

Using the scale below, please rate how accurately the following statements describe your experience.

Not at all Severely
0———1———2———3———4———5———6———7———8———9

1. I felt sick to my stomach ( )
2. I felt faint-like ( )
3. I felt annoyed/irritated ( )
4. I felt sweaty ( )
5. I felt queasy ( )
6. I felt lightheaded ( )
7. I felt drowsy ( )
8. I felt clammy/cold sweat ( )
9. I felt disoriented ( )
10. I felt tired/fatigued ( )

- Overall fatigue ( ) - Arm fatigue ( )

11. I felt nauseated ( )
12. I felt hot/warm ( )
13. I felt dizzy ( )
14. I felt like I was spinning ( )
15. I felt as if I may vomit ( )
16. I felt uneasy ( )

17. In general, how do you feel about your motion sickness relative to last session?

Much worse Much better

0 ----------5----------10

18. In general, do you think you are ready to take the main experiments? ◯ Yes ◯ No

Appendix F: Borg's Rating of Perceived Exertion [RPE]

How you might describe your exertion	**Borg rating of your exertion**	**Examples (for most adults <65 years old)**
None	6	Reading a book, watching television
Very, very light	7 to 8	Tying shoes
Very light	9 to 10	Chores like folding clothes that seem to take little effort
Fairly light	11 to 12	Walking through the grocery store or other activities that require some effort but not enough to speed up your breathing
Somewhat hard	13 to 14	Brisk walking or other activities that require moderate effort and speed your heart rate and breathing but don't make you out of breath
Hard	15 to 16	Bicycling, swimming, or other activities that take vigorous effort and get the heart pounding and make breathing very fast
Very hard	17 to 18	The highest level of activity you can sustain
Very, very hard	19 to 20	A finishing kick in a race or other burst of activity that you can't maintain for long

Source: Borg G. Borg's Perceived Exertion and Pan Scales. Champaign, IL: Human Kinetics, 1998.

Using the 15-point scale, please describe your experience.

	Shoulders	Center	Overall
750 meters into test			
1500 meters into test			
5-minutes post test			

Appendix G: Wheelchair User's Shoulder Pain Index (WUSPI)

Place a 'X' across the scale to estimate your level of pain with the following activities. Tick the box at right if the activity was not performed in the past week. Based on your experiences IN THE PAST WEEK, how much shoulder pain have you experienced when:

Not performed

1. Transferring from a bed to a wheelchair?

No pain _____ Worst pain ever experienced □

2. Transferring from a wheelchair to a car?

No pain _____ Worst pain ever experienced □

3. Transferring from a wheelchair to a bath or shower?

No pain _____ Worst pain ever experienced □

4. Loading your wheelchair into a car?

No pain _____ Worst pain ever experienced □

5. Pushing your wheelchair for 10 minutes or more?

No pain _____ Worst pain ever experienced □

6. Pushing up ramps or inclines outdoors?

No pain _____ Worst pain ever experienced □

7. Lifting objects down from an overhead shelf?

No pain _____ Worst pain ever experienced □

8. Putting on trousers?

No pain _____ Worst pain ever experienced □

9. Putting on a t-shirt or a jumper?

No pain _____ Worst pain ever experienced □

10.Putting on a button-down shirt?

No pain _____ Worst pain ever experienced □

11.Washing your back?

No pain _____ Worst pain ever experienced □

12.Usual daily activities Not performed

No pain _____ Worst pain ever experienced □

13.Driving?

No pain _____ Worst pain ever experienced □

14.Performing household chores?

No pain _____ Worst pain ever experienced □

15.Sleeping?

No pain _____ Worst pain ever experienced □

Adapted from original (Wheelchair User's Shoulder Pain Index (WUSPI), 1995).

Appendix H: Visual Analog Scale [VAS]

Using the scale below, please mark your current pain level on the line between the two end points.

Pretest:

No pain	_____	Pain as bad as it could be

Post-Test:

No pain	_____	Pain as bad as it could be

10 cm line.

Appendix I: Correction Factor Test Results

	Calibration Factor	Ergometer Distance (m)	Video Distance (m)	Ergometer to Video Ratio	New Calibration Factor
Left	0.195	15.80	10	1.58	0.12
	0.123	12.14	10	1.21	0.10
	0.102	8.67	10	0.87	0.12
	0.117	11.48	10	1.15	0.10
	0.102	10.77	10	1.08	0.09484248

	Calibration Factor	Ergometer Distance (m)	Video Distance (m)	Ergometer to Video Ratio	New Calibration Factor
Right	0.195	15.80	10	1.58	0.12
	0.123	12.40	10	1.24	0.10
	0.100	11.49	10	1.15	0.09
	0.087	9.22	10	0.92	0.09390707

Appendix J: Ergometer Velocity Versus Video Velocity

Ergometer						
Speed (m/s)	Side	Start Time (s)	End Time (s)	Distance Traveled (m)	Time (s)	Ergometer Velocity (m/s)
0.9	Left	9.001	38.023	10.77	29.022	0.371
	Right	10.001	36.003	9.22	26.002	0.355
1.2	Left	15.001	35.003	9.96	20.002	0.498
	Right	6.001	27.003	9.99	21.002	0.476
1.5	Left	8.001	23.022	9.00	15.021	0.599
	Right	7.001	23.002	9.93	16.001	0.621

Video				
Speed (m/s)	Side	Distance (m)	Time (s)	Video Velocity (m/s)
0.9	Left	10	29	0.345
	Right	10	26	0.385
1.2	Left	10	20	0.500
	Right	10	21	0.476
1.5	Left	10	15	0.667
	Right	10	16	0.625

Appendix K: Full-size Blueprint of Universiade Pavilion

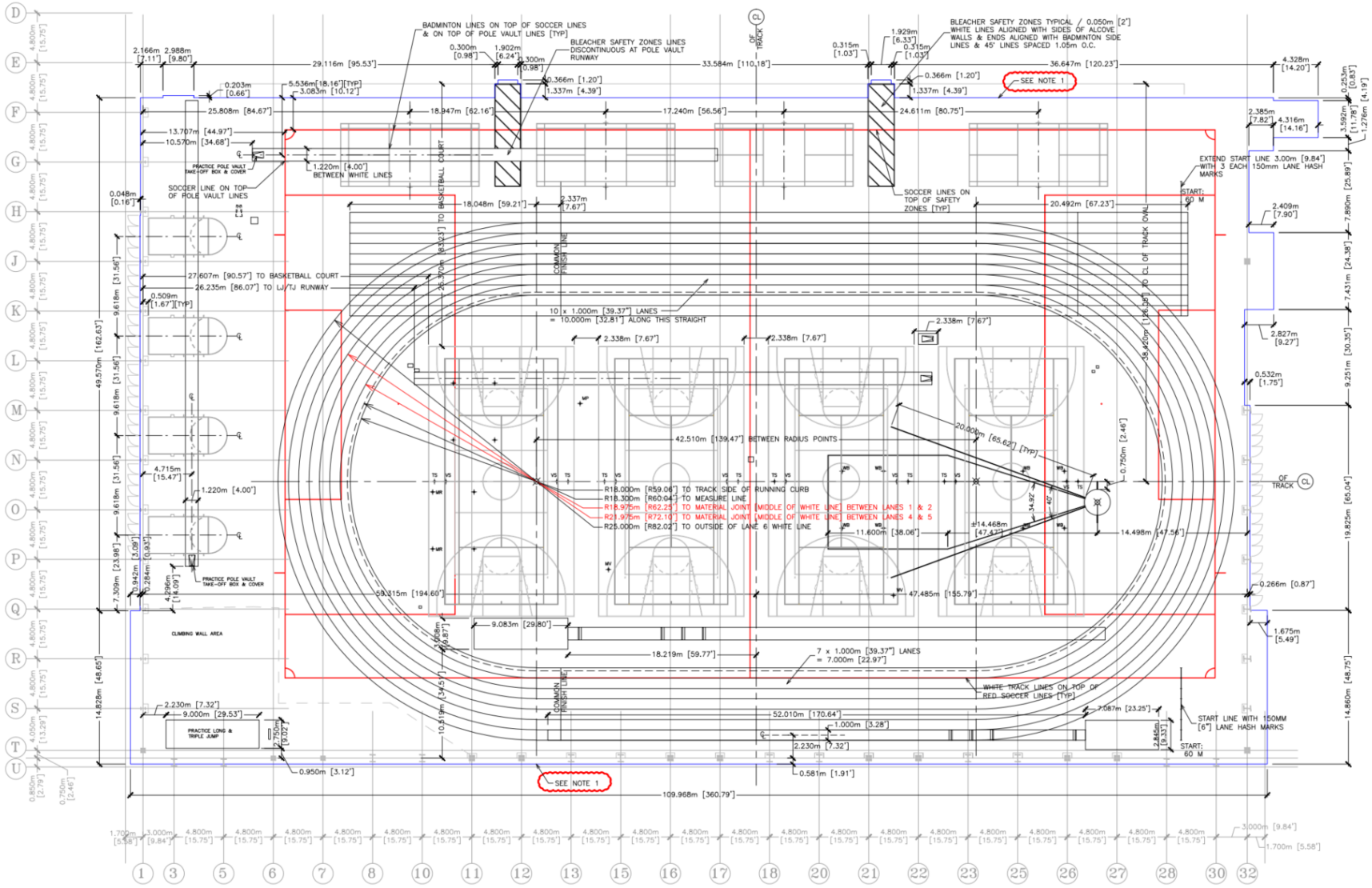

Appendix L: Rolling Resistance Data

VR		
Wheel	Session #	Resistance (m/s/s)
Right	1	-0.1028
	2	-0.0916
	3	-0.1734
	4	-0.1783
	5	-0.1508
	6	-0.2031
	Mean	-0.1500
Left	2	-0.1173
	3	-0.1653
	4	-0.2025
	5	-0.1751
	6	-0.2270
	Mean	-0.17744

RW		
Wheel	Session #	Resistance (m/s/s)
Right	1	-0.0980
	2	-0.0861
	3	-0.1022
	4	-0.0820
	5	-0.0849
	6	-0.1013
	Mean	-0.0924
Left	1	-0.0975
	2	-0.0951
	3	-0.1019
	4	-0.0986
	5	-0.0817
	6	-0.0914
	Mean	-0.0944

Appendix M: Track Compensator Indicator and Dial Code

TrackCompSerialPort.cs

```
public class DialSerialPort:  IDisposable
{
public static DialSerialPort Current;
public int DialValue { get; set; }

private SerialPort serialPort = null;
/// <summary>
/// Construct to connect the port with proper baudrate
/// </summary>
/// <param name="portName"></param>
public DialSerialPort(string portName) {
    //Initialize serialPort
    Current = this;
       serialPort = new SerialPort(portName, 38400, Parity.None, 8, StopBits.One);
    serialPort.ReadBufferSize = 8192;
}
/// <summary>
/// Dispose the serial port.
/// </summary>
public void Dispose() {
       Close();
}
public bool Open() {
       try {
              serialPort.Open();
              return true;
       }
       catch { return false; }
}
public void Read()
{
    int i = 30;
    int total = 0;
    int straightVal = -1;

    try {
        while (true)
        {
            Thread.Sleep(1);
            var remainHex = string.Empty;
            var packetRemainData = new List<string>();

            var totalbytes = serialPort.BytesToRead;
            if (totalbytes > 0)
            {
                //Load all the serial data to buffer
                var buffer = new byte[totalbytes];
                serialPort.Read(buffer, 0, buffer.Length);
                var hexFull = BitConverter.ToString(buffer);

                hexFull = remainHex + hexFull;

                //Console.WriteLine(hexFull);
```

```
                var packets = new List<DialPacket>();

                remainHex = ParsePacketHex(hexFull.Split('-').ToList(), packets);

                foreach (var packet in packets)
                {
                    //Total transmitted data is 16 byte long. 1 more byte should be
checksum. prefixchar is the extra header due to API Mode
                    int prefixCharLength = 7;
                    int byteArrayLength = 4;
                    int totalExpectedCharLength = prefixCharLength + byteArrayLength;

                    //Based on above variables to parse data coming from SerialPort
                    DialValue = ParseConvertRFDataHex(packet.Data, packetRemainData,
totalExpectedCharLength);


//This code is used to set the straight value for the Dial and create the turning
values

            if (straightVal == -1)
                straightVal = DialValue;
            if (i > 0)
            {
                total = total + DialValue;
                i--;
            }
            else
            {
                straightVal = total / 30;
            }

            if ((DialValue - straightVal) < -10 && (DialValue - straightVal) > -20)
            {
                DialValue = -1;
            }

            else if ((DialValue - straightVal) < -20 && (DialValue - straightVal) > -
40)
            {
                DialValue = -2;
            }

            else if ((DialValue - straightVal) > 8 && (DialValue - straightVal) < 19)
            {
                DialValue = 1;
            }

            else if ((DialValue - straightVal) > 19 && (DialValue - straightVal) < 30)
            {
                DialValue = 2;
            }

            else if ((DialValue - straightVal) > 30 && (DialValue - straightVal) < 41)
            {
                DialValue = 3;
            }

            else if ((DialValue - straightVal) > 41 && (DialValue - straightVal) < 52)
            {
                DialValue = 4;
            }
```

```
            else if ((DialValue - straightVal) > 52 && (DialValue - straightVal) < 70)
            {
                DialValue = 5;
            }

            else
            {
                DialValue = 0;
            }


        }
        finally {
               Close();
        }
}
public void Close() {
        if(serialPort != null) {
               try {
                      serialPort.Close();
                      serialPort.Dispose();
               }
               catch {
               }
        }
}


private static string ParsePacketHex(List<string> hexFull, List<DialPacket> packets) {
        var leftHex = string.Empty;
        var isWrongStart = false;

        //Each packet based on example above should be more than 20 bytes. 7E 00 10 81
66 66 24 00 7D 5E 00 07 01 01 55 55 00 00 00 53 0A
        while(hexFull.Count > 20) {
               if(hexFull[0] == "7E") {
                      var length = int.Parse(hexFull[1] + hexFull[2],
System.Globalization.NumberStyles.HexNumber);
                      if(length != 16) {
                             isWrongStart = true;
                      }
                      else {
                             var frameType = hexFull[3];

                             if(frameType == "81") {
                                    if(hexFull.Count < length + 4)
                                           break;

                                    var packetDataBytes = hexFull.GetRange(4, length);

                                    var source16Addess = string.Join("",
packetDataBytes.GetRange(0, 2));


                                    var RSSI = packetDataBytes[2];
                                    var receiveOption = packetDataBytes[3];
                                    var data = packetDataBytes.GetRange(4, length - 5);
                                    var checkSum = packetDataBytes[length - 1];

                                    DialPacket xbeePacket = new DialPacket();
                                    xbeePacket.StartDelimiter = hexFull[0];
```

```
                                        xbeePacket.Length = length;
                                        xbeePacket.FrameType = frameType;
                                        xbeePacket.Address16bit = source16Addess;
                                        xbeePacket.ReceiveOption = receiveOption;
                                        xbeePacket.Data = data;
                                        xbeePacket.CheckSum = checkSum;
                                        packets.Add(xbeePacket);
                                        hexFull.RemoveRange(0, 4 + length);
                                }
                                else
                                        isWrongStart = true;
                        }
                }
                else {
                        isWrongStart = true;
                }

                if(isWrongStart) {
                        if(hexFull.Count > 1) {
                                var idx = hexFull.IndexOf("7E", 1);
                                if(idx >= 0) {
                                        hexFull.RemoveRange(0, idx);
                                }
                                else {
                                        break;
                                }
                        }
                }
        }
        if(hexFull.Count > 0)
                return string.Join("-", hexFull) + "-";
        else
                return "";
}

/// The function is for parseing RF data values
/// RF data: 7E 00 07 01 01 55 55 00 00 00 53 from above example.
/// The actual data read from serial is actually 7D 5E 00 07 01 01 55 55 00 00 00 53
/// So instead of 7E, it's 7D 5E
/// </summary>
/// <param name="packetHexData"></param>
/// <param name="leftHexData"></param>
/// <param name="totalExpectedCharLength"></param>
/// <returns></returns>
private static int ParseConvertRFDataHex(List<string> packetHexData, List<string>
leftHexData, int totalExpectedCharLength) {

        if(packetHexData.Count() == totalExpectedCharLength) {
                if(packetHexData[0] == "7D" && packetHexData[1] == "5E") {
                        var length = int.Parse(packetHexData[2] + packetHexData[3],
System.Globalization.NumberStyles.HexNumber);
                        if(length != 7) {
                                return -1;
                        }
                        else {
                                //Based on the adrino code, I'm reading last two bytes
should be enough
                                int decValue = int.Parse(packetHexData[9],
System.Globalization.NumberStyles.HexNumber);
                  //int decValue = int.Parse(packetHexData[9] + packetHexData[10],
System.Globalization.NumberStyles.HexNumber);
                  return decValue;
```

```
                    }
                }
            }
            return -1;
}
}
}

namespace ConsoleErgometer.Hardware
{
public class TrackCompSerialPort : IDisposable
{
public static TrackCompSerialPort Current;
public int TrackCompValue { get; set; }

private SerialPort = null;
/// <summary>
/// Construct to connect the port with proper baudrate
/// </summary>
/// <param name="portName2"></param>
public TrackCompSerialPort(string portName2)
{
    //Initialize serialPort
    Current = this;
    serialPort = new SerialPort(portName2, 38400, Parity.None, 8, StopBits.One);
    serialPort.ReadBufferSize = 65536; //8192
}
/// <summary>
/// Dispose the serial port.
/// </summary>
public void Dispose()
{
    Close();
}
public bool Open()
{
    try
    {
        serialPort.Open();
        return true;
    }
    catch { return false; }
}

public void Read()
{
    int i = 30;
    int total = 0;
    int straightVal = -1;

    try
    {
        while (true)
        {
            Thread.Sleep(1);
            var remainHex = string.Empty;
            var packetRemainData = new List<string>();
            var totalbytes = serialPort.BytesToRead;
            if (totalbytes > 0)
            {
                //Load all the serial data to buffer
                var buffer = new byte[totalbytes];
```

```
                serialPort.Read(buffer, 0, buffer.Length);
                var hexFull = BitConverter.ToString(buffer);

                hexFull = remainHex + hexFull;

                // Console.WriteLine(hexFull);

                var packets = new List<TrackCompPacket>();

                remainHex = ParsePacketHex(hexFull.Split('-').ToList(), packets);

                // Console.WriteLine(packets);
                foreach (var packet in packets)
                {
                    //Total transmitted data is 30 byte long. 1 more byte should be
checksum. prefixchar is the extra header due to API Mode
                    int prefixCharLength = 21;
                    int byteArrayLength = 4;
                    int totalExpectedCharLength = prefixCharLength + byteArrayLength;

                    //Based on above variables to parse data coming from SerialPort
                    TrackCompValue = ParseConvertRFDataHex(packet.Data,
packetRemainData, totalExpectedCharLength);

                    Console.Write("Track Comp Value: " + TrackCompValue.ToString());


//This code is used to set the straight value for the track compensator indicator and
create the turning values

if (straightVal == -1)
    straightVal = TrackCompValue;
if (i > 0)
{
    total = total + TrackCompValue;
    i--;
}
else
{
    straightVal = total / 30;
}

// Use this for the racing chair the lab owns where the track compensator indicator
must be mounted above the track control device.

    if ((TrackCompValue - straightVal) < -200 && (TrackCompValue - straightVal) > -
350)
    {
        TrackCompValue = 1;
    }

    else if ((TrackCompValue - straightVal) < -350 && (TrackCompValue - straightVal) >
-600)
    {
        TrackCompValue = 2;
    }

    else if ((TrackCompValue - straightVal) < -600 && (TrackCompValue - straightVal) >
-850)
    {
        TrackCompValue = 3;
    }
```

```
    else if ((TrackCompValue - straightVal) < -850 && (TrackCompValue - straightVal) >
-1100)
    {
        TrackCompValue = 4;
    }

    else if ((TrackCompValue - straightVal) < -1100 && (TrackCompValue - straightVal)
> -3000)
    {
        TrackCompValue = 5;
    }

    else
    {
        TrackCompValue = 0;
    }


    //Use this for the 17 in red racing wheelchair from the Steadward Center where the
track compensator indicator must be mounted underneath the track control device.
    /*
if ((TrackCompValue - straightVal) > 150 && (TrackCompValue - straightVal) < 350)
    {
        TrackCompValue = 1;
    }

    else if ((TrackCompValue - straightVal) < -350 && (TrackCompValue - straightVal) >
-600)
    {
        TrackCompValue = 2;
    }

    else if ((TrackCompValue - straightVal) < -600 && (TrackCompValue - straightVal) >
-850)
    {
        TrackCompValue = 3;
    }

    else if ((TrackCompValue - straightVal) < -850 && (TrackCompValue - straightVal) >
-1100)
    {
        TrackCompValue = 4;
    }

    else if ((TrackCompValue - straightVal) < -1100 && (TrackCompValue - straightVal)
> -2000)
    {
        TrackCompValue = 5;
    }

    else
    {
        TrackCompValue = 0;
    }
    */
        }
        finally
        {
            Close();
        }
    }
```

```
    public void Close()
    {
        if (serialPort != null)
        {
            try
            {
                serialPort.Close();
                serialPort.Dispose();
            }
            catch
            {
            }
        }
    }

   private static string ParsePacketHex(List<string> hexFull, List<TrackCompPacket>
packets)
    {
        var leftHex = string.Empty;
        var isWrongStart = false;

    /*
        *
        * Packet for Track Comp gyro device
        *
        * RX (Receive) Packet 16-bit Address (API 2)
        *
        * 7E 00 1E 81 33 03 24 00 7D 5E 00 15 01 01 33 33 00 00 00 02 5D 8C 99 00 E1
00 12 00 00 00 02 00 17 07 92
        *
        * Start delimiter: 7E
        * Length: 00 1E (30)
        * Frame type: 81 (RX (Receive) Packet 16-bit Address)
        * 16-bit source address: 33 03
        * RSSI: 24
        * Options: 00
        * RF data: 7E 00 15 01 01 33 33 00 00 00 02 5D 8C 99 00 E1 00 12 00 00 00 02
00 17 07
        * Checksum: 92
        *
        */

    //Each packet based on example above should be more than 34 bytes.
    //7E 00 1E 81 33 03 24 00 7D 5E 00 15 01 01 33 33 00 00 00 02 5D 8C 99 00 E1 00 12
00 00 00 02 00 17 07 92
    //7E 00 1E 81 33 03 24 00 7D 5E 00 15 01 01 33 33 00 00 00 00 44 8C 74 00 F3 00 38
00 0A 00 01 00 17 06 92
    while (hexFull.Count > 30)
    {
        if (hexFull[0] == "7E")
        {
            var length = int.Parse(hexFull[1] + hexFull[2],
System.Globalization.NumberStyles.HexNumber);
            if (length != 30)
            {
                isWrongStart = true;
            }
            else
            {
                var frameType = hexFull[3];

                if (frameType == "81")
```

```
                {
                    if (hexFull.Count < length + 4)
                        break;

                    var packetDataBytes = hexFull.GetRange(4, length);

                    var source16Addess = string.Join("", packetDataBytes.GetRange(0,
2));


                    var RSSI = packetDataBytes[2];
                    var receiveOption = packetDataBytes[3];
                    var data = packetDataBytes.GetRange(4, length - 5);
                    var checkSum = packetDataBytes[length - 1];

                    TrackCompPacket xbeePacket = new TrackCompPacket();
                    xbeePacket.StartDelimiter = hexFull[0];
                    xbeePacket.Length = length;
                    xbeePacket.FrameType = frameType;
                    xbeePacket.Address16bit = source16Addess;
                    xbeePacket.ReceiveOption = receiveOption;
                    xbeePacket.Data = data;
                    xbeePacket.CheckSum = checkSum;
                    packets.Add(xbeePacket);
                    hexFull.RemoveRange(0, 4 + length);
                }
                else
                    isWrongStart = true;
            }
        }
        else
        {
            isWrongStart = true;
        }

        if (isWrongStart)
        {
            if (hexFull.Count > 1)
            {
                var idx = hexFull.IndexOf("7E", 1);
                if (idx >= 0)
                {
                    hexFull.RemoveRange(0, idx);
                }
                else
                {
                    break;
                }
            }
        }
    }
    if (hexFull.Count > 0)
        return string.Join("-", hexFull) + "-";
    else
        return "";
}

/// <summary>
/// The function is for parseing RF data values
/// RF data: 7E 00 15 01 01 33 33 00 00 00 02 5D 8C 99 00 E1 00 12 00 00 00 02 00 17
07 from above example (first iteration data packet)
```

```
/// The actual data read from serial is actually 7D 5E 00 15 01 01 33 33 00 00 00 02
5D 8C 99 00 E1 00 12 00 00 00 02 00 17 07
/// So instead of 7E, it's 7D 5E
///
/// The function is for parseing RF data values
/// RF data: 7E 00 07 01 01 55 55 00 00 00 53 from above example.
/// The actual data read from serial is actually 7D 5E 00 07 01 01 55 55 00 00 00 53
/// So instead of 7E, it's 7D 5E
/// </summary>
/// <param name="packetHexData"></param>
/// <param name="leftHexData"></param>
/// <param name="totalExpectedCharLength"></param>
/// <returns></returns>
private static int ParseConvertRFDataHex(List<string> packetHexData, List<string>
leftHexData, int totalExpectedCharLength)
{

    if (packetHexData.Count() == totalExpectedCharLength)
    {
        if (packetHexData[0] == "7D" && packetHexData[1] == "5E")
        {
            var length = int.Parse(packetHexData[2] + packetHexData[3],
System.Globalization.NumberStyles.HexNumber);
            //ToDo: float length = float.Parse(length);
            if (length == 30)
            {
                return -2;
            }
            else
            {
                //Based on the adrino code, I'm reading last two bytes should be
enough
                //int decValue = int.Parse(packetHexData[5],
System.Globalization.NumberStyles.HexNumber);
                int decValue = int.Parse(packetHexData[13] + packetHexData[14],
System.Globalization.NumberStyles.HexNumber);
                return decValue;
            }
        }
    }
    return -3;
}
}
}
```

Wheelchair.cs

```
namespace ConsoleErgometer.Model {
class Wheelchair {
private DialSerialPort dial = DialSerialPort.Current;
private TrackCompSerialPort trackComp = TrackCompSerialPort.Current;

private ErgoDataPacket lastPoint = new ErgoDataPacket();
private Vector2 forward = new Vector2(0, 1);

public Vector2 leftPosition = new Vector2(0, 0);
public Vector2 rightPosition = new Vector2(0, 0);
public Vector2 centerPosition = new Vector2(0, 0);
public double theta = 0;

private Queue<Vector2> oldVelocities = new Queue<Vector2>(5);
```

```
public IDataFilter alFilter = new MWADataFilter(5, 0), arFilter = new MWADataFilter(5,
0);

double coefficient = 0;

private Settings;

public double RadiusCorrectionFactor { get; private set; }
public double DistanceTraveledLeft { get; private set; }
public double DistanceTraveledRight { get; private set; }
public double LeftWheelRadius { get; private set; }
public double RightWheelRadius { get; private set; }

public Wheelchair(Settings settings) {
    this.settings = settings;
}

public void Update(ref ErgoDataPacket dp) {
// process the data
double dt = dp.t - lastPoint.t;

// calibrate
dp.velocityLeft *= settings.LeftCalibration;
dp.velocityRight *= settings.RightCalibration;

// integrate the position
double forwardVelocity = (dp.velocityLeft + dp.velocityRight) / 2;


/// BEGIN ZOHREH MODS
if (settings.EnableRotationCorrection) {
double MOIRoller = 0.66;
double mass = settings.WeightOfPerson;
double moiwheel = 0.115;
double inertiaFraction = (moiwheel + MOIRoller) / settings.MOIChair;
double radiusFraction = Math.Pow(settings.WheelSpan / settings.WheelRadius, 2) / 2;
if (dp.velocityLeft != 0 || dp.velocityRight != 0)
{
    if (dp.velocityLeft * dp.velocityRight > 0)
    {
        coefficient = 0.5 + 0.5 * Math.Min(Math.Abs(dp.velocityLeft),
Math.Abs(dp.velocityRight)) / Math.Max(Math.Abs(dp.velocityLeft),
Math.Abs(dp.velocityRight));
    }
    else
    {
        coefficient = 0.5 - 0.5 * Math.Min(Math.Abs(dp.velocityLeft),
Math.Abs(dp.velocityRight)) / Math.Max(Math.Abs(dp.velocityLeft),
Math.Abs(dp.velocityRight));
    }

    LeftWheelRadius = settings.LaneRadius + 0.33;
    RightWheelRadius = LeftWheelRadius + settings.WheelSpan;

    DistanceTraveledLeft = LeftWheelRadius * Math.PI;
    DistanceTraveledRight = RightWheelRadius * Math.PI;

    RadiusCorrectionFactor = DistanceTraveledLeft / DistanceTraveledRight;
```

```
//Syd Mods
//This portion is used to have the Dial Value change the velocity of the left roller
and turn the wheelchair.
    if (DialSerialPort.Current.DialValue == 0)
    {
        dp.velocityLeft *= ((inertiaFraction * radiusFraction + (1 - (inertiaFraction
* radiusFraction)) * coefficient));
        dp.velocityRight *= ((inertiaFraction * radiusFraction + (1 - (inertiaFraction
* radiusFraction)) * coefficient));
    }
    else if (DialSerialPort.Current.DialValue == 1)
    {
        dp.velocityLeft *= ((inertiaFraction * radiusFraction + (1 - (inertiaFraction
* radiusFraction)) * coefficient) * 0.99);
        dp.velocityRight *= (inertiaFraction * radiusFraction + (1 - (inertiaFraction
* radiusFraction)) * coefficient);
    }

    else if (DialSerialPort.Current.DialValue == 2)
    {
        dp.velocityLeft *= ((inertiaFraction * radiusFraction + (1 - (inertiaFraction
* radiusFraction)) * coefficient) * 0.98);
        dp.velocityRight *= (inertiaFraction * radiusFraction + (1 - (inertiaFraction
* radiusFraction)) * coefficient);
    }

    else if (DialSerialPort.Current.DialValue == 3)
    {
        dp.velocityLeft *= ((inertiaFraction * radiusFraction + (1 - (inertiaFraction
* radiusFraction)) * coefficient) * 0.97);
        dp.velocityRight *= (inertiaFraction * radiusFraction + (1 - (inertiaFraction
* radiusFraction)) * coefficient);
    }

    else if (DialSerialPort.Current.DialValue == 4)
    {
        dp.velocityLeft *= ((inertiaFraction * radiusFraction + (1 - (inertiaFraction
* radiusFraction)) * coefficient) * 0.96);
        dp.velocityRight *= (inertiaFraction * radiusFraction + (1 - (inertiaFraction
* radiusFraction)) * coefficient);
    }

    else if (DialSerialPort.Current.DialValue == 5)
    {
        dp.velocityLeft *= ((inertiaFraction * radiusFraction + (1 - (inertiaFraction
* radiusFraction)) * coefficient) * 0.95);
        dp.velocityRight *= (inertiaFraction * radiusFraction + (1 - (inertiaFraction
* radiusFraction)) * coefficient);
    }

    else if (DialSerialPort.Current.DialValue == -2)
    {
        dp.velocityLeft *= (inertiaFraction * radiusFraction + (1 - (inertiaFraction *
radiusFraction)) * coefficient);
        dp.velocityRight *= ((inertiaFraction * radiusFraction + (1 - (inertiaFraction
* radiusFraction)) * coefficient) * 0.98);
    }

else
    {
```

```
        dp.velocityLeft *= (inertiaFraction * radiusFraction + (1 - (inertiaFraction *
radiusFraction)) * coefficient);
        dp.velocityRight *= ((inertiaFraction * radiusFraction + (1 - (inertiaFraction
* radiusFraction)) * coefficient) * 0.99);
    }


    // This portion is used to have the Track Compensator Value change the velocity of
the left roller and turn the wheelchair.
    if (TrackCompSerialPort.Current.TrackCompValue == 0)
    {
        dp.velocityLeft *= ((inertiaFraction * radiusFraction + (1 - (inertiaFraction
* radiusFraction)) * coefficient));
        dp.velocityRight *= ((inertiaFraction * radiusFraction + (1 - (inertiaFraction
* radiusFraction)) * coefficient));
    }
    else if (TrackCompSerialPort.Current.TrackCompValue == 1)
    {
        dp.velocityLeft *= ((inertiaFraction * radiusFraction + (1 - (inertiaFraction
* radiusFraction)) * coefficient) * 0.99);
        dp.velocityRight *= (inertiaFraction * radiusFraction + (1 - (inertiaFraction
* radiusFraction)) * coefficient);
    }
    else if (TrackCompSerialPort.Current.TrackCompValue == 2)
    {
        dp.velocityLeft *= ((inertiaFraction * radiusFraction + (1 - (inertiaFraction
* radiusFraction)) * coefficient) * 0.985);
        dp.velocityRight *= (inertiaFraction * radiusFraction + (1 - (inertiaFraction
* radiusFraction)) * coefficient);
    }
    else if (TrackCompSerialPort.Current.TrackCompValue == 3)
    {
        dp.velocityLeft *= ((inertiaFraction * radiusFraction + (1 - (inertiaFraction
* radiusFraction)) * coefficient) * 0.98);
        dp.velocityRight *= (inertiaFraction * radiusFraction + (1 - (inertiaFraction
* radiusFraction)) * coefficient);
    }
    else if (TrackCompSerialPort.Current.TrackCompValue == 4)
    {
        dp.velocityLeft *= ((inertiaFraction * radiusFraction + (1 - (inertiaFraction
* radiusFraction)) * coefficient) * 0.975);
        dp.velocityRight *= (inertiaFraction * radiusFraction + (1 - (inertiaFraction
* radiusFraction)) * coefficient);
    }
    else
    {
        dp.velocityLeft *= ((inertiaFraction * radiusFraction + (1 - (inertiaFraction
* radiusFraction)) * coefficient) * 0.97);
        dp.velocityRight *= (inertiaFraction * radiusFraction + (1 - (inertiaFraction
* radiusFraction)) * coefficient);
    }

/// END ZOHREH MODS


dp.accelerationLeft = alFilter.filterPoint((dp.velocityLeft - lastPoint.velocityLeft)
/ dt);
dp.accelerationRight = arFilter.filterPoint((dp.velocityRight -
lastPoint.velocityRight) / dt);

double accelerationTerm = dp.accelerationRight - dp.accelerationLeft;
```

```
// update the rotation
double deltaTheta = ((dp.velocityRight - dp.velocityLeft) / settings.WheelSpan) * dt;

theta += deltaTheta;

// rotate it!
Matrix2x2 rotationMatrix = new Matrix2x2(Math.Cos(theta), -1 * Math.Sin(theta),
Math.Sin(theta), Math.Cos(theta));
Vector2 forwards = rotationMatrix * forward;

// move it!
leftPosition += (forwards * dp.velocityLeft) * dt;
rightPosition += (forwards * dp.velocityRight) * dt;
centerPosition = (leftPosition + rightPosition) / 2;

// store the old point
lastPoint = dp;
}

void Reset(double wheelSpan) {
lastPoint.velocityLeft = 0;
lastPoint.velocityRight = 0;

centerPosition = new Vector2(0, 0);
leftPosition = centerPosition + new Vector2(-wheelSpan / 2, 0);
rightPosition = centerPosition + new Vector2(wheelSpan / 2, 0);
theta = Math.PI;
}
```

Program.cs

```
private static void Ergometer_NewData(ErgoDataPacket dp) {
       wheelchair.Update(ref dp);
       UpdateEON();
    UpdateLabVIEW(dp, ergometer);

    TimeSpan timeSinceLastDisplay = DateTime.Now - LastDisplayTime;
       if(timeSinceLastDisplay.TotalSeconds >= 0.1) {
              LastDisplayTime = DateTime.Now;
              //Console.Write(string.Format("\rx: {0,6:0.0} m, y: {0,6:0.0} m, vl:
{0,5:0.00} m/s, vr: {1,5:0.00} m/s", wheelchair.centerPosition.x,
wheelchair.centerPosition.y, wheelchair.lastVelocityLeft,
wheelchair.lastVelocityRight));
              //Console.Write(string.Format("\rt: {0,5:0.00} s, vl: {1,5:0.00} m/s,
vr: {2,5:0.00} m/s -> ({3,5:0.00}, {4,5:0.00})@{5,5:0.00}", dp.t, dp.velocityLeft,
dp.velocityRight, wheelchair.centerPosition.x, wheelchair.centerPosition.y,
wheelchair.theta));

              //TODO:MusiUpdate to include dial value in console log
              Console.Write(string.Format("\rt: {0,5:0.00} s, vl: {1,5:0.00} m/s, vr:
{2,5:0.00} m/s -> ({3,5:0.00}, {4,5:0.00})@{5,5:0.00}, Dial: {6,5:0.00}, val2:
{7,5:0.00}", dp.t, dp.velocityLeft, dp.velocityRight, wheelchair.centerPosition.x,
wheelchair.centerPosition.y, wheelchair.theta, ergometer.DialValue,
ergometer.TrackCompValue));
       }
}
```